S ARCHIVE
97.06
RKS, S.

NAVAL POSTGRADUATE SCHOOL
Monterey, California



THESIS

INSTANTANEOUS AXIS OF ROTATION FOR CONTINUOUS HUMAN KNEE MOTION

by
Steven A. Parks

June, 1997

Thesis Advisor: Young W. Kwon

Approved for public release; distribution is unlimited.

DUDLEY KNOX LIBRARY
NAVAL POSTGRADUATE SCHOOL
MONTEREY CA 93943-5101

REPORT DOCUMENTATION PAGE

Form Approved
OMB No. 0704-0188

Public reporting burden for this collection of information is estimated to average 1 hour per response, including the time for reviewing instruction, searching existing data sources, gathering and maintaining the data needed, and completing and reviewing the collection of information. Send comments regarding this burden estimate or any other aspect of this collection of information, including suggestions for reducing this burden, to Washington headquarters Services, Directorate for Information Operations and Reports, 1215 Jefferson Davis Highway, Suite 1204, Arlington, VA 22202-4302, and to the Office of Management and Budget, Paperwork Reduction Project (0704-0188) Washington DC 20503.

1. AGENCY USE ONLY *(Leave blank)*	2. REPORT DATE	3. REPORT TYPE AND DATES COVERED
	June 1997	Master's Thesis

4. TITLE AND SUBTITLE
INSTANTANEOUS AXIS OF ROTATION FOR CONTINUOUS HUMAN KNEE MOTION

5. FUNDING NUMBERS

6. AUTHOR(S)
Parks, Steven

7. PERFORMING ORGANIZATION NAME(S) AND ADDRESS(ES)
Naval Postgraduate School
Monterey, CA 93943-5000

8. PERFORMING ORGANIZATION REPORT NUMBER

9. SPONSORING / MONITORING AGENCY NAME(S) AND ADDRESS(ES)

10. SPONSORING / MONITORING AGENCY REPORT NUMBER

11. SUPPLEMENTARY NOTES
The views expressed in this thesis are those of the author and do not reflect the official policy or position of the Department of Defense or the U.S. Government.

12a. DISTRIBUTION / AVAILABILITY STATEMENT
Approved for public release; distribution unlimited.

12b. DISTRIBUTION CODE

13. ABSTRACT *(maximum 200 words)*

Previous studies of human knee motion are based on finite rotation data collected using large rotation steps varying from 5 to 30 degrees. In some cases this rotation data is used to develop axes of rotation for the joint. For such analysis, the rotation axis developed may be significantly different from the joint's instantaneous axis of rotation because, in general, the axis of rotation developed using finite rotation steps only closely approximates the true instantaneous axis of rotation if the step size is small. For the current study, a device has been developed to record high frequency (15 Hz) rotation and translation data of the femur and tibia during knee flexion. Kinematic constraint equations have been developed to analyze the six degree of freedom rotation and translation data to obtain an accurate approximation to the instantaneous axis of rotation. Four cadaveric knees were analyzed with all ligaments intact. Motion characteristics common to all knees were identified. The most obvious characteristic, internal tibial rotation, was related to the initial varus/valgus orientation of each knee. The anterior cruciate ligaments (ACL) of these same knees were subsequently severed, the knees were measured, and the motion analyzed. Differences in the motion characteristics of each knee were detected after the ACL was cut.

14. SUBJECT TERMS	15. NUMBER OF PAGES
Biomechanics, Three Dimensional Rigid Body Motion, Knee Joint, Continuous Motion	128
	16. PRICE CODE

17. SECURITY CLASSIFICATION OF REPORT	18. SECURITY CLASSIFICATION OF THIS PAGE	19. SECURITY CLASSIFICATION OF ABSTRACT	20. LIMITATION OF ABSTRACT
Unclassified	Unclassified	Unclassified	UL

NSN 7540-01-280-5500

Standard Form 298 (Rev. 2-89)
Prescribed by ANSI Std. 239-18

Approved for public release; distribution is unlimited

INSTANTANEOUS AXIS OF ROTATION FOR CONTINUOUS HUMAN KNEE MOTION

Steven A. Parks
Lieutenant Commander, United States Navy
B.S., United States Naval Academy, 1982

Submitted in partial fulfillment of the
requirements for the degree of

MASTER OF SCIENCE IN MECHANICAL ENGINEERING

and

MECHANICAL ENGINEER

from the

NAVAL POSTGRADUATE SCHOOL
June 1997

NPS ARCHIVE
1997.06
PARKS, S.

KNOX LIBRARY
NAVAL POSTGRADUATE SCHOOL
CA 93943-5101

ABSTRACT

Previous studies of human knee motion are based on finite rotation data collected using large rotation steps varying from 5 to 30 degrees. In some cases this rotation data is used to develop axes of rotation for the joint. For such analysis, the rotation axis developed may be significantly different from the joint's instantaneous axis of rotation because, in general, the axis of rotation developed using finite rotation steps only closely approximates the true instantaneous axis of rotation if the step size is small. For the current study, a device has been developed to record high frequency (15 Hz) rotation and translation data of the femur and tibia during knee flexion. Kinematic constraint equations have been developed to analyze the six degree of freedom rotation and translation data to obtain an accurate approximation to the instantaneous axis of rotation. Four cadaveric knees were analyzed with all ligaments intact. Motion characteristics common to all knees were identified. The most obvious characteristic, internal tibial rotation, was related to the initial varus/valgus orientation of each knee. The anterior cruciate ligaments (ACL) of these same knees were subsequently severed, the knees were measured, and the motion analyzed. Differences in the motion characteristics of each knee were detected after the ACL was cut.

TABLE OF CONTENTS

I. INTRODUCTION 1

II. METHODS AND MATERIALS 11

A. BACKGROUND 11

B. OVERVIEW 12

C. MEASUREMENT APPARATUS 13
1. Rotation Measurement 13
2. Translation Measurement 16
3. Simulated Muscle Loading 18

D. DATA COLLECTION 19

E. KNEE SPECIMENS 20
1. Specimen Preparation 20

III. ANALYSIS 23

A. SMOOTHING DATA 23

B. COORDINATE SYSTEMS 23
1. Pretesting Alignment 23

C. MEASUREMENT OF KNEE MOTION 24

D. DEVELOPMENT OF ROTATION MATRICES 30
1. Tibial or Femoral to Inertial Coordinate System 30
2. Femoral to Tibial Coordinate System 34

E. INSTANTANEOUS AXIS OF ROTATION 35
1. Development of the Instantaneous Axis of Rotation 35
2. Calculation of the Differential Rotation Vector 40
3. Alternate Derivation of the Differential Rotation Vector 41

F. KINEMATIC DEGREES OF FREEDOM AND CONSTRAINT .. 42

G. LOCATION OF THE INSTANTANEOUS AXIS OF ROTATION WITHIN THE KNEE 46

H. FLEXION, VARUS-VALGUS, AND INTERNAL-EXTERNAL ROTATION 47

I. USE OF THE INSTANTANEOUS AXIS OF ROTATION FOR COMPUTER MODELING 49

IV. ACCURACY 51

V. RESULTS 53

A. SUMMARY OF FIGURES 54

B. ACL INTACT CONDITION 55

C. ACL DEFICIENT CONDITION 63

VI. CONCLUSIONS 103

VII. RECOMMENDATIONS 107

APPENDIX. ALTERNATIVE DERIVATIONS OF THE INSTANTANEOUS ANGULAR VELOCITY VECTOR 109

A. ANGULAR VELOCITY VECTOR CALCULATED UTILIZING DIFFERENTIAL EULER ANGLE DATA 109

B. ANGULAR VELOCITY VECTOR CALCULATED UTILIZING THE TIME DERIVATIVE OF THE TRANSFORMATION MATRIX 110

GLOSSARY OF MEDICAL TERMS 113

GLOSSARY OF ENGINEERING TERMS 115

LIST OF REFERENCES 117

INITIAL DISTRIBUTION LIST 119

I. INTRODUCTION

Impaired knee function, due to either injury or degenerative joint disease, occurs among people of all ages. Reconstructive surgical procedures range from ligament repair to total knee replacement. Regardless of the procedure, its effectiveness will depend on how closely the surgeon is able to restore motion characteristics of the original, uninjured or healthy knee. The instantaneous axis of rotation of the knee joint is one of the most significant parameters quantifying these motion characteristics. From a continuous time history of this axis, other clinically significant motion parameters can be calculated.

The instantaneous axis of rotation of the human knee joint is also important to the understanding of the muscle and load reaction forces within the knee. For any rigid body in motion, the forces and moments acting on that rigid body can be resolved into a force directed along the instantaneous axis of rotation and a moment acting about this axis. Accurate determination of the location of the instantaneous axis within the knee is necessary if forces in ligaments and tendons and contact forces between bones are to be predicted. Knowledge of these forces is useful to properly evaluate ligament repair and replacement techniques.

Finally, an accurate representation of the instantaneous axis of rotation of the knee would be invaluable to designers of total knee replacement components and external orthoses (braces) to correct congenital defects. The instantaneous axis of rotation gives such designers a benchmark for reproducing the normal internal kinematics of a knee [Ref. 1].

The role of the anterior cruciate ligament (ACL) and the posterior cruciate ligament (PCL) in normal knee function is not completely understood. Early theories postulated that the ACL, PCL, and the articulating surfaces of the femur and tibia acted as a four bar linkage with no significant deformation of the ligaments and the motion of the knee was constrained to the sagital plane [Ref. 2]. However, the attachment sites of the cruciate ligaments do not lie within the sagital plane and they possess complex nonlinear viscoelastic properties [Refs. 3, 4, and 5]. Therefore, the actual motion of the femur with respect to the tibia is three dimensional with a continually moving instantaneous axis of rotation. Until the past 3 decades, the planar four bar linkage model was the accepted standard for developing the "instant center" of rotation. The term "instant center" only applies to two dimensional motion, for the more general three dimensional case the concept of an "instantaneous axis" must be applied.

Recent experimental work has focused on quantifying the true three dimensional motion of the knee. A variety of experimental procedures and equipments have been used. Previously reported studies conducted by Kurosawa *et al.* [Ref. 1], Blankevoort *et al.* [Refs. 6,7], and Essinger *et al.* [Ref. 8] developed axes of rotation for the human knee using discrete motion data to approximate continuous motion. In these and similar studies the discrete motion data is recorded using finite rotation steps up to 20° per step. Knee motion was stopped at each flexion step to record data.

In the study performed by Kurosawa, *et al.*, the tibia was fixed and a single load weight was cantilevered off the posterior side of the proximal end of the femur. The load was connected to the quadriceps tendon just above the patella. The flexion angle was

controlled by adjusting the length of the cable attaching the load weight to the quadriceps tendon. For each 15 degree flexion step, radiographs were taken and the motion of the lateral and medial femoral condyle centers were analyzed from flexion step to flexion step to generate the axis of rotation.

The mathematical model of the knee joint developed by Essinger, *et al.* is based on data collected with an experimental setup identical to that used by Kurosawa. They did not report development of any kind of rotation axis, however they did report internal/external tibia rotation and varus/valgus rotational component values that were predicted by their model. These rotational components are directly related to the location and direction of the instantaneous axis of rotation, as will be demonstrated later.

Blankevoort, *et al.*, used a more complex experimental setup. The knee was loaded and flexed by a complicated arrangement of linkages allowing six degrees of freedom between the tibia and the femur. The knee was flexed in prescribed steps varying from 5 to 30 degrees per step. Radiographs were taken at each flexion step and the axis of rotation was developed using stereophotogrammetry. To provide landmarks, small tantalum pellets were fixed to the bone surface prior to testing.

The flexed knee stance rig, or "Oxford rig", used by Bourne and Biden [Ref. 9] closely approximates physiologic loading of the knee joint, however, this is still a static device where knee motion is stopped to record data.

The axis of rotation developed using such analyses will, in general, differ from the instantaneous axis of rotation because of the path dependent nature of rigid body rotation. If the instantaneous axis of rotation of any joint is not fixed within the joint, but rather, is

free to move, significant error can exist between the direction and placement of a rotation axis calculated using large rotation steps and the actual instantaneous axis of rotation. This difference may introduce errors such that any axis of rotation calculated with large finite rotation steps cannot be used to accurately predict ligament forces during knee flexion or extension.

A finite, rigid body rotation does not satisfy the parallelogram law of vector addition and as such is not a true vector quantity. To illustrate, consider a finite rigid body rotation through an arbitrary angle around an axis oriented in an arbitrary direction. If this rotation were a vector quantity it could be decomposed into its components along each of the coordinate axes. The total rotation could be viewed as a series of rotations, each around a separate coordinate axis. The total rotation would be the rotation about the x axis, followed by rotation about the y axis, and finally rotation about the z axis. Furthermore, if the parallelogram law of vector addition were valid, the order of the rotation would be immaterial, with the rotation order x-y-z being equivalent to z-y-x, etc. This is not the case. If the order of rotation is changed, the final configuration of the rigid body will be different. Therefore, finite rotation is path dependent and is not a vector.

However, an infinitesimal rotation is a vector quantity and is path independent [Ref. 10]. The instantaneous axis of rotation is the direction of an infinitesimal rotation vector. If calculated using any value of finite rotation, the resulting axis is only an approximation of the instantaneous axis of rotation. The smaller the finite rotation step, the more accurate will be the approximation.

Figures 1 and 2 give a two dimensional illustration of the effect of rotation step size on the location of the axis of rotation. For both Figures 1 and 2, the total rigid body motion from orientation A to orientation B follows the same trajectory. Figure 2 contains an intermediate step A' along the trajectory from A to B. It can be clearly seen that a difference in rotation step size can significantly change the location of the center of rotation. As the rotation step size decreases, the axis of rotation approximates the instantaneous center of rotation more closely.

The study performed by Hollister, *et al.*, was the only one identified where continuous motion data was analyzed to develop rotation axes for the knee [Ref. 11]. In this study time lapse photography was used to analyze the path described by light emitting diodes (LED) as the knee is flexed. A flexion-extension (FE) axis was identified using a mechanical axis finder. Once found, a hole was drilled along this axis and a pin was inserted. A camera was aligned along this axis and the LEDs were installed on a pin oriented along the tibial longitudinal rotation (LR) axis. The femur was fixed to a platform and the camera recorded time lapse photographs of the LEDs as the tibia was flexed on the femur. The paths described by the LEDs were then analyzed for concentricity to demonstrate the FE axis of rotation. This investigation effectively demonstrated the FE axis of rotation, however, it did not develop a true instantaneous axis of rotation since it did not take into account the internal/external tibia rotation that was occurring during joint flexion. The LEDs were mounted on the pin inserted along the LR axis, thereby negating any effects tibia rotation would have on the analysis. Also, the joint was not loaded during testing.

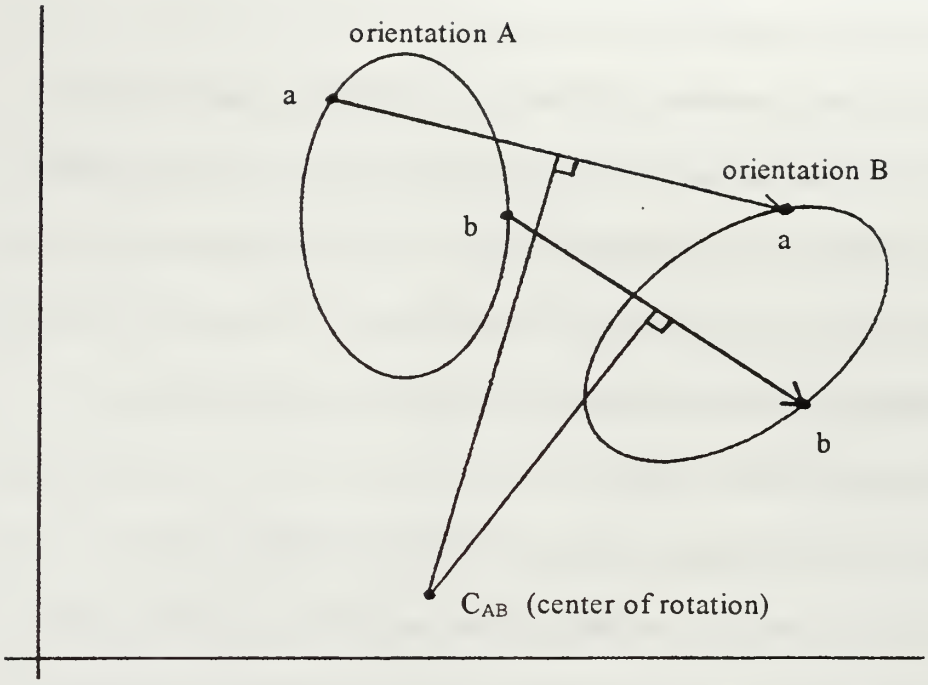


Figure 1: Center of rotation for two dimensional rigid body motion from orientation A to orientation B

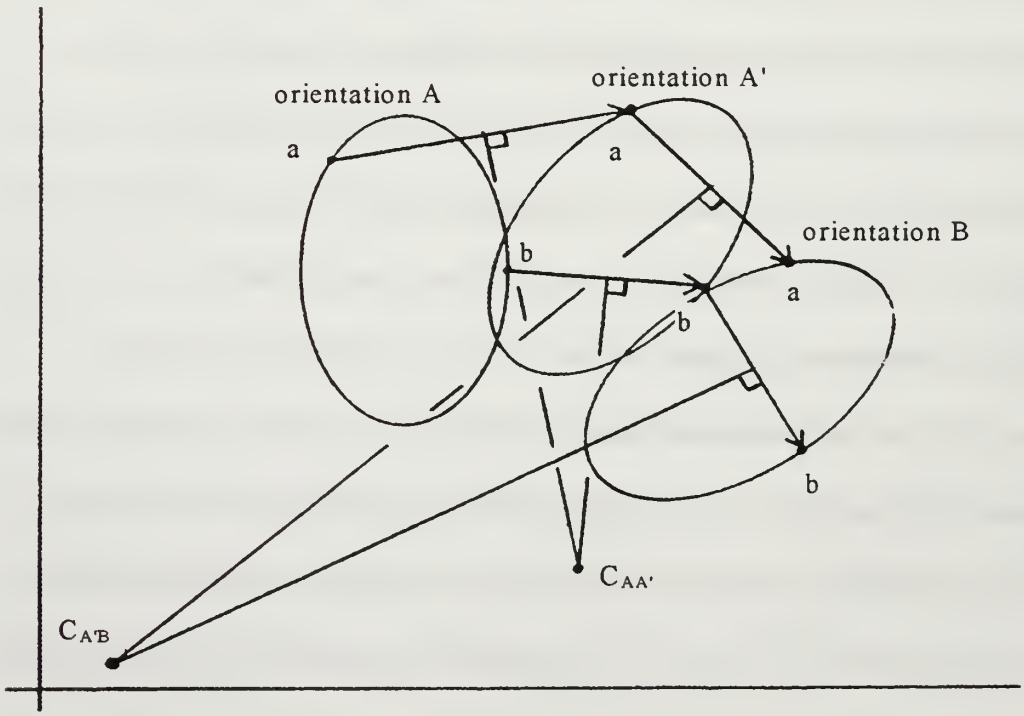


Figure 2: Centers of rotation for two dimensional rigid body motion from orientation A to orientation B with an intermediate orientation A'

The motion analysis developed in this thesis is based on rotation data collected at a 15 Hz sample frequency during continuous motion. The measurement apparatus allows variable loading, up to approximately physiologic conditions, and allows high frequency motion recording during flexion and extension. Higher data collection frequencies are possible, although not necessary for the flexion speed of the measuring device. The maximum differential rotation between data points is no larger than 0.3 degrees, sufficiently small for an accurate approximation of the instantaneous axis of rotation. The result is an analysis that may be used to directly calculate the magnitude of a particular joint's internal/external tibial rotation and varus/valgus rotation throughout the entire range of flexion.

The continuous motion measurement apparatus was used to investigate the motion characteristics of four cadaveric knees. The objective was to identify common motion characteristics between different specimens and correlate these characteristics to externally identifiable landmarks. Figures 3 and 4 provide details of the anatomy of the knee joint, showing the anatomic features referred to in this study.

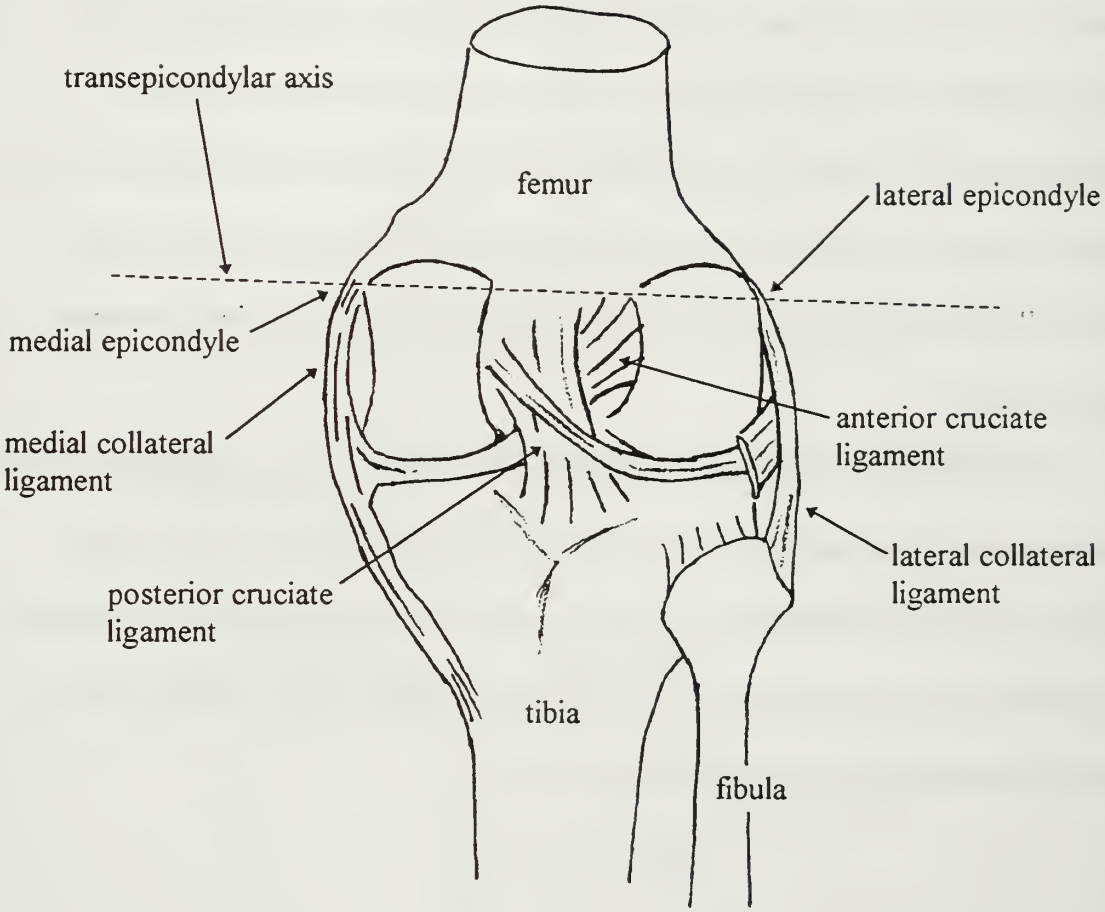


Figure 3: Posterior view of a typical knee [Ref. 12]

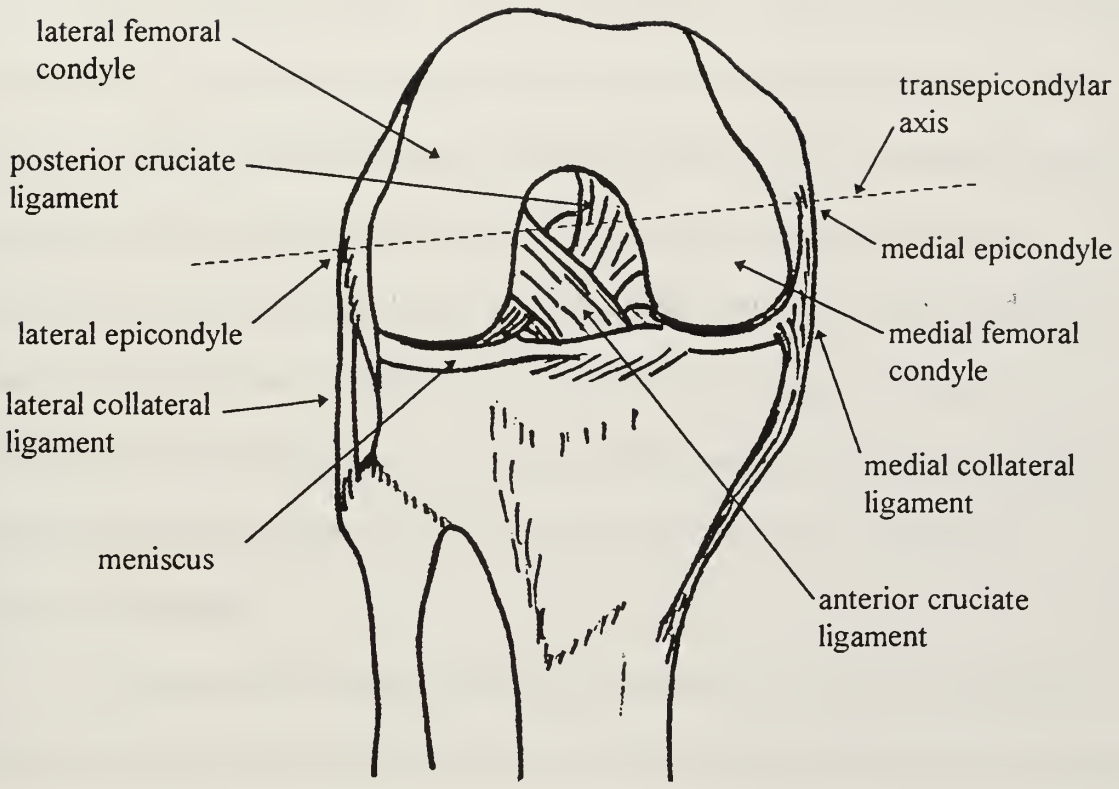


Figure 4: Anterior view of a typical knee in flexion [Ref. 12].

II. METHODS AND MATERIALS

A. BACKGROUND

The accuracy of kinematic analysis improves as the data analyzed more closely approximates continuous motion. Continuous analog data is, however, difficult to collect and analyze. Discrete motion data, if collected at a high enough sample frequency, can closely approximate continuous data. By measuring motion with a computerized analog to digital collection scheme, data can be collected without interrupting knee motion. Curves are then fit to the data to allow numerical differentiation, whereby the rigid body motion of both the femur and the tibia can be completely described. In addition, uninterrupted knee motion improves accuracy while measuring small translations and rotations by minimizing any hysteresis effects caused by the motion sensors and mechanical linkages.

Load simulating the main muscle groups involved in knee motion was applied to the vector sum points for the muscle groups and directed along the long axes of the femur and tibia. The proximal end of the femur and the distal end of the tibia were constrained to translate with one degree of freedom, closely approximating physiologic conditions encountered during squatting or sitting. The knee is flexed (or extended) while measuring Eulerian rotations of the tibia and the femur in the inertial frame. Translation of the femur is measured in the body fixed tibial frame with three degrees of freedom.

The instantaneous angular velocity vector is an important parameter characterizing rigid body motion. This vector, along with translation data for any point fixed with

respect to a rigid body, completely describes the motion of that body. An infinitesimal rotation of a rigid body can be treated as a vector quantity [Ref. 10] and the differential rotation vector that results differs from the instantaneous angular velocity vector only in scalar magnitude. The discrete motion data collected at 15 Hz can be used to calculate approximations to the differential translation and rotation vectors of the femur and the tibia. Knowledge of the differential rotation and translation allows the calculation of an instantaneous axis of rotation for the knee joint.

B. OVERVIEW

Data was recorded for four cadaveric knees. Each knee was measured with an apparatus capable of measuring six degrees of freedom for the femur, three relative translations with respect to the tibia and three rotations, and three rotational degrees of freedom for the tibia. As each knee was flexed or extended, eleven channels of data were recorded at a 15 Hz sample rate per channel through the entire range of motion from 0 to 110 degrees of flexion. The eleven data channels consisted of six rotations, three for the tibia and three for the femur, and five translations, lateral and medial anterior-posterior (A-P) translation, lateral and medial side distraction-compression (D-C) translation, and lateral side lateral-medial (L-M) translation. This provided high frequency continuous motion data for the knee, sufficient to fully describe the rotation and translation of the femur with respect to the tibia or both the femur and tibia with respect to the inertial frame.

C. MEASUREMENT APPARATUS

The measurement apparatus consists of a rigid frame with a fixed horizontal plate and a moving horizontal plate (Figure 5). The moving horizontal plate is driven up or down vertically at 3.175 mm/sec by a threaded leadscrew driven by a constant speed electric motor (Velmex Unislide model B4018P40J).

1. Rotation Measurement

An arrangement of three rotational linear variable potentiometers (Maurey Instrument 87-P82-103) (Figure 6) is anchored to the fixed horizontal plate, serving as the attachment point for the distal end of the tibia. A similar arrangement is anchored to the moving horizontal plate, serving as the attachment point for the proximal end of the femur.

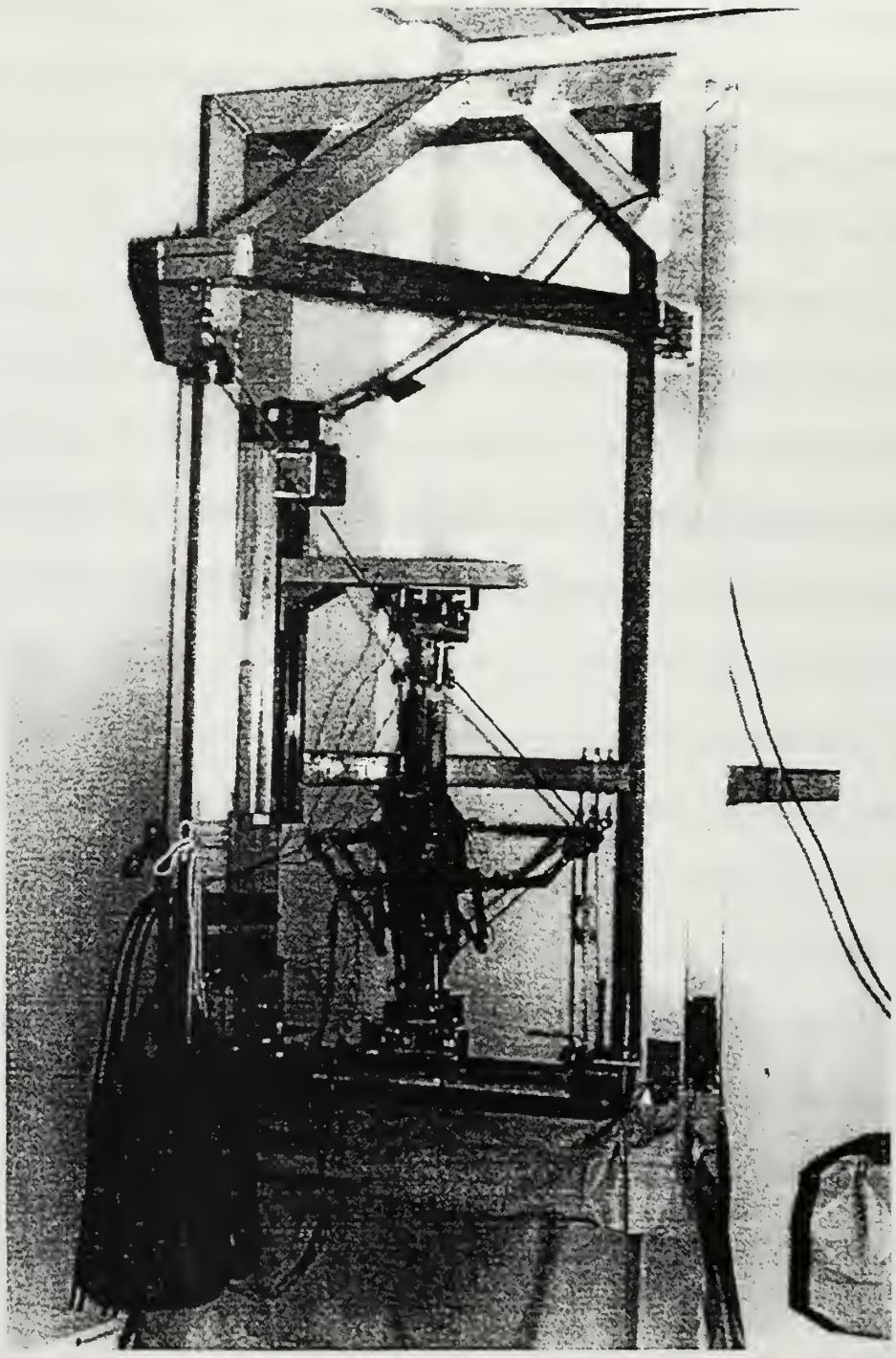


Figure 5: Knee motion measurement device

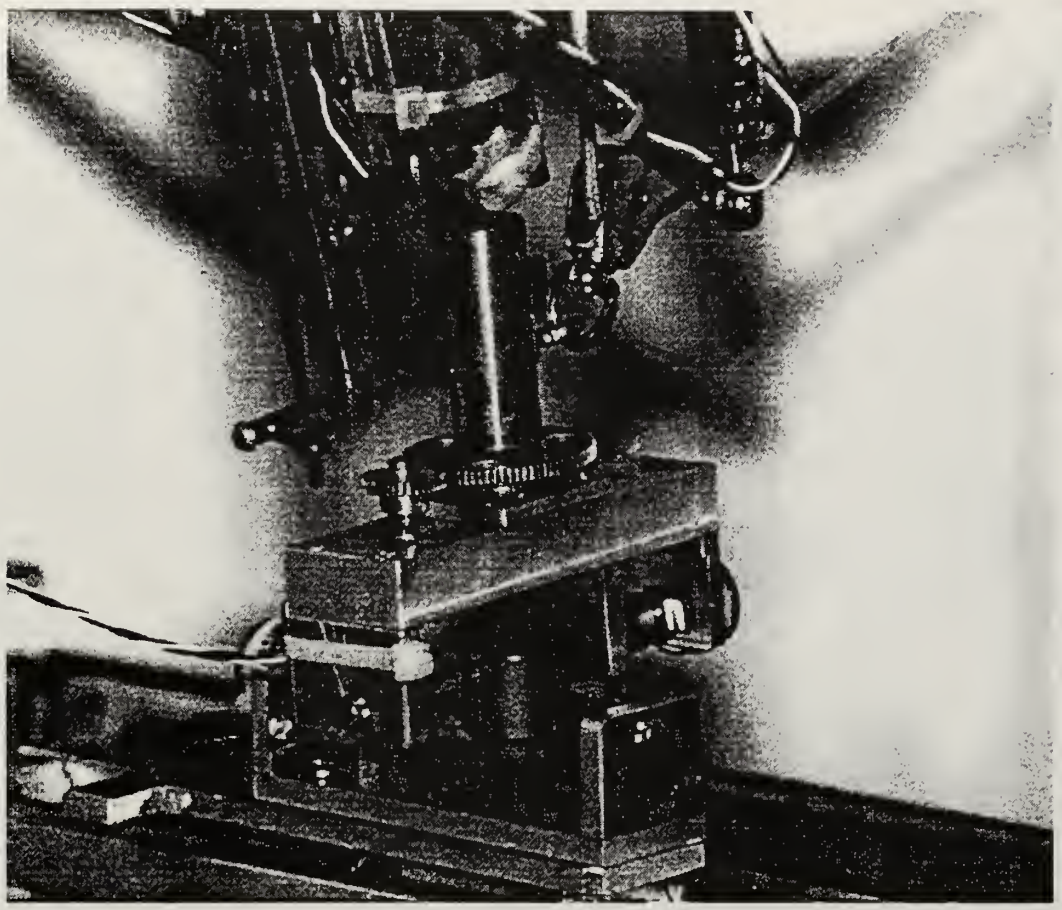


Figure 6: Details of rotary sensor array

The axes of these sensors intersect at a common point and they measure the Eulerian angles of rotation of the femur and the tibia with respect to the inertial frame. This particular sequence of rotation is also sometimes referred to as Bryant angles of rotation [Ref. 13].

2. Translation Measurement

An orthogonal arrangement of translation sensors (Maurey Instrument P2080-2-103) is fixed to the tibia approximately midway between the tibial plateau and the distal end (Figure 7). Each femur was through drilled and a pin inserted along the transepicondylar axis defined by the lateral and medial epicondyles[1]. The translation sensors are attached to these pins at the femur surface. These sensors form an orthogonal coordinate system that is body fixed in the tibia, moving with the tibia as the knee is flexed. The lateral side translation sensors measure the A-P, C-D, and L-M translation of the lateral side of the femoral epicondyle with respect to the moving, body fixed, tibial coordinate system. The two other sensors measure the A-P and C-D translation of the medial epicondyle. Since the length of the transepicondylar axis (femur width) is invariant during coordinate transformations, the L-M translation of the medial epicondyle can be calculated using the measured A-P and C-D translation of the medial epicondyle. L-M translation is defined positive for lateral to medial translation of the femur with respect to the tibia. A-P translation is defined positive for posterior to anterior translation of the femur with respect to the tibia. C-D translation is defined positive for distraction translation of the femur with respect to the tibia.

[1] Any reference to lateral or medial refers to the equipment setup for a left knee. Only left knees were tested in this study.

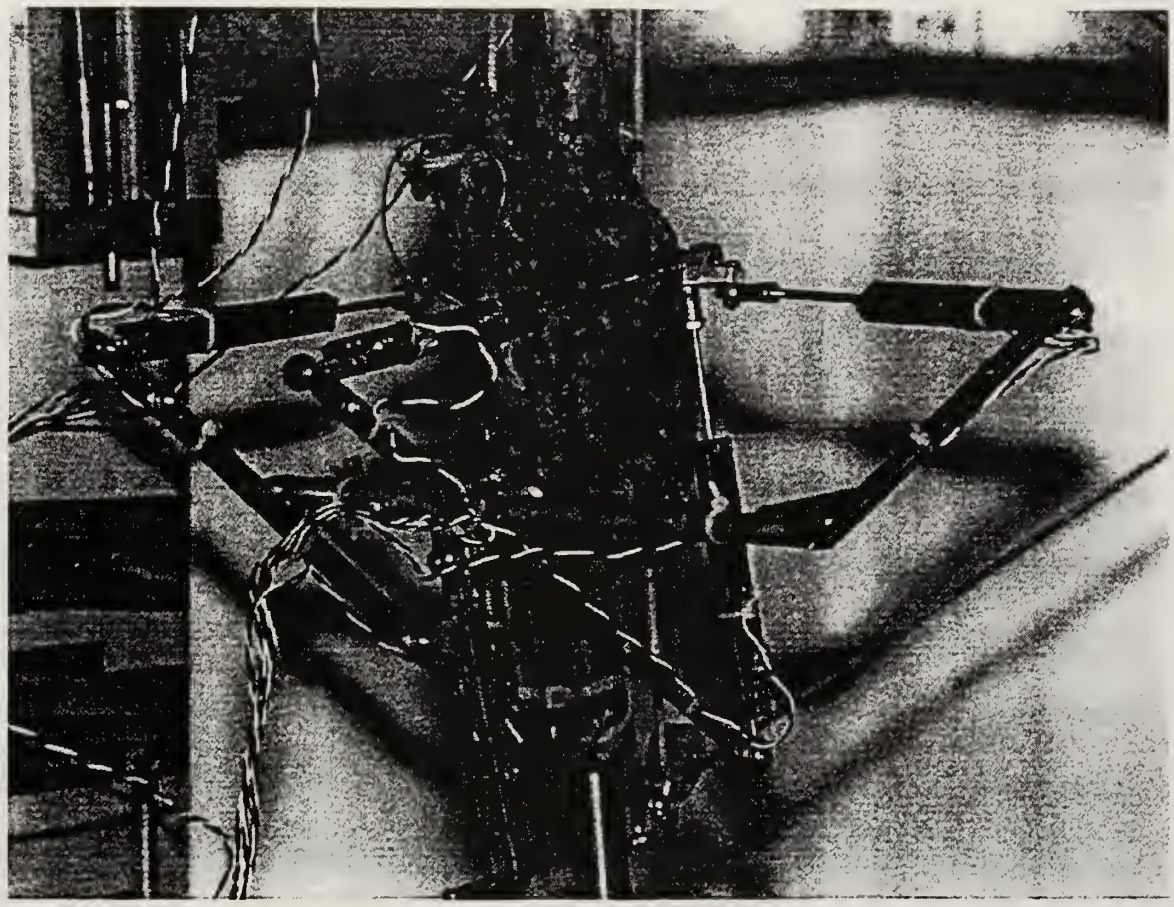


Figure 7: Details of translation sensor array

3. Simulated Muscle Loading

To simulate muscle loading, eye bolts are installed directly into the tibia and femur at the vector sum points for the gastrocnemius, hamstring, and quadriceps muscle groups. Eye bolts are used to achieve single, reproducible, muscle forces while eliminating error induced by clamp slippage. Bony anatomic landmarks are used to place the eye bolts, improving consistency between specimens. The quadriceps extension force is applied to the bony prominence on the tibial tubercle. The hamstring force is applied to a point halfway between the semimembranosus and biceps tendons, roughly corresponding to the inferior apex of the popliteal fossa. The gastrocnemius force is applied to a point midway between the two gastrocnemius heads, roughly corresponding to the superior apex of the popliteal fossa [Ref. 14]. Weights are attached to these eye bolts by means of nylon traction cord or steel cable (depending on load) directed along the axis of the long bones. For this particular study, the quadriceps load was simulated with a 40 lbf weight, the hamstring load was simulated with a 20 lbf weight, and the gastrocnemius load was simulated with a 20 lbf weight. These loads are double the 20/10/10 pound loads applied during a previous study conducted with this same measuring device [Ref. 14]. Only flexion data was recorded because during extension unknown distraction loads could possibly be induced by the worm drive and the loading configuration of the knee.

At the beginning of flexion, all internal and external forces and moments are in equilibrium. The simulated muscle forces remain constant throughout the flexion cycle. The knee flexes when the threaded leadscrew translates the moving horizontal plate downward.

D. DATA COLLECTION

The output of the translation and rotation sensors is sampled and recorded with a 15 Hz sample rate per channel. Because the data is recorded during continuous motion of the knee it includes the effects of kinetic friction at the knee joint. If the knee were stopped at intervals to record data the motion measurements would be affected by static friction which would not be present during knee motion. The magnitude of static friction can be greater than the magnitude of kinetic friction. Also, discontinuous data collection is subject to error induced by the viscoelastic nature of soft tissue. Stopping to collect data will subject the measurements to error caused by time dependent deformation (creep). The high sample rate of 15 Hz also ensures the recorded data closely approximates continuous motion data, allowing the calculation of angular rotation vectors necessary for the kinematic analysis.

Three data runs of flexion were recorded for each knee with the ACL intact. Approximately 1500 data points per channel were recorded and displayed in an 11 column ASCII format (six rotations, five translations). All three data runs per knee were recorded in immediate sequence with no adjustments made to the knee mounting between runs. This was necessary to ensure the data for each run was recorded from the same starting position on the rotary and linear sensors. The data runs for each knee were compared between runs to observe consistent motion characteristics to verify reliable equipment operation.

Immediately following the data runs with ACL intact, the ACL was severed and three data runs of flexion were recorded. The knees were not removed from the motion

measuring device between the ACL intact and the ACL severed runs. This ensured the knees had the same alignment relative to the motion measuring device frame and rotational sensors. Therefore, any changes in the knee motion characteristics could be readily observed and not masked by alignment inaccuracies.

E. KNEE SPECIMENS

1. Specimen Preparation

Four left human knee specimens were used to conduct the research. Each knee was verified to have a normal, intact PCL, ACL, and menisci. The specimens were prepared by removing tissue leaving the quadriceps mechanism, cruciate ligaments, and capsule intact. Following this initial preparation each knee was maintained frozen at 258 Kelvin until immediately prior to testing. Each knee was fitted with a 10 mm diameter steel rod cemented into the medullary canal of both the tibia and the femur. The rod length was sized to ensure each knee maintained approximately the same range of motion for flexion and extension. Eye bolts were inserted into the bones at the vector sum points for the muscle groups. A pin was inserted in a drilled hole along the transepicondylar axis defined by the LCL and MCL femoral insertion sites. This pin served as the attachment point for the femoral translation sensors. This group of knee specimens had been used for a previous test using lighter muscle force loads [Ref. 14] and the preparations described were performed prior to that test. In the interim between the previous testing and the current study the knees were kept frozen at 258 degrees Kelvin.

After thawing, each knee was mounted in the measurement apparatus. The rods that had been cemented into the tibia and femur medullary canals were inserted into

sockets attached to the rotation sensors and the muscle force simulation weights attached (Figure 8).

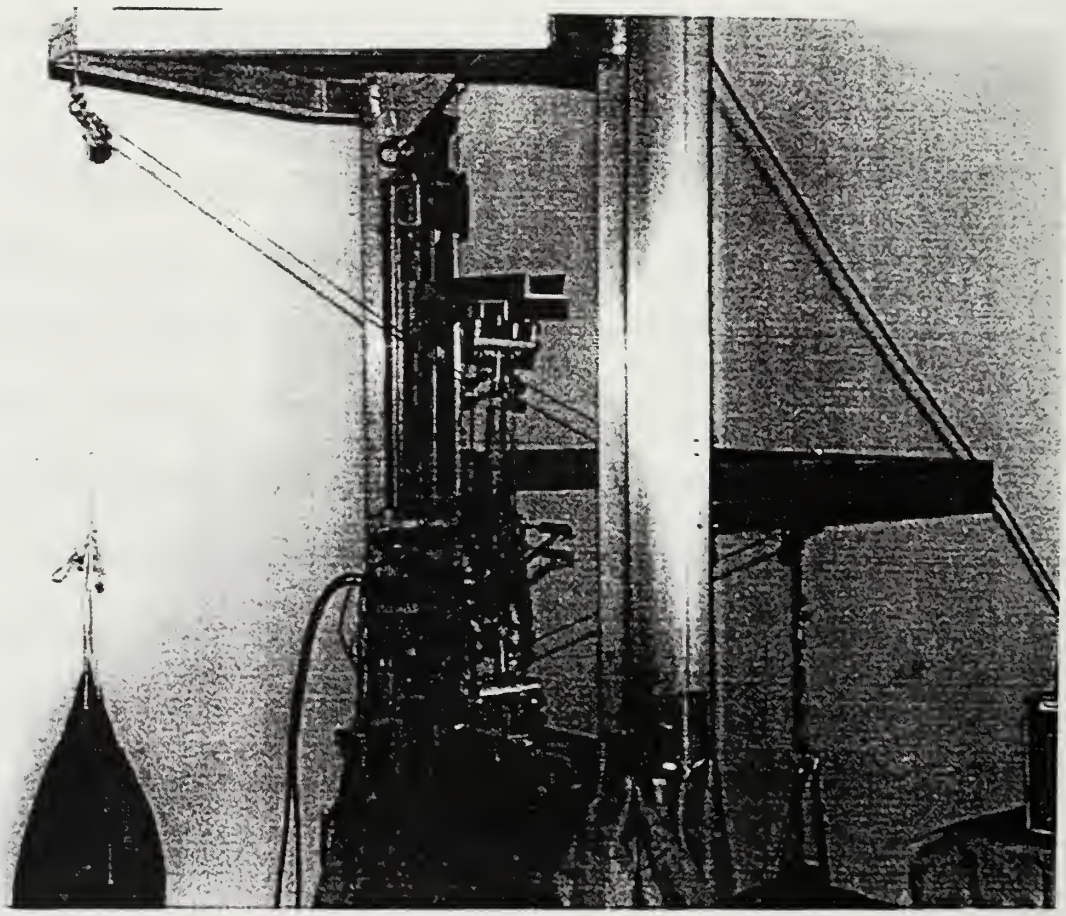


Figure 8: Arrangement of loading weights

III. ANALYSIS

A. SMOOTHING DATA

Prior to any analysis the raw data collected was smoothed by performing a 9^{th} order polynomial fit. A 9^{th} order polynomial was chosen because it gave the best fit to the data with the minimum least square error. This provided smooth data values to improve the accuracy of the numerical differentiation required to calculate differential rotation and angular and linear velocities.

B. COORDINATE SYSTEMS

Three separate coordinate systems are utilized by the measuring apparatus. The first is an inertial reference system, denoted X, Y, Z, fixed to the measuring device frame. The second is a body fixed system, denoted x_f, y_f, z_f, fixed to the femur and free to translate and rotate along with the femur. The third is a body fixed system, denoted x_t, y_t, z_t, fixed to the tibia and free to translate and rotate along with the tibia. The x_t and x_f axes correspond to the L-M axis of the tibia and femur respectively. The y_t and y_f axes correspond to the A-P axis of the tibia and femur respectively. The z_t and z_f axes are parallel to the longitudinal axis of the tibia and femur respectively.

1. Pretesting Alignment

Prior to collecting any data the rotational sensor arrays are aligned by placing a rigid rod in the knee mounting sockets. The sensor arrays are then adjusted until they are congruent. Once this is accomplished, data is recorded from the stationary rotation

sensors and this becomes the zero rotation reference against which data is compared during knee flexion and extension.

Once a knee is installed, and prior to any motion, the origins of the two body-fixed femoral and tibial coordinate systems coincide and are located at the common attachment point of the three orthogonal translation sensors on the lateral side of the transepicondylar axis (Figures 9 and 10). Their initial rotational configuration will depend on the initial rotational configuration of the bones to which they are attached. The origin of the inertial coordinate system may be placed at any convenient point.

C. MEASUREMENT OF KNEE MOTION

The raw rotational data collected from the six degree of freedom measuring apparatus consists of Euler angles of rotation of both the tibia and femur with respect to the inertial frame. The construction of the measuring apparatus dictates the order in which the rotations are accomplished (Figure 11). Rotation about the x axis occurs first resulting in the x',y',z' coordinate system. Rotation about the y' axis occurs next resulting in the x'',y'',z'' coordinate system. Finally, rotation occurs about the z'' axis resulting in the x''',y''',z''' coordinate system which is the final position of the rotated tibia or femur (Figure 12).

The Euler angles measured by the apparatus cannot be used to directly transform the tibial and femoral surfaces during knee flexion and extension. Transformation matrices must be developed for both the tibia and the femur using the Euler angles. These transformation matrices map coordinates in either the femoral or tibial system to the inertial reference system. These transformation matrices may also be combined to map

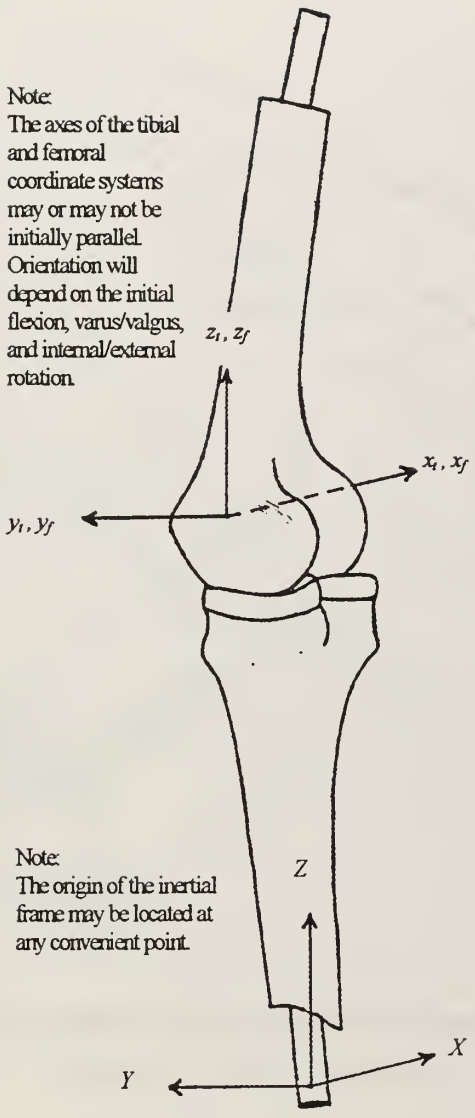


Figure 9: Body-fixed and inertial coordinate systems, knee fully extended

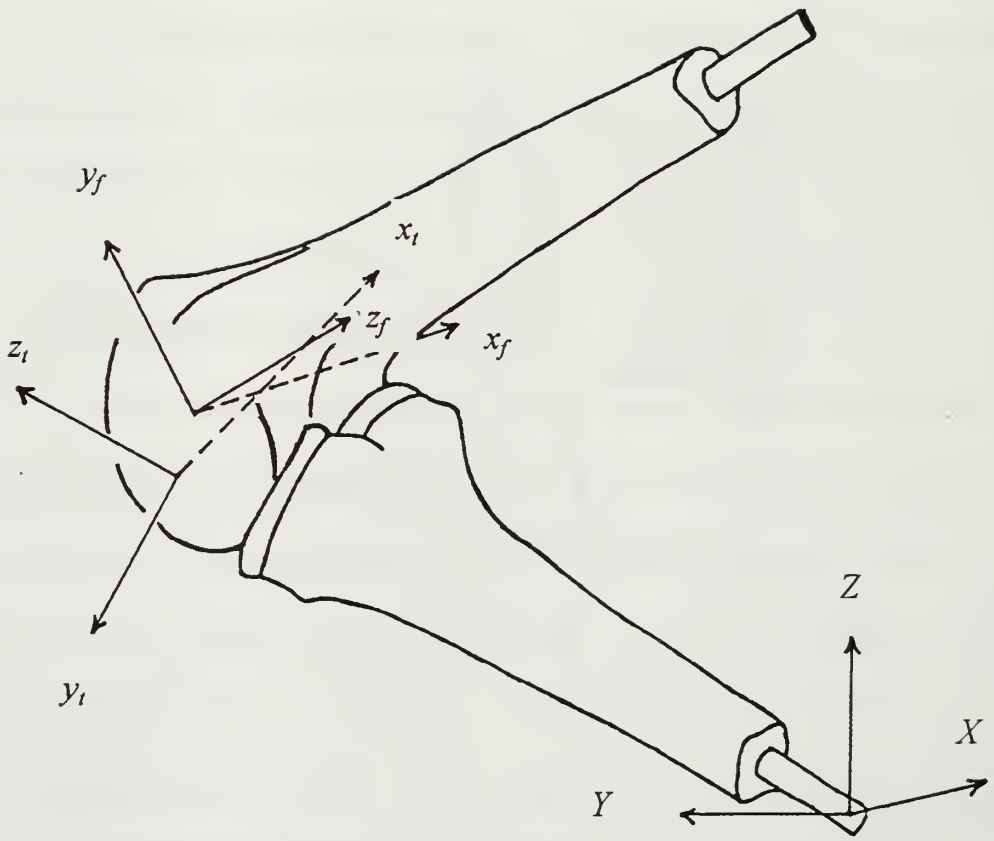


Figure 10: Body-fixed and inertial coordinate systems, knee fully flexed

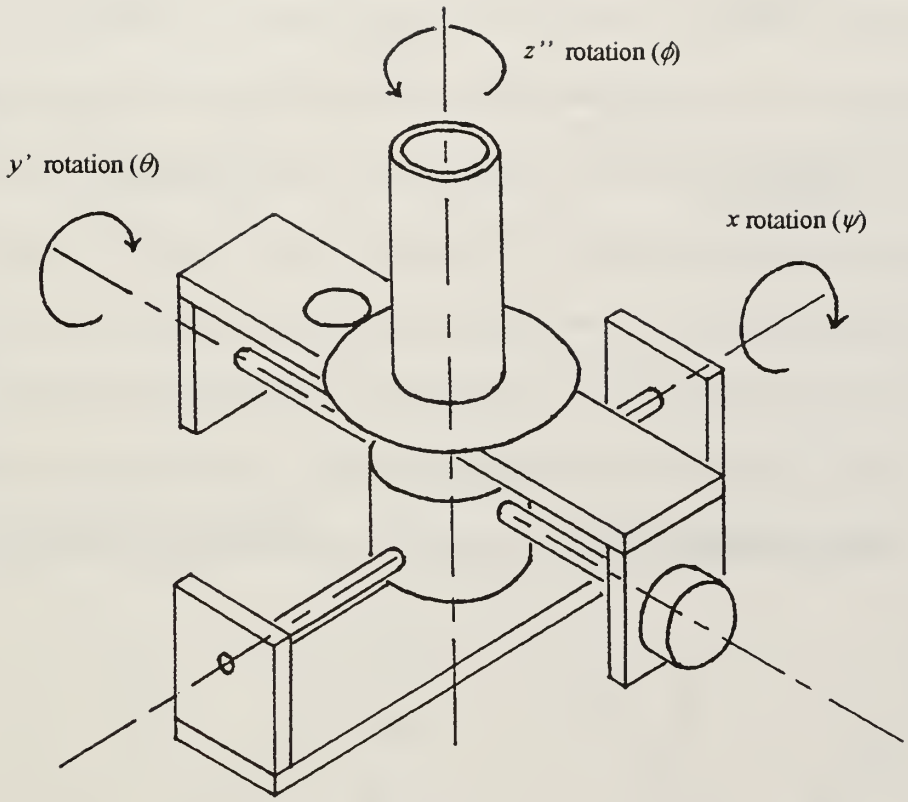


Figure 11: Rotary sensor array

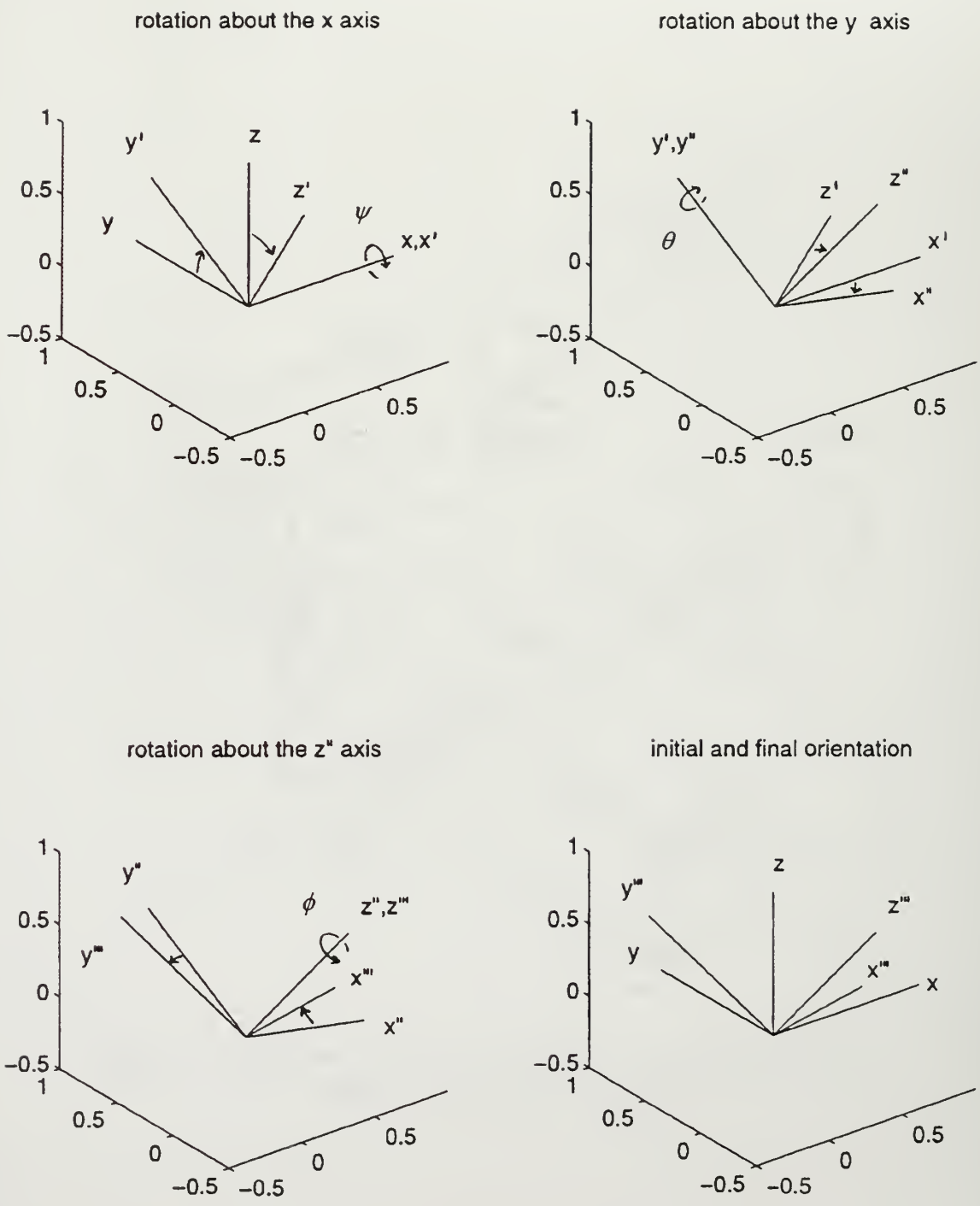


Figure 12: Successive Euler rotations

coordinates from the femoral system directly into the tibial system, or vice versa. This overall transformation from the femoral system to the tibial system is desired in order to describe the motion of the femur with respect to the tibia.

The variable end of the translation sensors are attached to the origin of the femoral coordinate system at the lateral end of the transepicondylar axis. This arrangement results in the direct measurement of femoral coordinate system translation components in the tibial coordinate system. It is not necessary to transform the measured translation because it is measured directly in the tibial coordinate system throughout the range of knee motion. The measured translation, together with the overall rotation matrix between the femur and tibia, define the rigid body motion (translation and rotation) of the femur with respect to the tibia. This allows the vector components of the femur surface to be mapped into the tibial coordinate system as the femur moves relative to the tibia while the knee is flexed or extended. The overall result is a model that will describe any motion of the femur with respect to the tibia using the parameters measured by the measuring apparatus.

D. DEVELOPMENT OF ROTATION MATRICES

1. Tibial or Femoral to Inertial Coordinate System

Each of the three coordinate systems, inertial, tibial, and femoral, utilized by the measurement apparatus is a right handed Cartesian coordinate system. To develop the rotation matrices for these systems in terms of Euler angles we consider three successive rotations, each about a separate axis. The angles of rotation about these axes are the actual parameters measured by the rotation sensors of the measurement apparatus. In the development of the rotation matrices a right hand rotation will be assumed to be positive. Rotation matrices will be developed such that they map local coordinates (primed) into the global (unprimed) coordinate system by the relation

$$\{s\} = [A]\{s'\} \tag{1}$$

where $\{s\}$ is a vector in the inertial (global) system and $\{s'\}$ is a vector in the body fixed (local) system. The sequence of rotation matrix development will be rotation about the x axis followed by rotation about the y' axis followed by rotation about the z'' axis. This order is consistent with the order of rotation imposed by the construction of the measuring apparatus.

First, consider rotation about the x axis (Figure 13). The angle of rotation is denoted by ψ. The coordinate transformation is accomplished by the following matrix equation:

$$\begin{Bmatrix} x \\ y \\ z \end{Bmatrix} = \begin{bmatrix} 1 & 0 & 0 \\ 0 & \cos(\psi) & -\sin(\psi) \\ 0 & \sin(\psi) & \cos(\psi) \end{bmatrix} \begin{Bmatrix} x' \\ y' \\ z' \end{Bmatrix} \tag{2}$$

$$\{s\} = [\Psi]\{s'\} \tag{3}$$

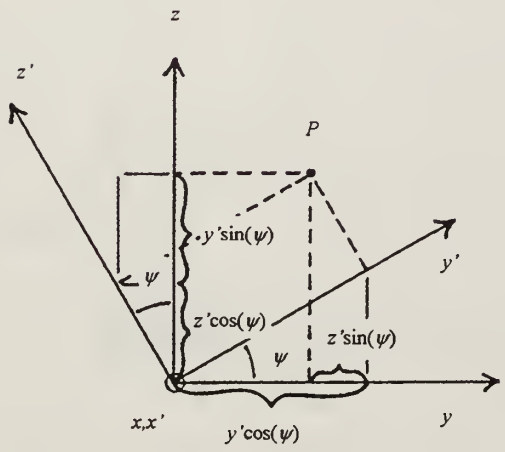


Figure 13: Rotation about the x axis

Next consider rotation about the y' axis (Figure 14). The angle of rotation is denoted by θ. The coordinate transformation is accomplished by the following matrix equation:

$$\begin{Bmatrix} x' \\ y' \\ z' \end{Bmatrix} = \begin{bmatrix} \cos(\theta) & 0 & \sin(\theta) \\ 0 & 1 & 0 \\ -\sin(\theta) & 0 & \cos(\theta) \end{bmatrix} \begin{Bmatrix} x'' \\ y'' \\ z'' \end{Bmatrix} \tag{4}$$

$$\{s'\} = [\Theta]\{s''\} \tag{5}$$

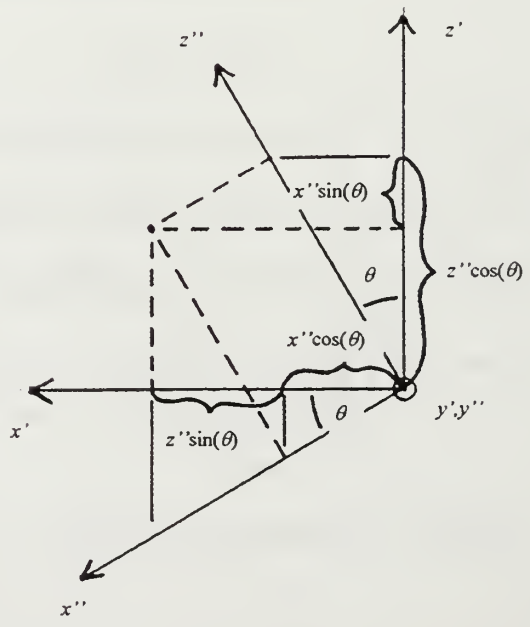


Figure 14: Rotation about the y' axis

Finally, consider rotation about the z'' axis (Figure 15). The angle of rotation is denoted by ϕ. The coordinate transformation is accomplished by the following matrix equation:

$$\begin{Bmatrix} x'' \\ y'' \\ z'' \end{Bmatrix} = \begin{bmatrix} \cos(\phi) & -\sin(\phi) & 0 \\ \sin(\phi) & \cos(\phi) & 0 \\ 0 & 0 & 1 \end{bmatrix} \begin{Bmatrix} x''' \\ y''' \\ z''' \end{Bmatrix} \tag{6}$$

$$\{s''\} = [\Phi]\{s'''\} \tag{7}$$

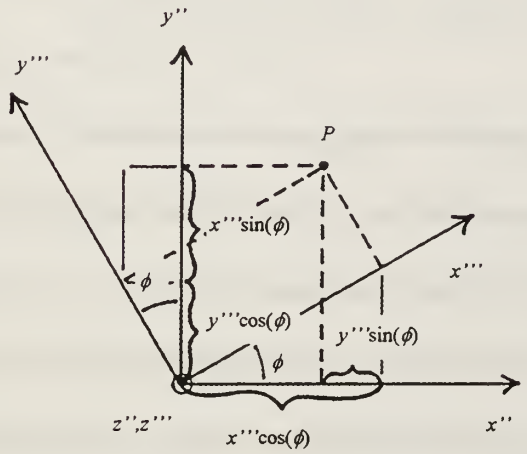


Figure 15: Rotation about the z'' axis

To develop the rotation matrix, the individual rotation matrices are applied in the correct order to transform the local coordinates of the rotated vector back to the global coordinate system.

$$\{s\} = [\Psi][\Theta][\Phi]\{s'''\} \tag{8}$$

The rotation matrix, $[T_f]$ or $[T_t]$, is given by

$$[T_{f,t}] = [\Psi_{f,t}][\Theta_{f,t}][\Phi_{f,t}] \tag{9}$$

or by carrying out the matrix multiplication:

$$[T_{f,t}] = \begin{bmatrix} \cos(\theta_{f,t})\cos(\phi_{f,t}) & -\cos(\theta_{f,t})\sin(\phi_{f,t}) & \sin(\theta_{f,t}) \\ \cos(\psi_{f,t})\sin(\phi_{f,t}) + & \cos(\psi_{f,t})\cos(\phi_{f,t}) - & -\sin(\psi_{f,t})\cos(\theta_{f,t}) \\ \sin(\psi_{f,t})\sin(\theta_{f,t})\cos(\phi_{f,t}) & \sin(\psi_{f,t})\sin(\theta_{f,t})\sin(\phi_{f,t}) & \\ \sin(\psi_{f,t})\sin(\phi_{f,t}) - & \sin(\psi_{f,t})\cos(\phi_{f,t}) + & \cos(\psi_{f,t})\cos(\theta_{f,t}) \\ \cos(\psi_{f,t})\sin(\theta_{f,t})\cos(\phi_{f,t}) & \cos(\psi_{f,t})\sin(\theta_{f,t})\sin(\phi_{f,t}) & \end{bmatrix} \tag{10}$$

where $\psi_{f,t}$, $\theta_{f,t}$, and $\phi_{f,t}$ are the Euler angles of rotation of the femur or tibia measured by the measurement apparatus about the x, y', and z'' axes respectively.

2. Femoral to Tibial Coordinate System

To develop the overall rotation matrix from the tibial to the femoral coordinate system consider two separate transformations. The first applies the femoral rotation matrix, $[T_f]$, to transform a vector from the femoral coordinate system to the inertial coordinate system. The second applies the inverse[2] of the tibial rotation matrix, $[T_t]^T$, to transform the same vector from the inertial system to the tibial coordinate system. Therefore,

$$[T] = [T_t]^T[T_f] \tag{11}$$

[2] Rotation matrices are orthogonal. The inverse of an orthogonal matrix is the matrix transpose.

where T is the overall rotation matrix.

E. INSTANTANEOUS AXIS OF ROTATION

According to *Chasles' theorem,* the motion of any rigid body can be decomposed into a translation of a point in the body and a rotation about an axis through the same point [Ref. 15]. A refinement of this theorem is helical[3] or "screw" motion of a rigid body. This is motion decomposed into a rotation about an axis and a translation along the same axis. This is a three dimensional analog of the concept of a two dimensional "instant center" of rotation. If the direction of this axis is chosen to be the same as the direction of the body's instantaneous angular velocity vector, the velocity of any point fixed with respect to the body can be decomposed into a translational component along the axis, and a rotational component perpendicular to the axis.

1. Development of the Instantaneous Axis of Rotation

The direction of the angular velocity vector of a rigid body is the direction of the instantaneous axis of rotation of the rigid body. The angular velocity vector can be calculated in a straightforward manner from the data recorded by the motion measuring device. The relationship between the angular velocity of a rigid body (ω_ξ, ω_η, ω_ζ) expressed in an arbitrary orthogonal, body-fixed coordinate system (ξ, η, ζ) and the time rate of change of the body's Euler angles $\left(\dot{\psi},\ \dot{\theta},\ \dot{\phi}\right)$ is given by the following matrix expression [Ref. 13]:

[3] The terms "helical axis of rotation" and "instantaneous axis of rotation" are synonymous throughout this paper. The description "helical axis of rotation" will be used only when referring to references where this particular term was used.

$$\begin{Bmatrix} \omega_\xi \\ \omega_\eta \\ \omega_\varsigma \end{Bmatrix} = \begin{bmatrix} \cos(\theta)\cos(\phi) & \sin(\phi) & 0 \\ -\cos(\theta)\sin(\phi) & \cos(\phi) & 0 \\ \sin(\theta) & 0 & 1 \end{bmatrix} \begin{Bmatrix} \dot{\psi} \\ \dot{\theta} \\ \dot{\phi} \end{Bmatrix} \qquad (12)$$

The matrix contained in equation (12) is a function of the total Euler angles between the body fixed orthogonal coordinate system (ξ, η, ζ) and the inertial frame.

Although this calculation will determine the direction of the instantaneous axis of rotation, it does not indicate where this axis is to be located within the knee. This information can be obtained from the data recorded by the motion measuring device, but not as easily as the angular velocity vector alone. In order to explain how this is accomplished some key concepts should be reviewed.

Every point on a rigid body undergoing rotation will experience the same angular velocity. Therefore, angular velocity vector is a "free vector" and can be applied to any point on a rigid body. The motion of any other point on the rigid body can be fully described by the translation of the application point, the angular velocity vector applied at that point, and the vector from the application point to the point of interest. This concept is illustrated in Figures 16 and 17.

In Figure 16 the angular velocity vector is applied to point A. The motion of point B in the inertial frame can be described as the translation of point A in the inertial frame ($r_{AA'}$) plus the rotation of the vector from point A to point B as the rigid body is rotated through a finite angle (θ). Similarly, the angular rotation vector may also be applied to point B. Figure 17 illustrates how the motion of point A can be described by the translation of point B ($r_{BB'}$) in the inertial frame plus the rotation of the vector from point

B to point A as the rigid body is rotated through the same finite angle (θ). In both cases the motion of the rigid body is identical.

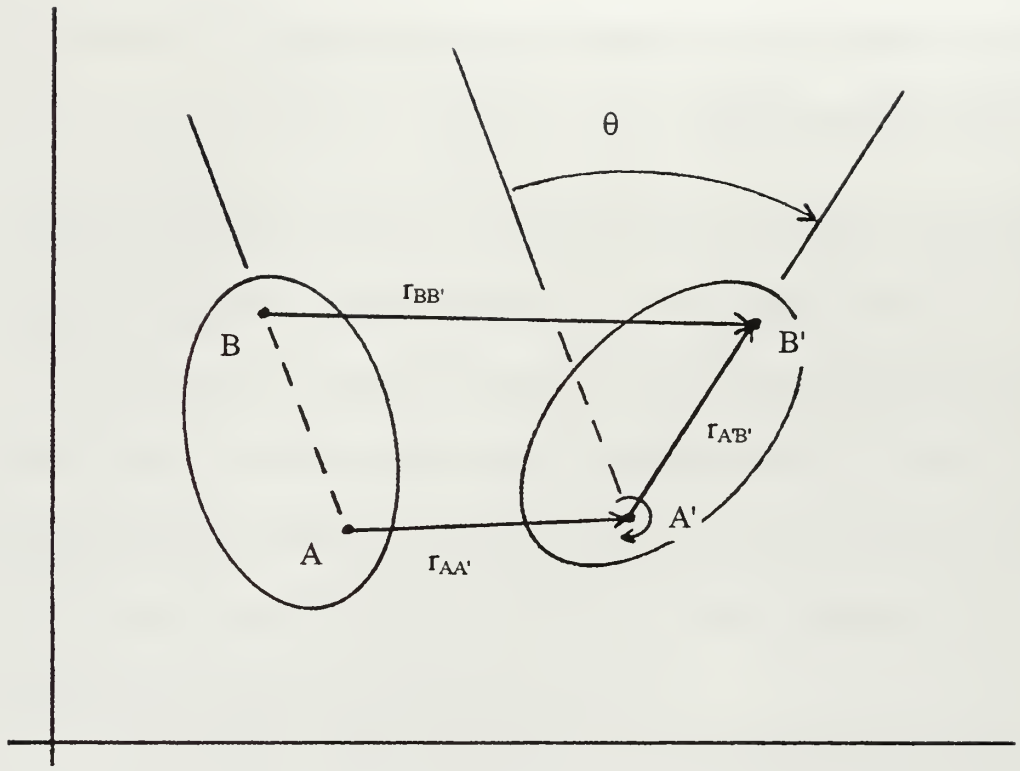


Figure 16: Two dimensional rigid body motion with rotation applied at point A.

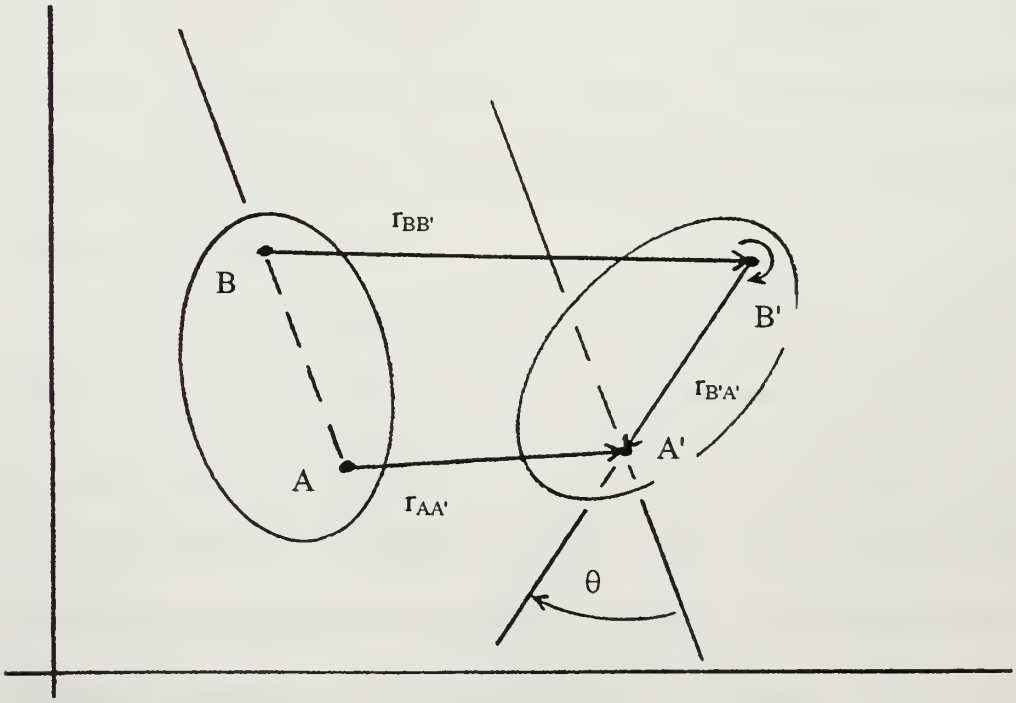


Figure 17: Two dimensional rigid body motion with rotation applied at point B.

The angular velocity vector coincides with the instantaneous axis of rotation when it is applied to the location where the velocity of any point on the rigid body can be resolved into a rotational component about the instantaneous axis and a translational component along the axis. This location may be internal or external to the rigid body.

This description of rigid body motion is possible because the angular velocity vector can be applied at any point in, on, or outside the body. In general, the same is not possible using finite rotation instead of velocities because, as discussed earlier, a finite rotation is not a vector quantity. However, an infinitesimal angular displacement is a vector quantity [Ref. 10]. The small discrete rotations recorded by the knee motion measurement device closely approximate infinitesimal rotation. The following approximation is valid for discrete data with small rotation steps:

$$\{\omega\} \approx \frac{\{\delta\theta\}}{\delta t} \tag{13}$$

where $\{\omega\}$ is the angular velocity vector, $\{\delta\theta\}$ is the differential rotation vector, and δt is the time step between data points. The differential rotation vector and the angular velocity vector have the same direction but different magnitudes. Therefore, any analysis applied to vector velocities can be applied to vector displacements because the vectors involved only differ by a constant in magnitude. In the case of this analysis the constant is 15 seconds (the reciprocal of the data collection time step).

2. Calculation of the Differential Rotation Vector[4]

In order to simplify the analysis it is necessary to express the differential rotation vector of the femur with respect to the tibia in the orthogonal, body fixed, tibial coordinate system. This will allow direct application of the differential translation data recorded for the lateral and medial ends of the transepicondylar axis to locate the instantaneous rotation axis within the knee.

Equation (12) gave the relationship between the time rate of change of the Euler angles measured in the inertial frame and the angular velocity vector expressed in the body fixed orthogonal coordinate system. Because this study involves discrete data with a short time step (1/15 sec), it is reasonable to approximate both the Euler angle time rate of change and the angular velocity expressed in the body-fixed orthogonal coordinate system as a differential rotation multiplied by the reciprocal of the time step. Therefore, equation (12) can be expressed in terms of differential Euler rotations as

$$\begin{Bmatrix} \beta_\xi \\ \beta_\eta \\ \beta_\varsigma \end{Bmatrix} = \begin{bmatrix} \cos(\theta)\cos(\phi) & \sin(\phi) & 0 \\ -\cos(\theta)\sin(\phi) & \cos(\phi) & 0 \\ \sin(\theta) & 0 & 1 \end{bmatrix} \begin{Bmatrix} \delta\psi \\ \delta\theta \\ \delta\phi \end{Bmatrix} \qquad (14)$$

where $\bar{\beta}$ is the differential rotation vector of the rigid body expressed in the orthogonal, body-fixed coordinate system (ξ, η, ζ).

Equation (14) can be applied to the rotation data collected for both the tibia and femur to develop their respective differential rotation vectors expressed in their own body fixed coordinate system. In order to describe the differential rotation of the femur with

[4] Alternative derivations for the instantaneous angular velocity vector are presented in Appendix A.

respect to the tibia expressed in the body fixed tibial coordinate system, the transformation matrix of equation (11) must be applied as follows:

$$\{\beta_{f/t}\} = [\mathrm{T}]\{\beta_f\} - \{\beta_t\} \tag{15}$$

Once this transformation is complete, the direction of the vector $\{\beta_{f/t}\}$ closely approximates that of the instantaneous axis of rotation.

3. Alternate Derivation of the Differential Rotation Vector

The knee motion measurement device records the Euler angles of rotation of the femur and the tibia relative to the inertial coordinate frame. It provides more than enough data to fully describe the motion of the femur with respect to the tibia. The effect of measurement error can be minimized by only using the proper data necessary to describe the motion and selectively using the parameters provided by sensors with the best accuracy. Because of these concerns an alternative derivation of the differential rotation vector was desired to compare to the previous analysis to cross check accuracy.

The translation sensors are precision linear resistors and are more accurate than the rotational sensors. Of the six rotational sensors, the sensors providing rotation around the x axis are considered the most accurate because they are measuring a much larger angle and travel in only one direction throughout flexion. As a result, the hysteresis error is negligible for the x rotation sensors. It may not be negligible for the sensors measuring rotation about the y' and z'' axes because the magnitude of rotation about these sensors may be small and the rotation may change direction during flexion or extension. This sensitivity to measurement error when the measured rotations are small was also identified by Blankevoort, *et al.* in their development of the helical (instantaneous) axis of rotation

[Ref. 6]. Therefore, in order to minimize susceptibility to this type of error, it is desirable to use the data provided by the translation sensors and the x rotation sensors when developing the differential rotation vector. It is demonstrated in the following section that these parameters are independent degrees of freedom for the rotation problem and they are sufficient to fully describe the motion.

F. KINEMATIC DEGREES OF FREEDOM AND CONSTRAINT

To determine the minimum parameters necessary to describe the motion of the knee, kinematic constraints must be identified to determine the motion degrees of freedom. In general, there are six degrees of freedom associated with rigid body motion, three translational and three rotational. The orientation of the body is described by the rotational degrees of freedom while location of the body is described by the translational degrees of freedom [Ref. 16]. The three rotational degrees of freedom are satisfied by the Euler angles of rotation between the femur and the tibia. However, it is desired to prescribe knee rotation using x rotation and translation measurements. To do this we must establish generalized coordinates that include these parameters and then formulate constraint equations to reduce the degrees of freedom to the three required to describe the body orientation.

To describe the rotation of the femur with respect to the tibia six generalized coordinates are selected. These are:

coordinate	definition
X	$(x_{\text{medial}} - x_{\text{lateral}})$
Y	$(y_{\text{medial}} - y_{\text{lateral}})$
Z	$(z_{\text{medial}} - z_{\text{lateral}})$
ψ	(euler angle of rotation along the x axis)
θ	(euler angle of rotation along the y' axis)
ϕ	(euler angle of rotation along the z'' axis)

The first three generalized coordinates are merely the components of the vector describing the transepicondylar axis expressed in the body fixed, tibial coordinate system. The last three generalized coordinates are the Euler rotation angles of the femur with respect to the tibia expressed in the body fixed, tibial coordinate system.

Equation (1) and equation (10) are used to develop the equations of constraint. This analysis assumes differential rotation. Therefore, the small angle approximations, $\cos(\alpha)=1$, and $\sin(\alpha)=\alpha$, are used to linearize equation (10). The following derivation is valid for small angles only. Applying these approximations and neglecting second order multiplications of small angles, equation (10) simplifies to the following:

$$\left[\overline{\mathrm{T}}\right] = \begin{bmatrix} 1 & -\phi & \theta \\ \phi & 1 & -\psi \\ -\theta & \psi & 1 \end{bmatrix} \tag{16}$$

This transformation matrix is applied to the vector representing the transepicondylar axis resulting in the following:

$$\begin{Bmatrix} X_1 \\ Y_1 \\ Z_1 \end{Bmatrix} = \begin{bmatrix} 1 & -\phi & \theta \\ \phi & 1 & -\psi \\ -\theta & \psi & 1 \end{bmatrix} \begin{Bmatrix} X_0 \\ Y_0 \\ Z_0 \end{Bmatrix} \tag{17}$$

$[X_1\ Y_1\ Z_1]^T$ are the transformed components of $[X_0\ Y_0\ Z_0]^T$ due to the small rotation $[\psi\ \theta\ \phi]^T$. Carrying out the multiplication and rearranging terms yields

$$\begin{Bmatrix} (X_1 - X) \\ (Y_1 - Y) \\ (Z_1 - Z) \end{Bmatrix} = \begin{bmatrix} 0 & Z & -Y \\ -Z & 0 & X \\ Y & -X & 0 \end{bmatrix} \begin{Bmatrix} \psi \\ \theta \\ \phi \end{Bmatrix} \tag{18}$$

Since equation (18) is only valid for small rotations, it will be restated in differential form for clarity:

$$\begin{Bmatrix} dX \\ dY \\ dZ \end{Bmatrix} = \begin{bmatrix} 0 & Z & -Y \\ -Z & 0 & X \\ Y & -X & 0 \end{bmatrix} \begin{Bmatrix} d\psi \\ d\theta \\ d\phi \end{Bmatrix} \tag{19}$$

Since the differential equations contained in equation (19) are non-integrable in closed form, they constitute three nonholonomic constraints for the rotation. The length of the transepicondylar axis vector is invariant during transformation, an additional algebraic constraint equation is given by

$$X^2 + Y^2 + Z^2 = \text{constant} \tag{20}$$

So far there are six degrees of freedom and four equations of constraint. Three independent degrees of freedom are necessary to describe the rigid body orientation of the femur with respect to the tibia. Also, the coefficient matrix of equation (19) is singular and no unique solution exists for the linear system. To resolve these discrepancies the

known differential x Euler rotation is applied to the constraint matrix resulting in the following:

$$\begin{Bmatrix} d\psi \\ dY \\ dZ \end{Bmatrix} = \begin{bmatrix} 1 & 0 & 0 \\ -Z & 0 & X \\ Y & -X & 0 \end{bmatrix} \begin{Bmatrix} d\psi \\ d\theta \\ d\phi \end{Bmatrix} \tag{21}$$

Equations (20) and (21) constitute a complete set of constraint equations to describe the rigid body rotation of the femur with respect to the tibia. Considering these constraint equations, it can be seen that there are only three independent degrees of freedom, two of X, Y, or Z, and $d\psi$, corresponding to the minimum required to describe rigid body orientation. The three dependent degrees of freedom, the remaining X, Y, or Z, and $d\theta$, $d\phi$, can be calculated utilizing the constraint equations. The measured $d\psi$ values applied as an independent degree of freedom are obtained by calculating the differential rotation vectors of both the tibia and the femur in their respective orthogonal, body-fixed coordinate systems utilizing equation (11), and then transforming the femoral differential rotation vector to the tibial system to calculate the total differential rotation vector using equation (15).

The three independent translational degrees of freedom are obtained from the lateral epicondyle translation data. No transformations are required for this data because the femoral translation is measured directly in the orthogonal, body fixed, tibial coordinate system.

An important point that must be realized in the analysis is that differential Euler rotations determined in equation (21) form the differential rotation vector, i.e., the vector

$\{d\psi, d\theta, d\phi\}^T$ is the same as the vector $\{\beta_\xi, \beta_\eta, \beta_\zeta\}^T$ calculated in equation (14). This is because an infinitesimal, differential rotation is independent of the order of rotation [Ref. 17]. The vector $\{d\psi, d\theta, d\phi\}^T$ of equation (21) differs from the vector $\{\delta\psi, \delta\theta, \delta\phi\}^T$ of equation (14) in that the former is the differential rotation vector expressed in the orthogonal, body-fixed, tibial coordinate system (x_t, y_t, z_t) while the latter is a vector of the differential Euler rotations recorded by the motion measurement device along the generally nonorthogonal x, y', and z'' axes.

Equations (15) and (21) are applied to calculate values for $d\theta$ and $d\phi$. This is done to develop values for these parameters that are unique and accurate for the measured independent degrees of freedom. The measured independent degrees of freedom are those sensed with the highest accuracy. The calculated parameters are also measured redundantly by the knee motion measurement device and these measured values are used to verify analysis accuracy.

G. LOCATION OF THE INSTANTANEOUS AXIS OF ROTATION WITHIN THE KNEE

The differential translation of the lateral epicondyle is calculated from the lateral side translation data. This differential translation is composed of a purely translational component along the instantaneous rotation axis and a purely rotational component, perpendicular to this axis. The translational component is determined by the vector projection of the lateral side differential translation vector onto the instantaneous axis. This translational component is subtracted from the lateral side differential translation vector to obtain the purely rotational component.

The rotational component of the lateral epicondyle differential rotation vector will be tangential to a circle drawn around the instantaneous axis of rotation with the plane of the circle perpendicular to the instantaneous axis (see Figure 18 next page). This requires that the rotational component be perpendicular to the radius vector drawn from the instantaneous axis to the rotational component. The cross product of this rotational component with the instantaneous axis defines a direction which is mutually perpendicular to both the instantaneous axis of rotation and the rotational component. This mutually perpendicular direction will be the direction of the radius vector from the instantaneous axis to the tangential rotational component of the lateral epicondyle differential translation vector. The magnitude of the radius vector is the magnitude of the rotational component of the lateral epicondyle differential translation divided by the magnitude of femoral differential angular rotation vector. Figure 18 illustrates this relationship.

H. FLEXION, VARUS-VALGUS, AND INTERNAL-EXTERNAL ROTATION

Throughout the data analysis, femoral angular displacement, rotation matrices, and the instantaneous rotation axis are calculated with respect to the body-fixed tibial coordinate system. This allows straightforward calculation of anatomical parameters of tibial flexion, varus-valgus rotation, and internal-external tibial rotation. Because the differential angular displacement of the femur with respect to the tibia is calculated for each data step, flexion, varus-valgus rotation, and internal-external rotation of the tibia for any instant in time can be calculated as the time integral of the x_t, y_t, and z_t components of the differential angular displacement, respectively. Flexion and varus/valgus rotation is

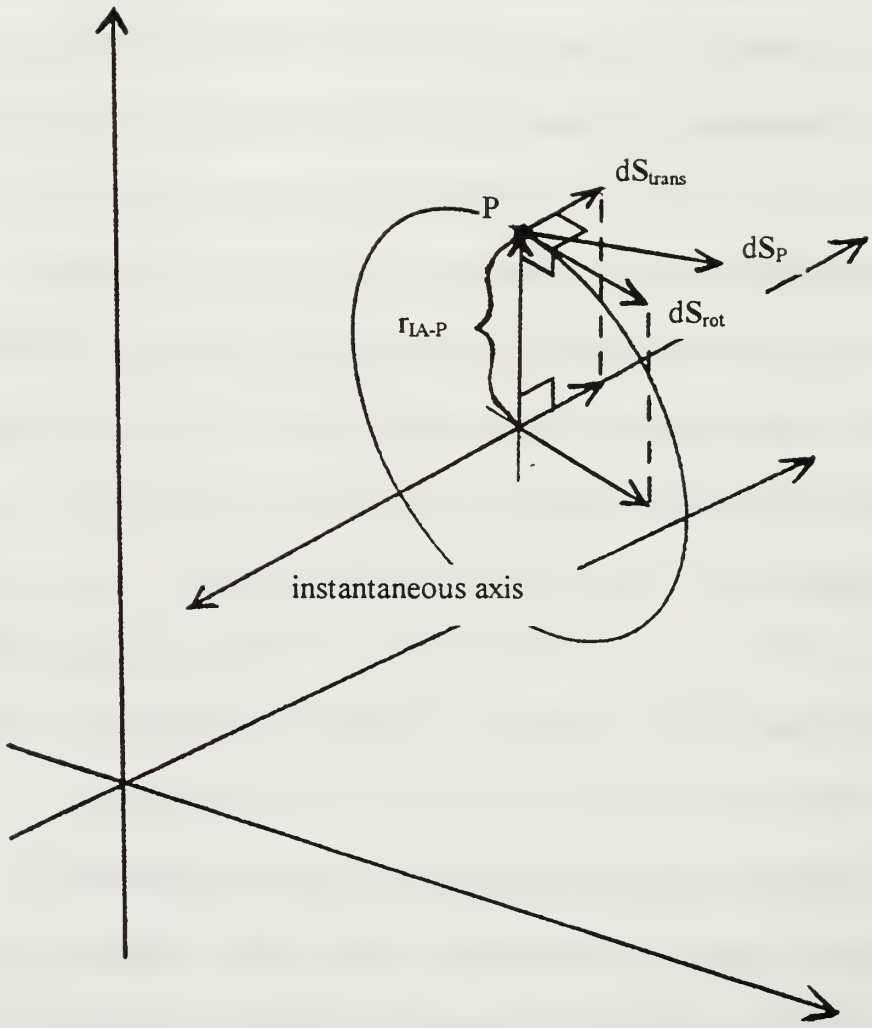


Figure 18: Differential motion of point P (dS_P) resolved into translation along the instantaneous axis of rotation and rotation about the instantaneous axis of rotation.

reported as the femur with respect to the tibia and internal rotation is reported as the tibia with respect to the femur.

I. USE OF THE INSTANTANEOUS AXIS OF ROTATION FOR COMPUTER MODELING

Once the differential rotation vector of the femur with respect to the tibia is calculated, this rotation vector can be used to develop a differential rotation matrix of the femur with respect to the tibia. An efficient method is to develop the rotation matrix in terms of the instantaneous rotation axis and the magnitude of the differential rotation. Euler parameters are calculated and the rotation matrix developed in terms of the Euler parameters as follows [Ref. 17]:

Euler parameters:

$$\theta_0 = \cos\left(\frac{\theta}{2}\right) \tag{22}$$

$$\theta_1 = \upsilon_1 \sin\left(\frac{\theta}{2}\right) \tag{23}$$

$$\theta_2 = \upsilon_2 \sin\left(\frac{\theta}{2}\right) \tag{24}$$

$$\theta_3 = \upsilon_3 \sin\left(\frac{\theta}{2}\right) \tag{25}$$

Transformation matrix:

$$[\mathrm{T}] = \mathrm{I} + 2\tilde{\tilde{\theta}}\left(\mathrm{I}\theta_0 + \tilde{\tilde{\theta}}\right) \tag{26}$$

where:

θ = magnitude of the differential rotation

$\upsilon_1, \upsilon_2, \upsilon_3$ = components of a unit vector in the direction of the instantaneous axis of rotation.

$$\tilde{\tilde{\theta}} = \begin{bmatrix} 0 & -\theta_3 & \theta_2 \\ \theta_3 & 0 & -\theta_1 \\ -\theta_2 & \theta_1 & 0 \end{bmatrix}$$

The transformation matrices are used to transform an array of vectors to points on the surface of the femur to simulate rotation of the femur with respect to the tibia.

IV. ACCURACY

Three data runs were recorded for each knee. The data was highly repeatable between runs. The standard error of the sample mean was calculated to demonstrate repeatability as follows:

$$\sigma_{\hat{\rho}} = \frac{s_{\hat{\rho}}}{\sqrt{n}} \qquad (27)$$

The standard error of the sample mean is the standard deviation of the distribution of the sample mean, which will be Gaussian. With 95% confidence, the actual mean will fall within two standard errors of the average of the recorded values of each parameter for the three data runs.

Table 1 gives the standard error for each measured parameter calculated over three data runs for each knee.

knee number	L31	L66	L67	L210
femur x rotation (degs)	0.4678	0.2479	0.2273	0.1716
femur y' rotation (degs)	0.1049	0.1434	0.0449	0.0772
femur z'' rotation (degs)	0.0939	0.4348	0.0863	0.3450
tibia x rotation (degs)	0.6788	0.1901	0.1981	0.1505
tibia y' rotation (degs)	0.0496	0.0754	0.0872	0.0648
tibia z'' rotation (degs)	0.2389	0.5270	0.1746	0.1739
lateral x_t translation (mm)	0.0580	0.1098	0.0280	0.0397
lateral y_t translation (mm)	0.8545	0.5036	0.4296	0.2461
lateral z_t translation (mm)	0.2140	0.5103	0.0324	0.1831
medial y_t translation (mm)	0.5447	0.3619	0.1117	0.0977
medial z_t translation (mm)	0.1137	0.2311	0.1807	0.0387

Table 1: Standard error

The standard error between data runs is on the order of 1% to 2% of the full range measured by each sensor. The instrumentation was quite reliable.

V. RESULTS

The goal of this study was to calculate a vector representation of the knee's instantaneous axis of rotation and calculate the location of this axis within the knee for the ACL intact and ACL deficient conditions. This was accomplished for each of the subject knees. Other studies have resolved knee motion into different coordinate systems. Hollister, *et al.*, identified a two axis system defining a longitudinal rotation (LR) axis coincident with the long axis of the tibia and a flexion extension (FE) axis extending through the femur connecting the attachment sites of the lateral collateral and medial collateral ligaments (LCL, MCL) [Ref. 11]. Blankevoort, *et al.*, resolved knee motion into rotation about a helical axis and translation along that axis [Ref. 6]. This is the same description of motion utilized in this study. However, Blankevoort utilized finite rotations of up to 15° per rotation step, and concluded that motion results were relatively insensitive to rotation step size. In fact, he states that due to measurement inaccuracies, the overall accuracy of the rotation axis is inversely proportional to step size. Measurement inaccuracies are minimized if continuous motion is measured because hysteresis and viscoelasticity have a minimum effect. Sensitivity to rotation step size was not tested as part of the current study.

The starting point of measurement for each knee was determined by the knee's natural fully extended position. The origin of the body fixed tibial coordinate system and the origin of the body fixed femoral coordinate system coincided at the lateral epicondyle. The coordinate axes were not necessarily parallel, depending on the initial values of

internal/external, varus/valgus, and flexion rotation of the femur with respect to the tibia. Prior to installing each knee in the measurement device, a rigid rod was placed in the sockets of the rotation sensors and the sensors were positioned orthogonally with the respective rotation axes of the two rotary sensor arrays parallel. Data was recorded to define the zero rotation position and this correction was applied to the recorded knee rotation data to establish the zero starting point for rotation measurements. Each knee had different values of internal, varus/valgus, and flexion rotation at the start of each data run, and these are reflected in the analysis.

A. SUMMARY OF FIGURES

Figures 19 through 38 show, in the body-fixed tibial coordinate system, the location of the instantaneous axis of rotation of the femur with respect to the tibia for the ACL intact condition. The location of the instantaneous axis is presented for 0°, 10°, 20°, 30°, and 90° of flexion. These angles were chosen because the most dramatic shift in the axis occurs during the first 30 degrees of flexion. In these figures the instantaneous axis of rotation is superimposed over a wireframe representation of the articulating surfaces of the tibia and femur. These wireframe surfaces were created from coordinate data measured on a foam casting of a "generic" knee and not from the actual knees themselves. Therefore, they are not meant to be an accurate representation of the articulating surfaces of the actual knees, rather, they are intended to serve as an aid to visualize the relative placement of the axis within the knee.

Figures 39 through 46 display the instantaneous axis of rotation for each knee through a full flexion cycle. The axis is shown for each 8 degrees of flexion.

Figures 47 through 54 provide information on the magnitude of tibia rotation and the apparent translation of the medial and lateral epicondyles vs flexion.

Figures 55 through 58 provide information on the trajectories of the epicondyles and the instantaneous axis of rotation. The view is from medial to lateral. These figures indicate the location of the instantaneous axis of rotation relative to the epicondyles throughout the range of flexion.

Figures 59 and 60 demonstrate how two points can appear to translate along a given direction due to pure rotation. All figures are located at the end of the chapter.

B. ACL INTACT CONDITION

A strong component of internal rotation can be clearly seen in each knee during the first 30° of flexion (Figures 47, 49, 51, and 53). This motion corresponds to the observed "screw home" mechanism of knee extension [Ref. 19]. The internal rotation that occurs during flexion is the knee "unscrewing" from the locked position of full extension. Following this period of pronounced internal rotation, the instantaneous axis of rotation then shifts to approximately the position of the transepicondylar axis where it remains relatively constant until the femur begins to rotate off the posterior horn of the meniscus.

In Figures 39 through 46 the variation of internal tibia rotation can be clearly seen as the axis of rotation for each knee tends toward the horizontal as flexion increases. The component of the instantaneous axis of rotation along the z (compression-distraction) axis represents internal (or external) tibia rotation.

Despite the overall similarities, there are also differences between the motion characteristics of each knee. This corroborates the findings of Blacharski, *et al.* who

concluded each knee displays different motion characteristics which are the result of the shape of the joint articulating surfaces [Ref. 20]. Hollister, *et al.*, identified a constant FE axis that is located in approximately the same position in each knee [Ref. 11]. This constant axis was located independent of the rotation along the tibial LR axis. If the rotation about the LR axis varies from knee to knee, as suggested by the current study, the resulting composite instantaneous axis of rotation will not be constant.

The particular path followed by the instantaneous axis as it moves through the entire range of flexion varies from knee to knee. However, some common characteristics were identified.

Each knee displayed pronounced internal rotation during the first 20 to 30 degrees of flexion (Figures 47,49,51, and 53). The initial period of internal rotation was followed by a period of less pronounced rotation for the remainder of the flexion range up to 120°. The magnitude of the total internal rotation varied between knees.

Two of the knees displayed somewhat peculiar internal/external rotation characteristics. One knee (L67) alternated between internal and external rotation throughout the range of flexion (Figure 47). Following testing, this knee was dissected and examined and found to have advanced osteoarthritis in the medial side. This condition was not identified by the pretesting arthroscopic examination. The unusual internal/external rotation characteristics could be explained by abnormally shaped articulating surfaces as well as an increase in the coefficient of kinetic friction between the articulating surfaces caused by the degenerated articular cartilage on the medial side. The other knee (L31) displayed consistent external rotation following the initial internal

rotation. Examination of this knee following testing revealed no readily identifiable reason for this behavior. Both knees (L67 and L31) displayed peak internal rotation of approximately 6 degrees, one half the magnitude of the two other knees in the study (L66 and L210). By clinical examination, the L67 knee was strongly varus (3 degrees), consistent with the degenerated articular cartilage on the medial side, and the L31 knee was only slightly valgus. The other two knees in the study (L66 and L210) were normal valgus knees and they displayed the more normal 12-15 degrees internal rotation throughout flexion. Although the sample size of four knees is too small to draw any definitive conclusions, this result seems to suggest the more severe the initial valgus orientation of a knee, the larger will be the magnitude of internal tibial rotation necessary to keep the tibia and femur in the sagital plane during flexion. Table 2 summarizes these findings.

Knee Number	varus/valgus angle	total internal rotation
L66	10° valgus	18° internal
L210	9° valgus	14° internal
L31	2° valgus	7° internal
L67	3° varus	6° internal

Table 2: Tibia Rotation vs Varus/Valgus Angle

Figures 55, 56, 57, and 58 present the apparent A-P translation of the lateral and medial ends of the transepicondylar axis. The translation is of the femur with respect to

the tibia and it is described as "apparent" translation because the actual motion is a combined rotation and translation, not a pure translation.

The following consideration should be taken into account when interpreting the A-P translation data. The lateral and medial points presented are the lateral and medial attachment points for the translation sensor arrays. These points are intended to coincide with the lateral and medial epicondyles and are actually the ends of a vector that is being rotated through space. Therefore, the relative orientation of the instantaneous axis of rotation and the transepicondylar axis will determine the apparent translation of these points relative to the tibia. In other words, based on the initial orientation of the transepicondylar axis and the instantaneous axis of rotation it is possible to cause these points to appear to translate in a manner that would suggest internal tibial rotation when, in fact, none was occurring. Figures 59 and 60 illustrate this possibility. From the figures it would appear that point B has a larger translation along the y axis than point A. If only y translation were considered, many different combinations of translation and rotation could result in the same y translations, including rotation about an axis parallel to the z axis. Therefore, complete knowledge of the rotation axis is required before the translation of point A or B along any axis can be properly evaluated. No attempt was made to make a quantitative correlation of the observed apparent translation to internal or external tibial rotation.

The transepicondylar axis was chosen as the reference axis for motion analysis after work performed by Hollister [Ref. 11]. The epicondyles are also easy to locate by clinical examination. The lateral and medial side translation sensors of the knee motion

measurement apparatus were attached to the ends of the transepicondylar axis. The medial end of the transepicondylar axis displayed consistent motion characteristics between knees. The medial point moved anteriorly for a short distance during the first 20°-30° of flexion followed by consistently posterior motion for the remainder of flexion. The lateral end of the transepicondylar axis displayed mixed motion characteristics. For two of the knees (L66 and L210) the lateral point moved consistently posterior. For the other two knees (L67 and L31) the lateral point moved posterior for the first 30° of flexion followed by anterior movement for approximately the next 20° of flexion and finally posterior movement again for the remaining flexion to 120°. These two knees were also the knees that displayed the unusual tibia internal rotation described previously.

One of the knees (L66) displayed minimal motion of the medial point. The translation was limited to a 10 mm diameter circle until the final stages of full flexion, indicating this particular point did indeed lie close to the joint's instantaneous axis of rotation. These exceptions not withstanding, the overall motion of the medial end of the transepicondylar axis was also posterior through the full range of flexion. These findings are consistent with the movement of the medial and lateral centers of rotation reported by Kurosawa, *et al.* [Ref. 1].

The motion of the lateral and medial ends of the transepicondylar axis will depend on their location relative to the instantaneous axis of rotation. If the instantaneous axis of rotation is superior to either point, that point will move anterior with respect to the tibia as the knee flexes. Conversely, if the instantaneous axis of rotation is inferior to either point, that point will move posterior with respect to the tibia as the knee flexes.

The lateral and medial side translation sensors were attached to a pin installed in a hole drilled along the transepicondylar axis. The placement of the drill guide was based on an external examination of each knee. Between knees, the error in placement of the drill guide was on the order of 5 to 10 mm. Therefore, variations are expected in the observed motion of the attachment points from knee to knee. As the distance from the lateral or medial side attachment point to the instantaneous axis of rotation increases, the magnitude of the observed translation of the attachment point should increase. This is evident in the motion characteristics of the knees in this study. The knees which display the most pronounced translation of the lateral and medial side points also have the largest distance from the instantaneous axis of rotation to these points. The differences in distance which cause the variation in translation from knee to knee are of the same order as the error in location of the epicondyles by external examination. If this error were kept minimum, the motion of the epicondyles may agree more closely from knee to knee than was evident from this study.

Comparison of the instantaneous axis of rotation of each knee with the constant FE axis identified in the study by Hollister, *et al.*[Ref. 11], reveals some similarities:

Hollister identified a constant FE axis, corresponding to the transepicondylar axis, directed from anteriosuperior on the medial side to posterioinferior on the lateral side passing through the origins of the MCL and the LCL. During flexion from approximately 30° through 120°, the instantaneous axis of rotation identified in the current study was also directed approximately parallel to this FE axis.

Hollister decomposed knee motion into flexion about the FE axis located in the posterior femoral condyle and tibial rotation about an independent LR axis parallel with the long axis of the tibia. The instantaneous axis of rotation identified in the current study is a single axis describing the overall motion of the joint, including the tibia internal rotation. The differences between the two can be reconciled when the effects of tibia rotation are applied to the constant FE axis identified by Hollister.

The instantaneous axis of rotation identified in the current study is located in the posterior femoral condyle, same as the FE axis identified by Hollister. However, the instantaneous axis of rotation developed here includes the component of internal/external tibial rotation. This causes it to tend from inferior on the lateral side to superior on the medial side for internal tibial rotation and superior on the lateral side to inferior on the medial side for external tibial rotation. This effect is more pronounced during periods of significant internal/external tibial rotation.

The instantaneous rotation axis in the current study is located just under the epicondyles. Hollister also concludes that the fixed FE axis is located just under the epicondyles. After the initial 20 to 30 degrees of flexion there is a period of less severe internal rotation, or even external rotation, lasting to approximately 90 degrees of flexion. During this period, the instantaneous axis of rotation remains relatively constant within the femoral condyle and is located 5 to 17 mm below the epicondyles depending on the knee. The Hollister study reported the lateral joint surface closer to the FE axis than medial, the same was true in the current study.

In the beginning of flexion, the instantaneous rotation axis is located closer to the joint articulating surface than later in flexion. As the joint flexes, the instantaneous rotation axis moves closer to the transepicondylar axis, remaining essentially constant for approximately 60 to 70 degrees of flexion. This motion is consistent with the varying ratio of rolling to sliding believed to exist at the joint articulating surface. An instantaneous axis of rotation closer to the joint articulating surface indicates less sliding. In the limit, if the instantaneous axis of rotation were located at the joint articulating surface there would be no sliding and the joint would undergo pure rolling. The observation that the instantaneous axis of rotation moves away from the joint articulating surface as the joint flexes indicates the ratio of sliding to rolling increases. This continues to a point occurring at approximately 30 to 40 degrees of flexion when the instantaneous rotation axis remains relatively constant, indicating a period of constant rolling to sliding ratio. In the last 30 degrees of joint flexion (90-120° total flexion), the instantaneous axis of rotation again moves closer to the joint articulating surface. This occurrence can be correlated to the beginning of hyperflexion where the femur is starting to pivot on the posterior horn of the meniscus.

The period of flexion occurring around a relatively constant axis from approximately 30 to 90 degrees of flexion indicates the femoral condyles have a circular profile of constant radius. This finding is consistent with a study conducted by Kurosawa *et al.*, where it was concluded the posterior profile of the femoral condyles can be closely represented by a circular arc [Ref. 1].

C. ACL DEFICIENT CONDITION

Figures 47 through 54 present tibia rotation versus flexion angle and A-P apparent translation of the lateral and medial attachment points for the translation sensors versus flexion angle for the ACL deficient condition. The same caution applies to interpreting this A-P translation data as a measure of tibial internal rotation as applies for the ACL intact condition. Also, this data should not be viewed as a measure of the absolute translation of the femur with respect to the tibia for the same reason.

The primary function of the ACL is to limit anterior tibial displacements while serving as a major secondary restraint to tibial internal rotation and minor secondary restraint to tibial external rotation [Ref. 22 and 23]. Figures 47,49, and 51 show a marked increase in overall tibial internal rotation for the ACL deficient condition compared to the ACL intact condition. Figure 53 shows knee L210 to be an exception. Also, each knee is initially more internally rotated prior to flexion for the ACL deficient condition. This result is consistent with the role of the ACL. The anomalous behavior of the L210 knee is unexplained.

As the knee is extended from full flexion, the ACL anterior fibers become increasingly taut [Ref. 24]. The ACL tends from posterio-lateral on the femur to anterio-medial on the tibia. Together, these facts indicate that the ACL should serve to provide a pivot point to pull the lateral femoral condyle forward as the knee extends. If the ACL is ruptured, this pivot point is no longer functional and the knee will not fully rotate externally upon extension. This was the case for the knees tested in this study.

The ACL of each knee was severed while the knee was installed in the motion measuring device. The knees were not removed from their mountings between data runs for the ACL intact and deficient conditions. In each case during the first flexion run following ACL severance the knee did not fully "screw home". This was observed visually as well as recorded by the motion measuring device. For subsequent data runs the knees underwent approximately the same magnitude of internal rotation as for the ACL intact case, however, the knee was initially more internally rotated at flexion start. (The exception was the L210 knee and although it did not fully rotate externally upon extension, same as the other knees, the total magnitude of its internal rotation excursion was significantly less after the ACL was cut.) These results do indeed confirm that the ACL serves to limit internal rotation. Once the ACL was cut, the tibia of each knee was allowed to continue internal rotation during flexion until other restraining mechanisms, such as the lateral and medial collateral ligaments, the tibial eminence, or the posterior oblique ligament, became controlling.

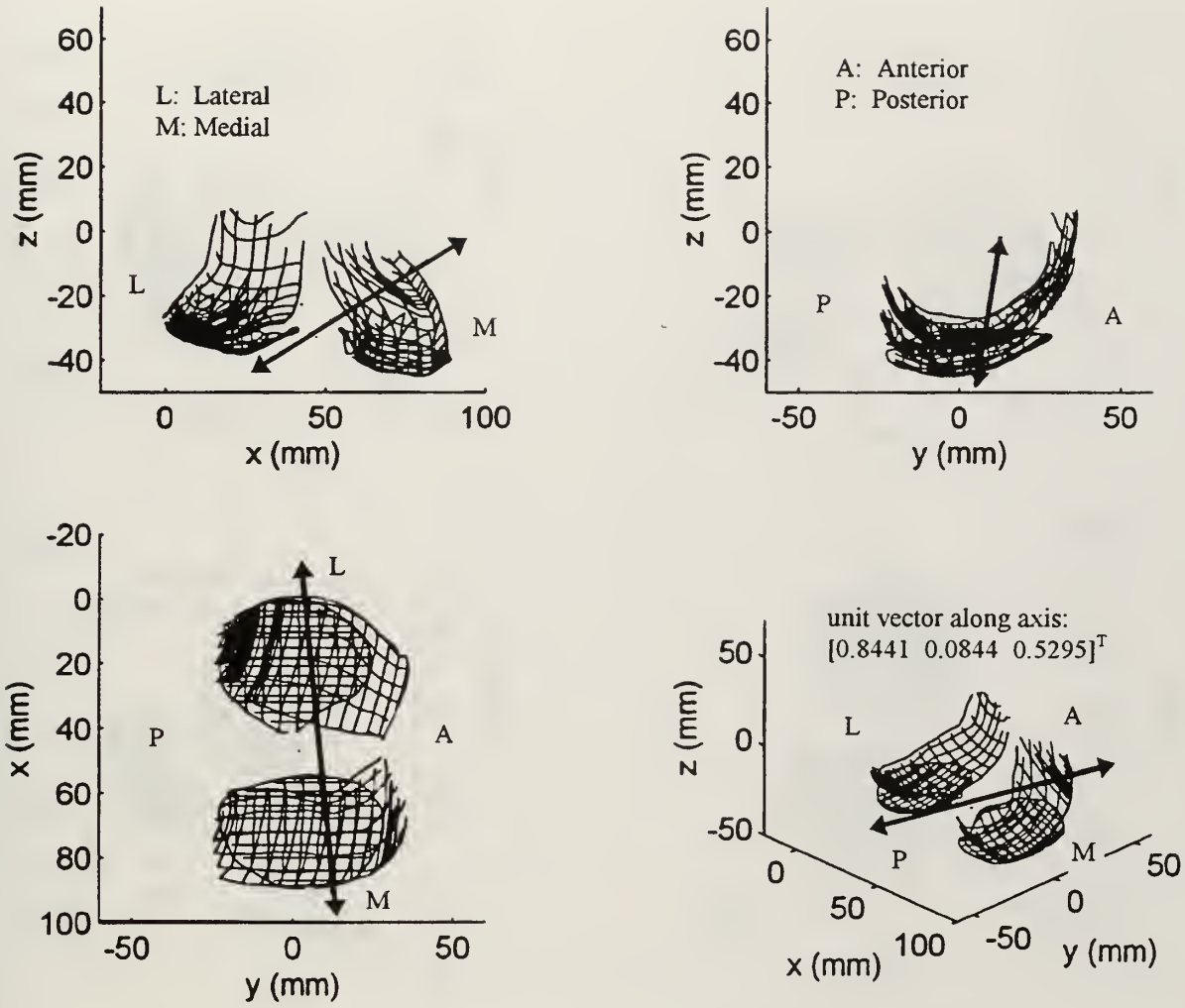


Figure 19: Instantaneous rotation axis, L67 knee, 0 degrees flexion

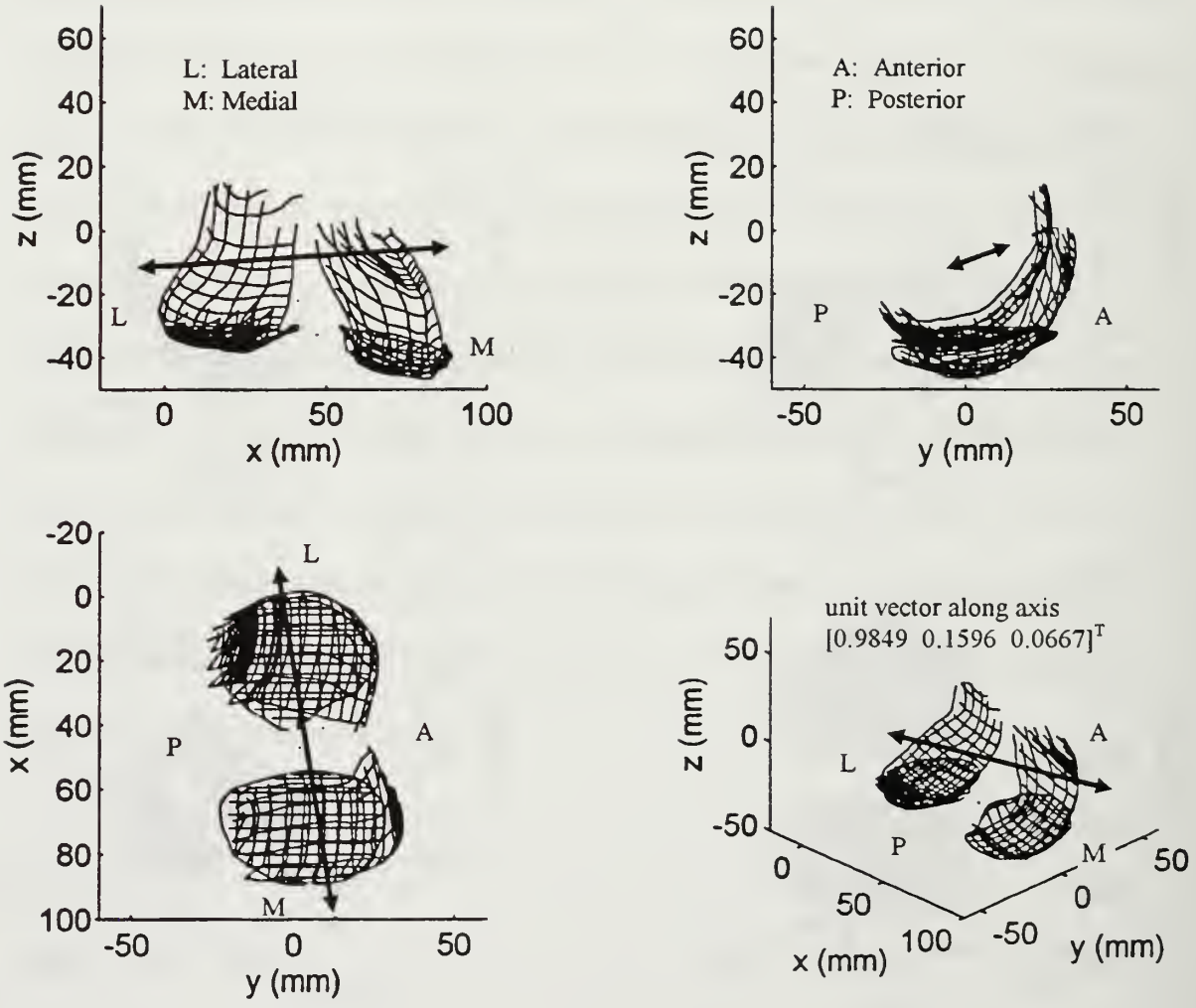


Figure 20: Instantaneous rotation axis, L67 knee, 10 degrees flexion

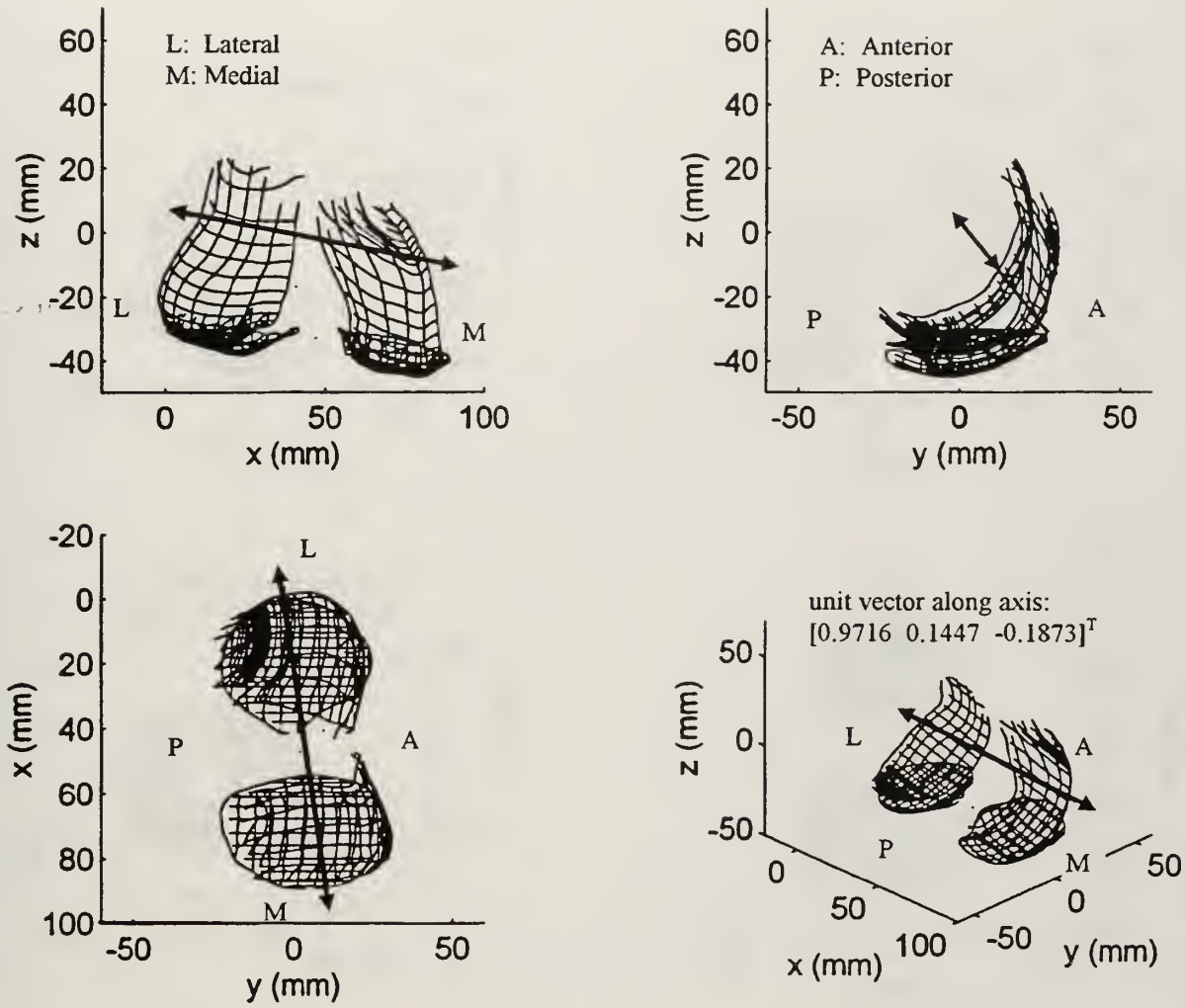


Figure 21: Instantaneous rotation axis, L67 knee, 20 degrees flexion

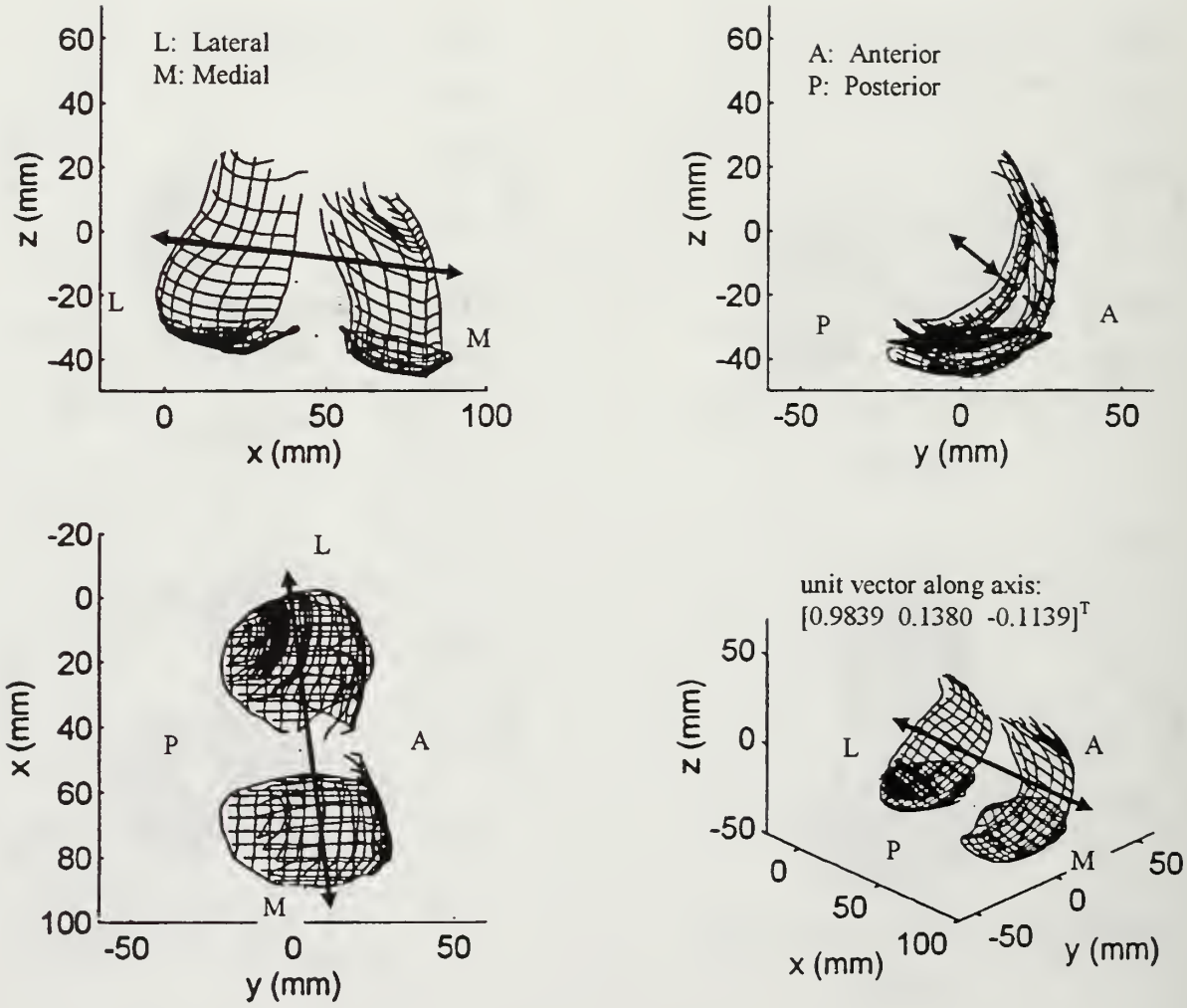


Figure 22: Instantaneous rotation axis, L67 knee, 30 degrees flexion

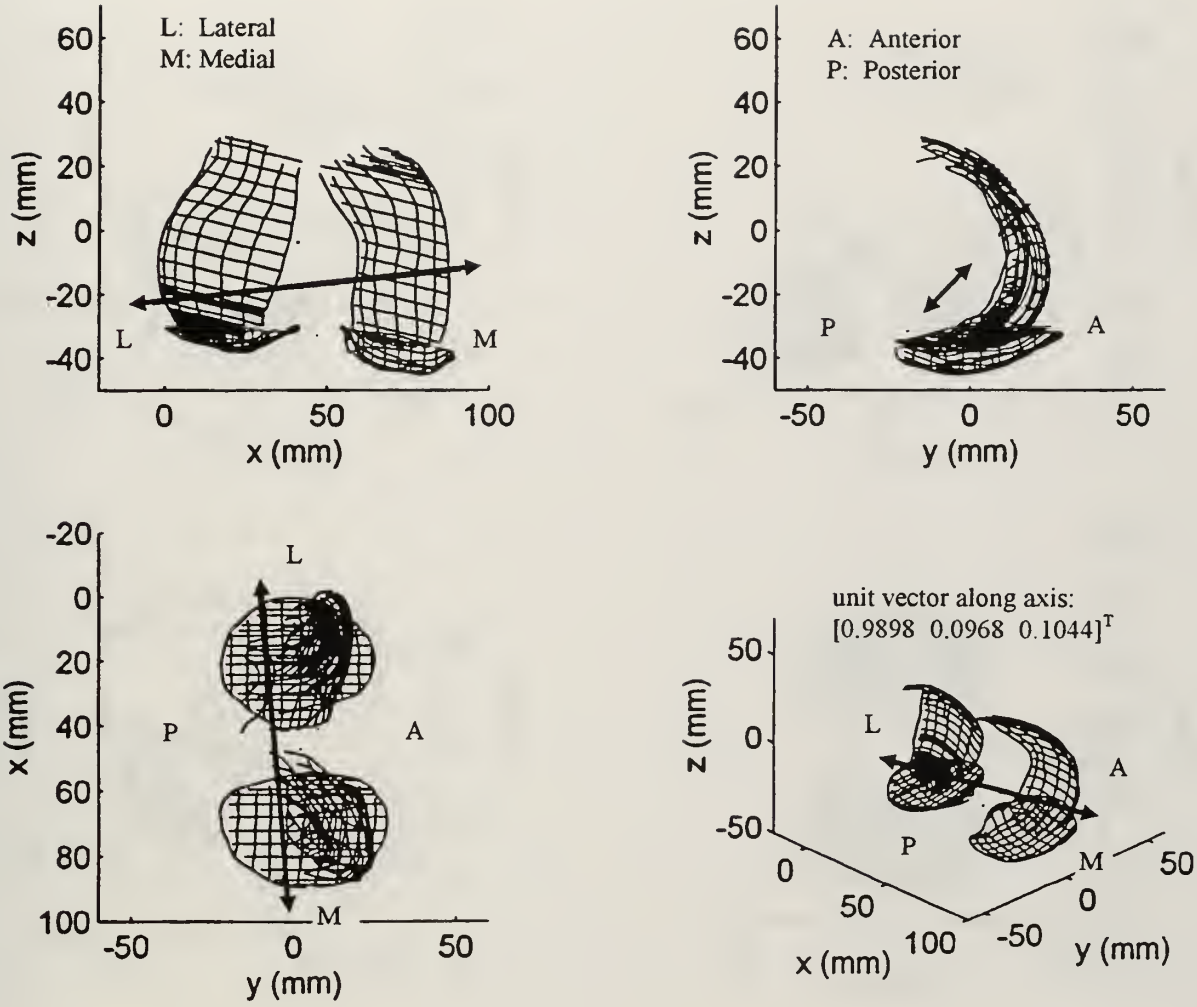


Figure 23: Instantaneous rotation axis, L67 knee, 90 degrees flexion

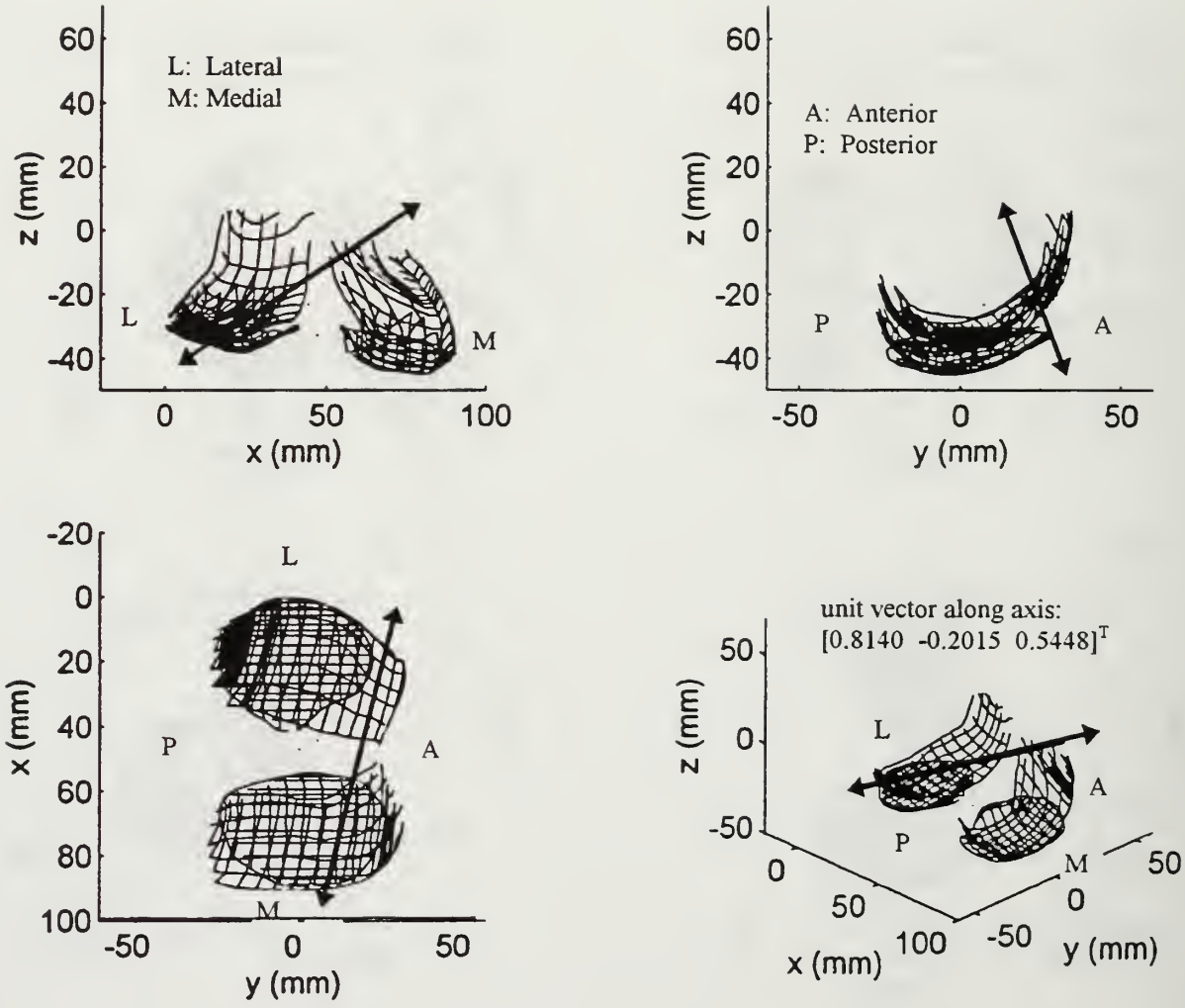


Figure 24: Instantaneous rotation axis, L66 knee, 0 degrees flexion

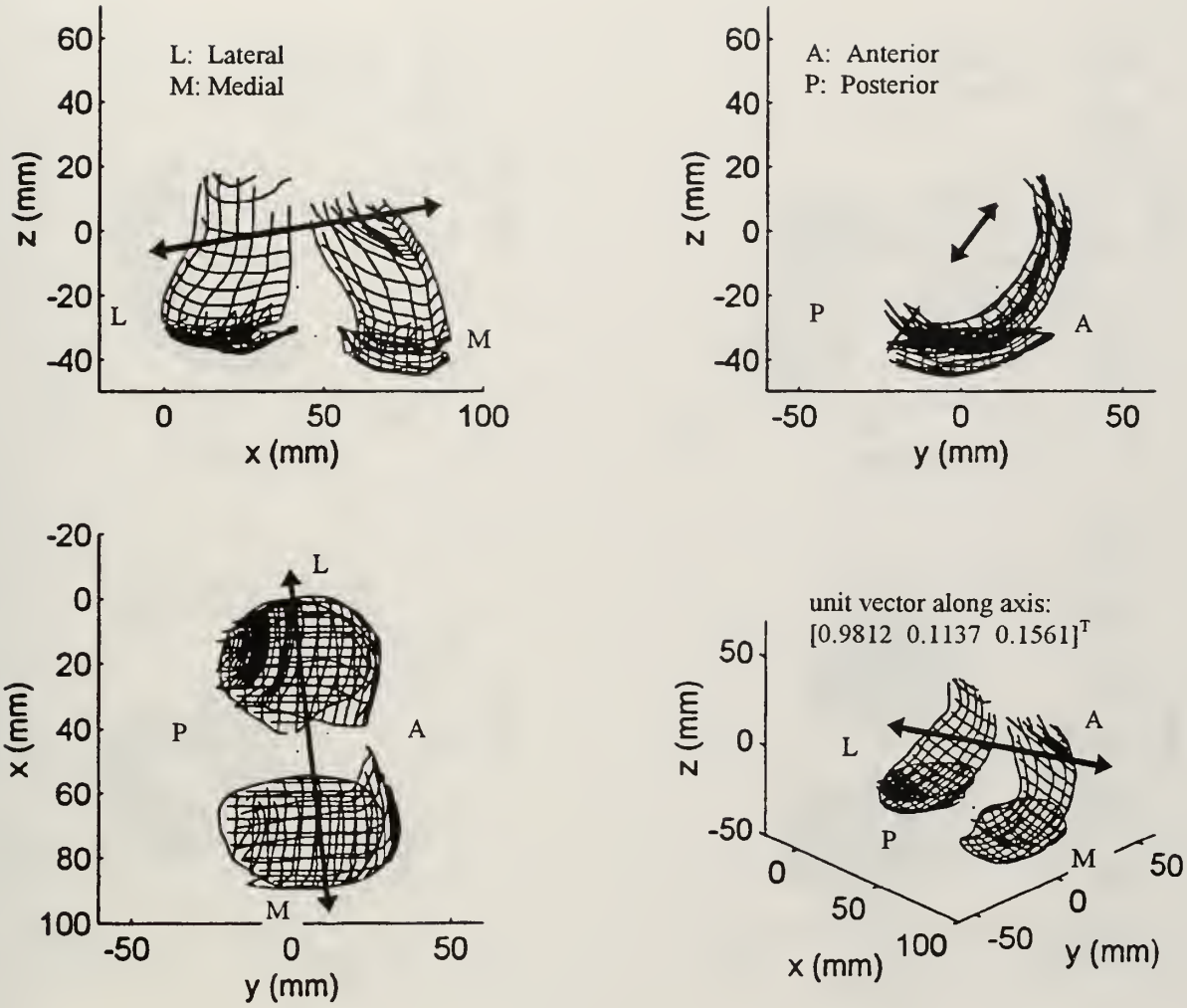


Figure 25: Instantaneous rotation axis, L66 knee, 10 degrees flexion

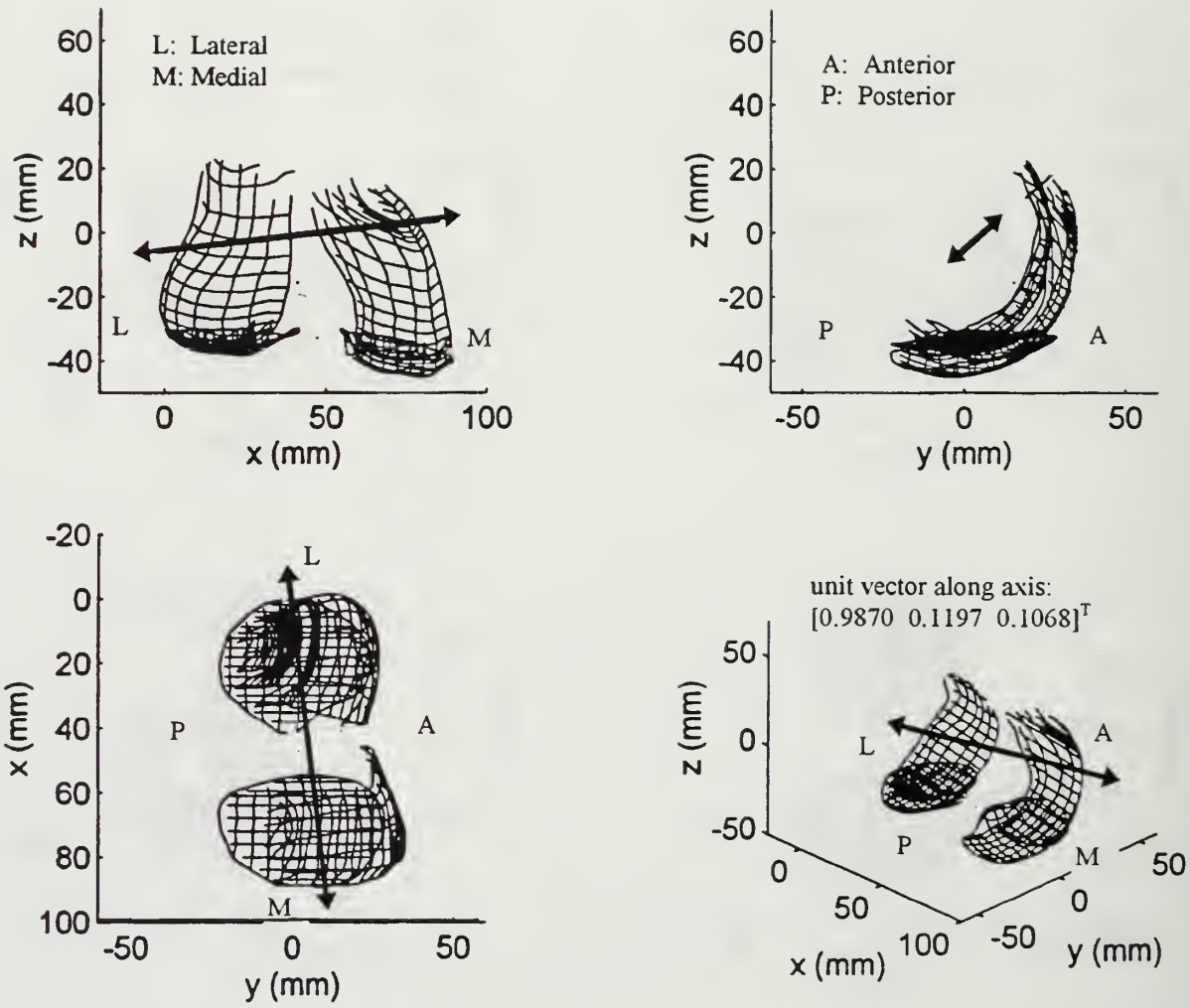


Figure 26: Instantaneous rotation axis, L66 knee, 20 degrees flexion

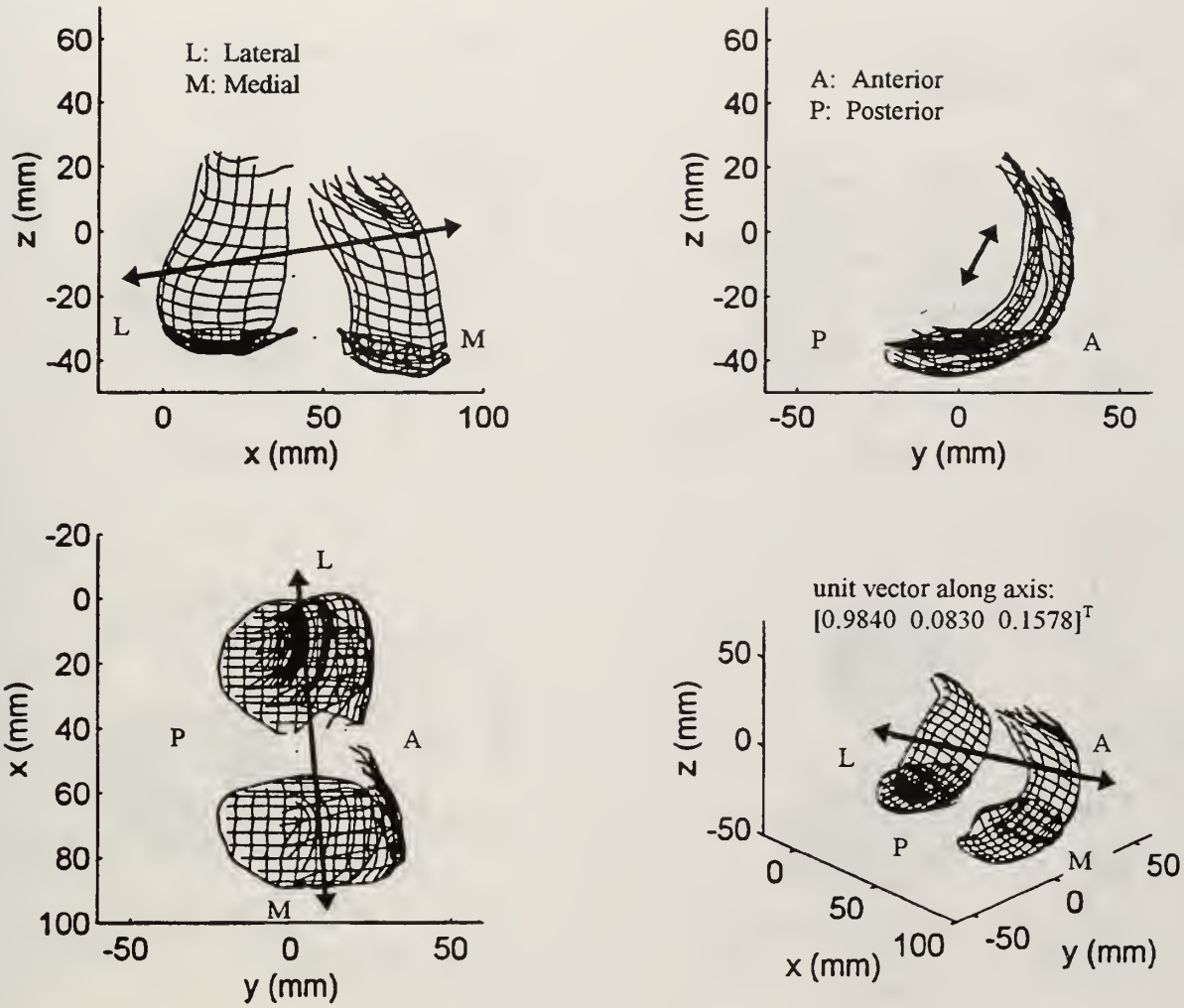


Figure 27: Instantaneous rotation axis, L66 knee, 30 degrees flexion

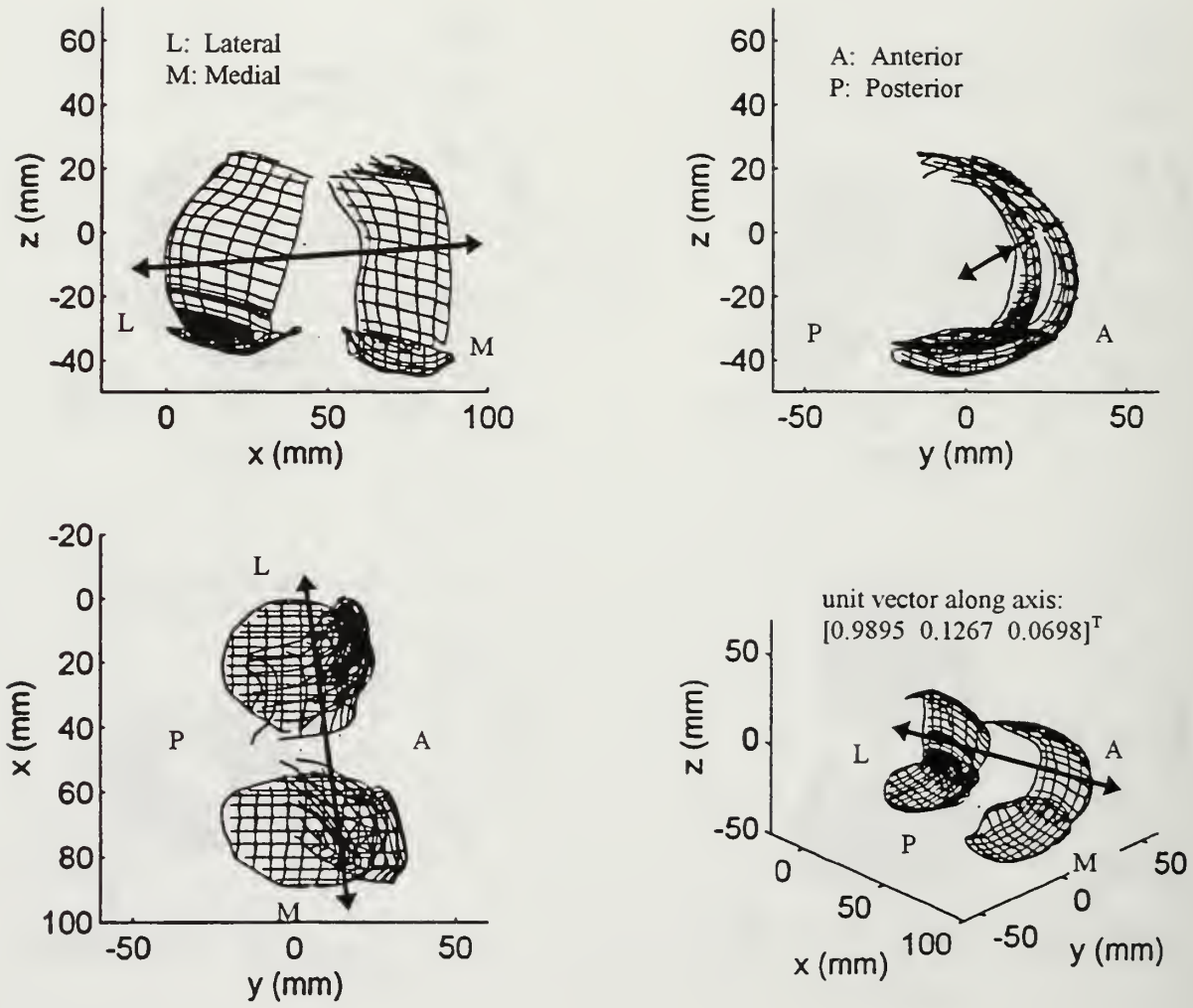


Figure 28: Instantaneous rotation axis, L66 knee, 90 degrees flexion

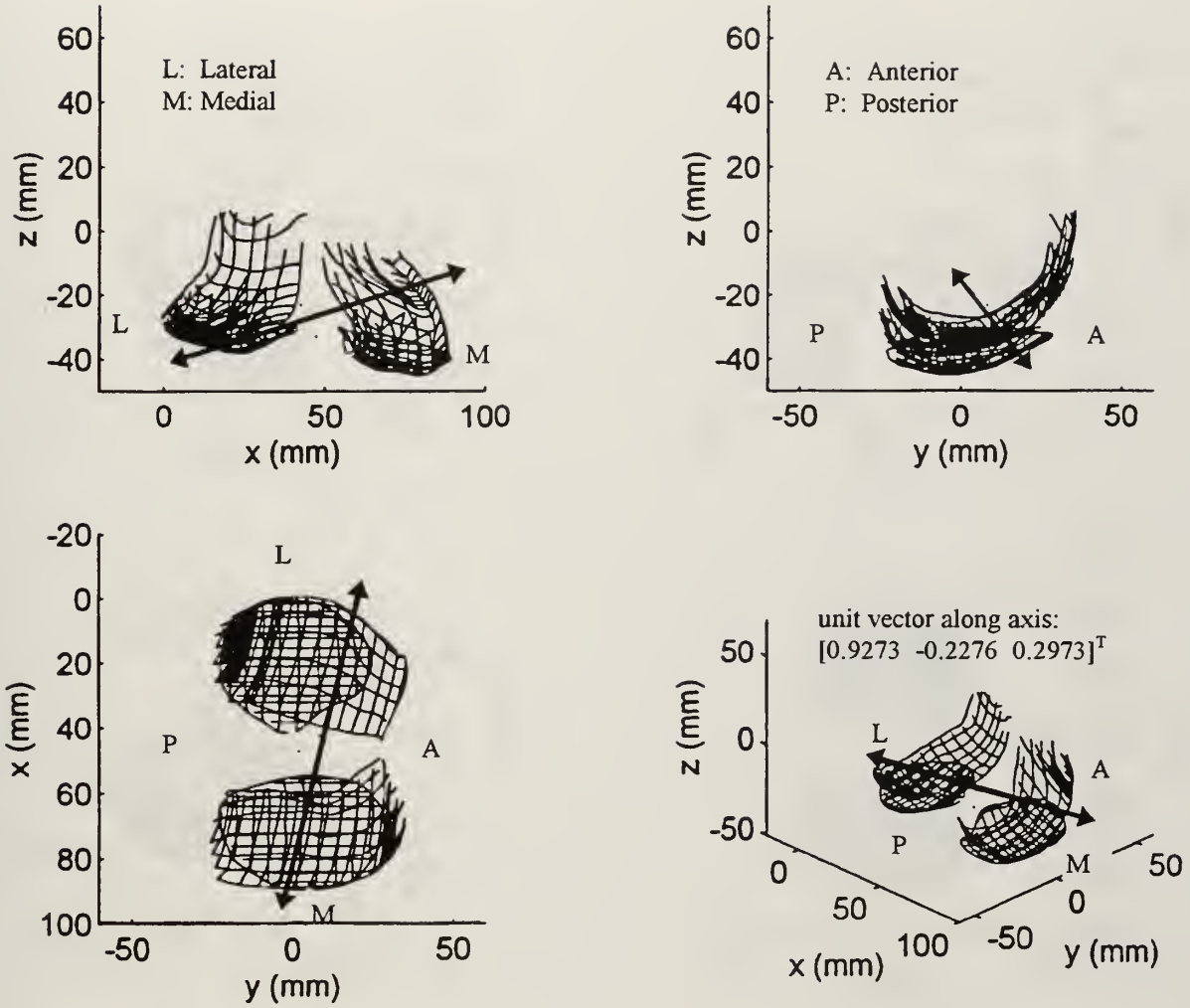


Figure 29: Instantaneous rotation axis, L31 knee, 0 degrees flexion

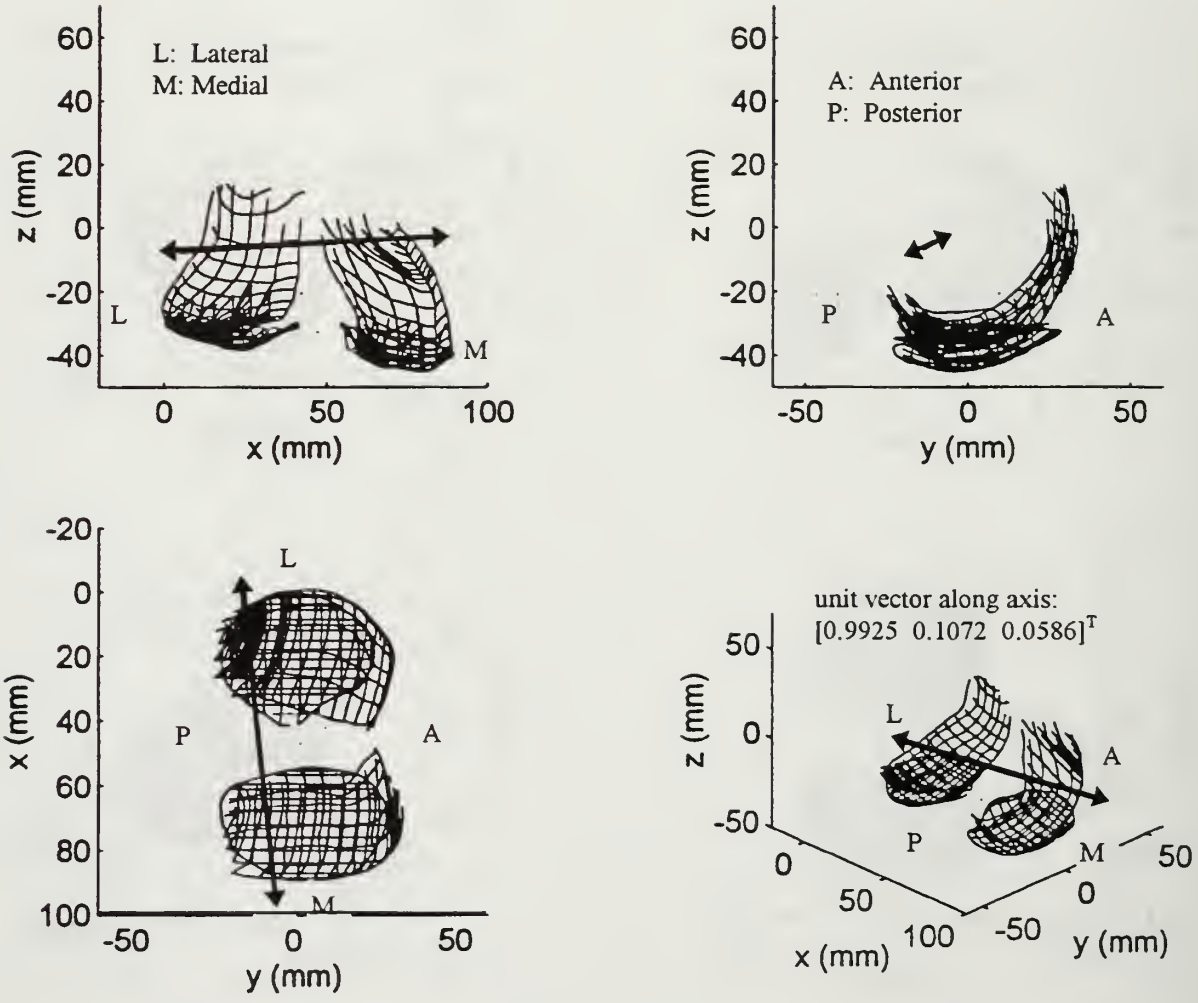


Figure 30: Instantaneous rotation axis, L31 knee, 10 degrees flexion

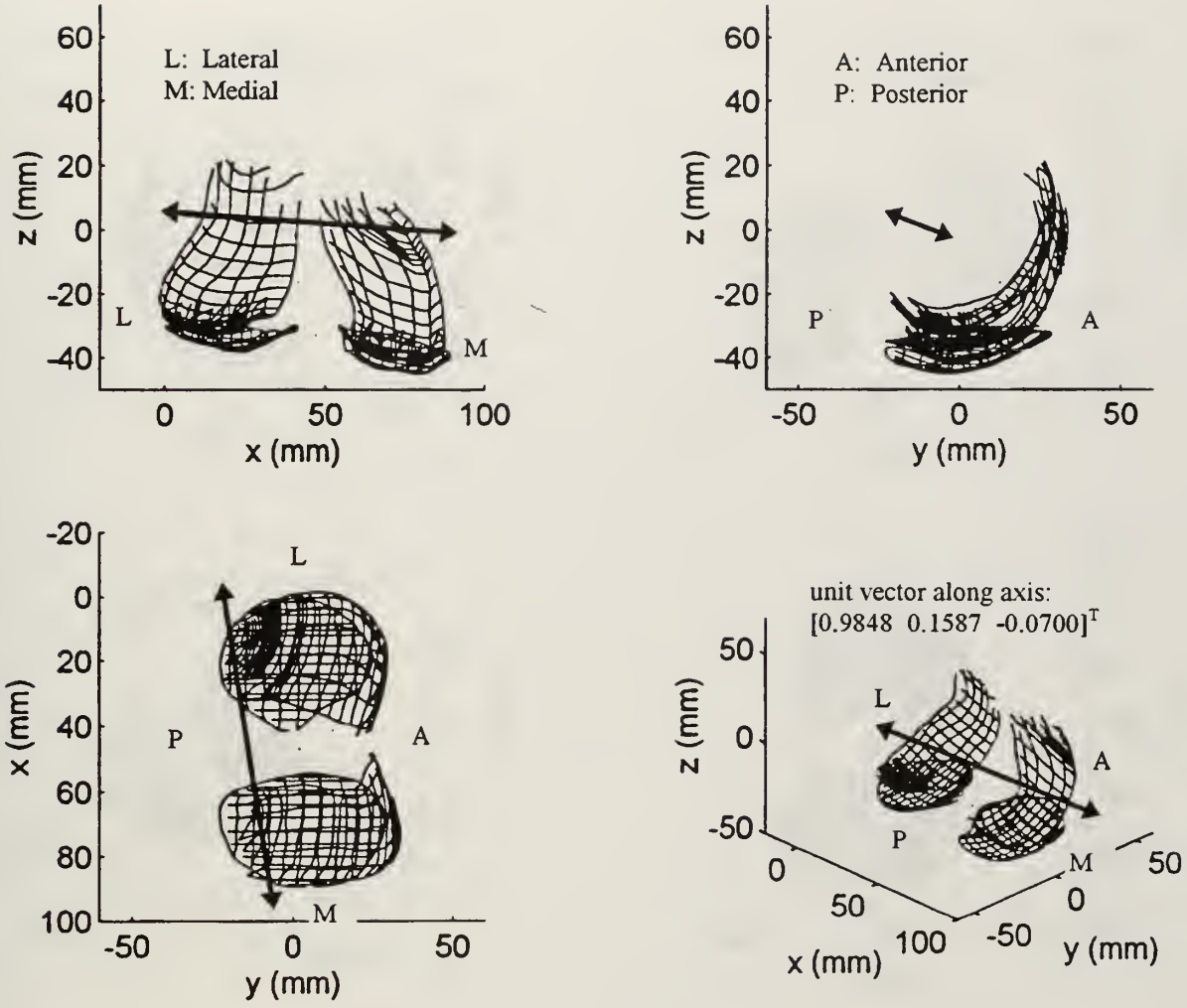


Figure 31: Instantaneous rotation axis, L31 knee, 20 degrees flexion

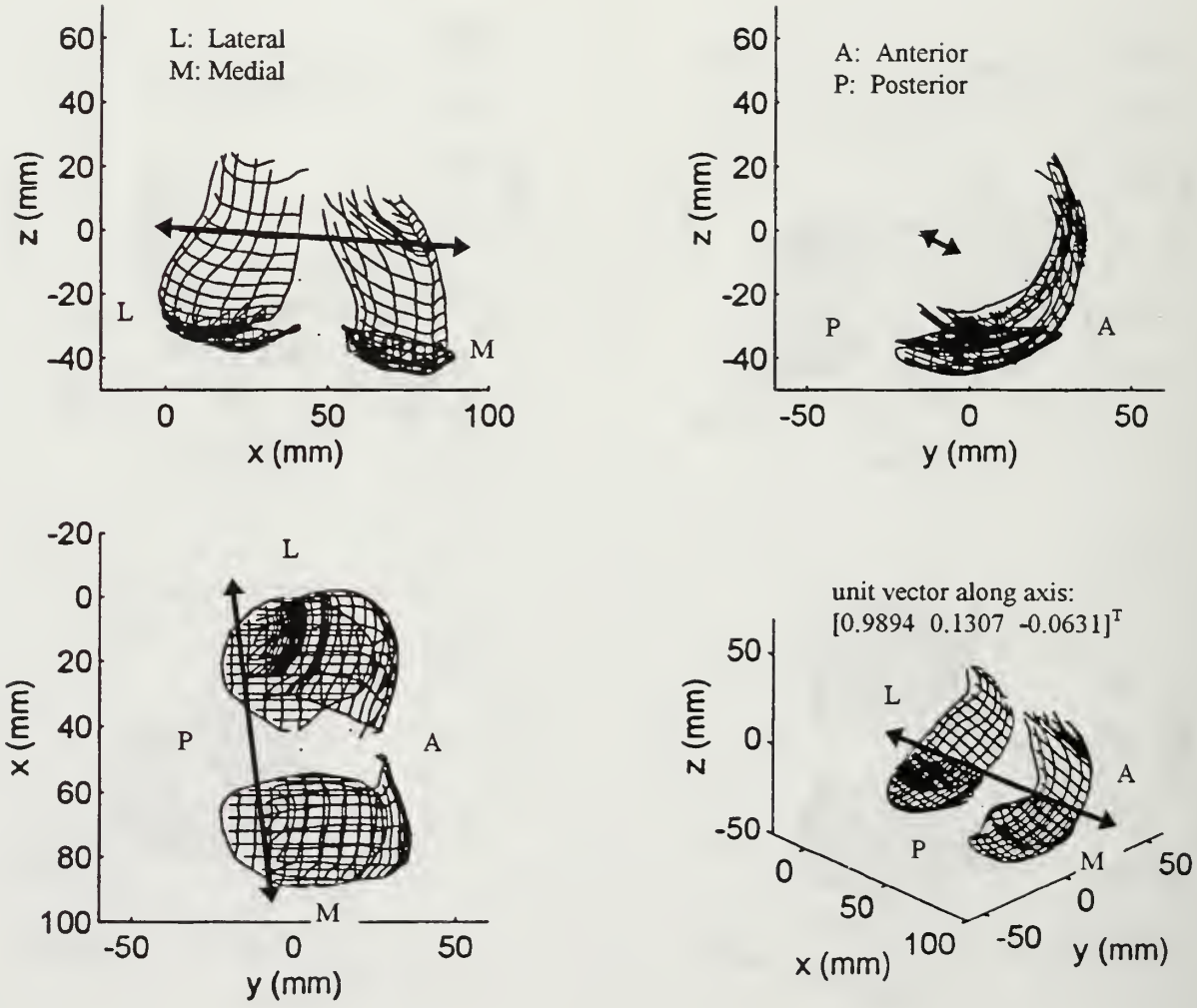


Figure 32: Instantaneous rotation axis, L31 knee, 30 degrees flexion

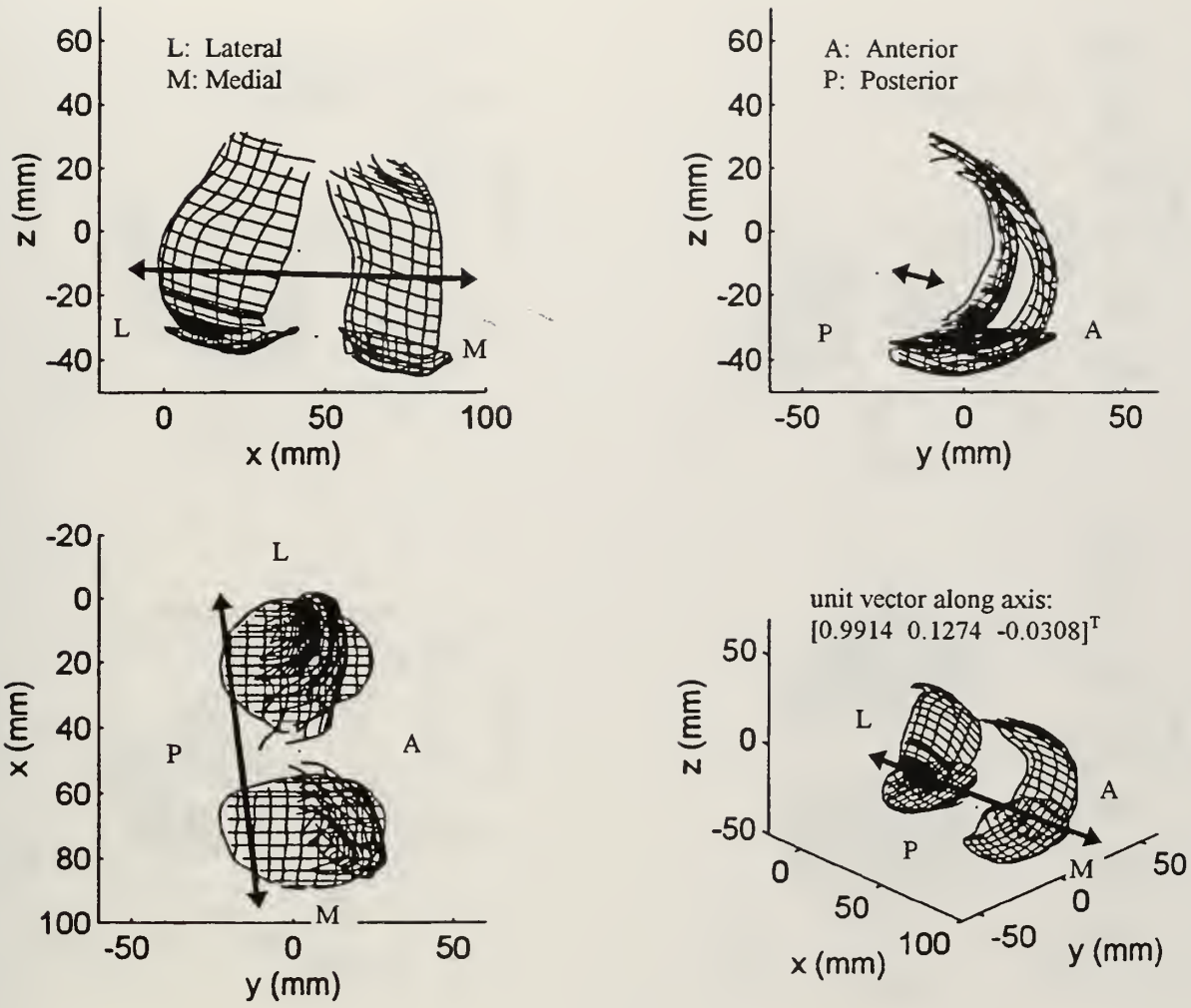


Figure 33: Instantaneous rotation axis, L31 knee, 90 degrees flexion

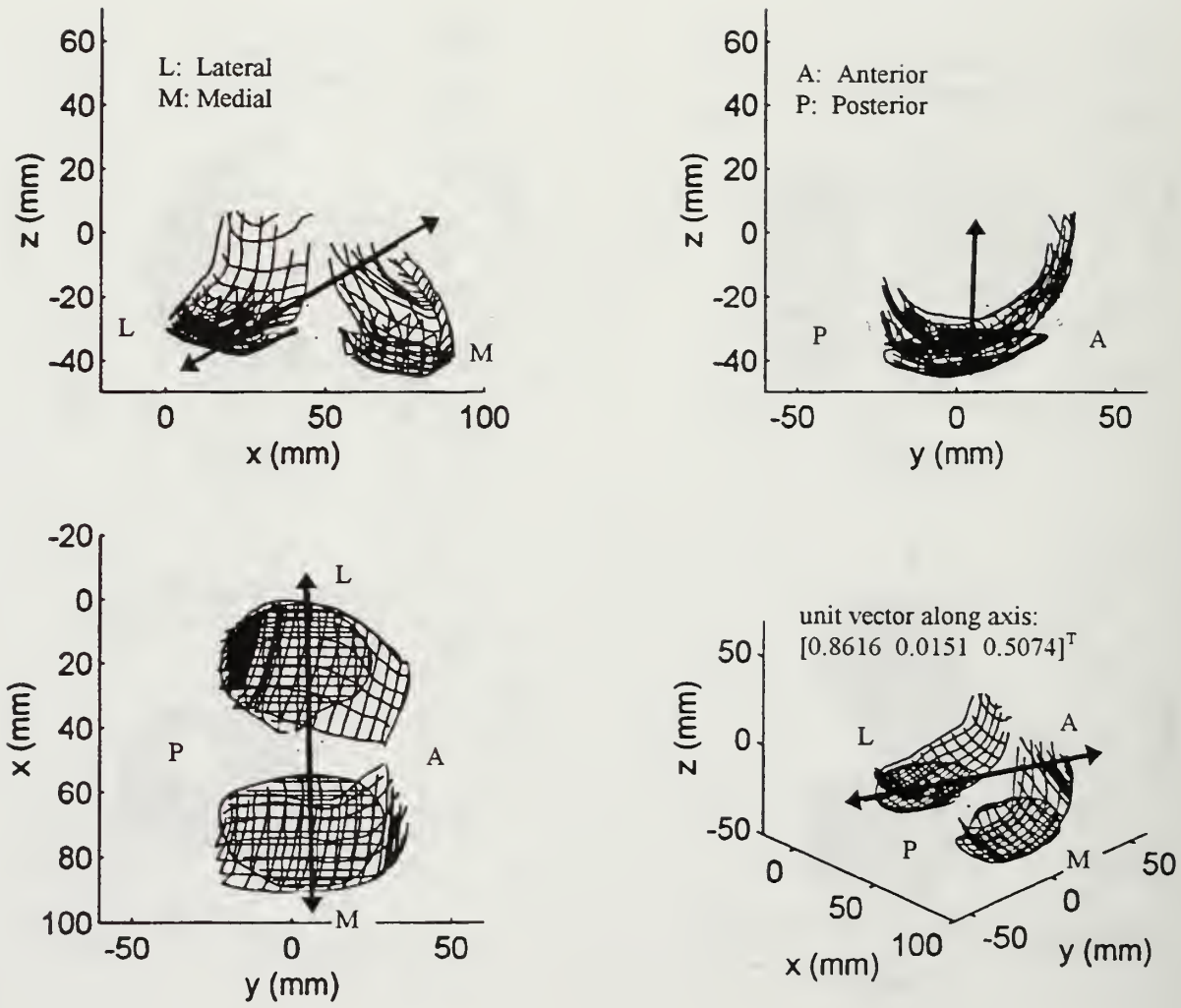


Figure 34: Instantaneous rotation axis, L210 knee, 0 degrees flexion

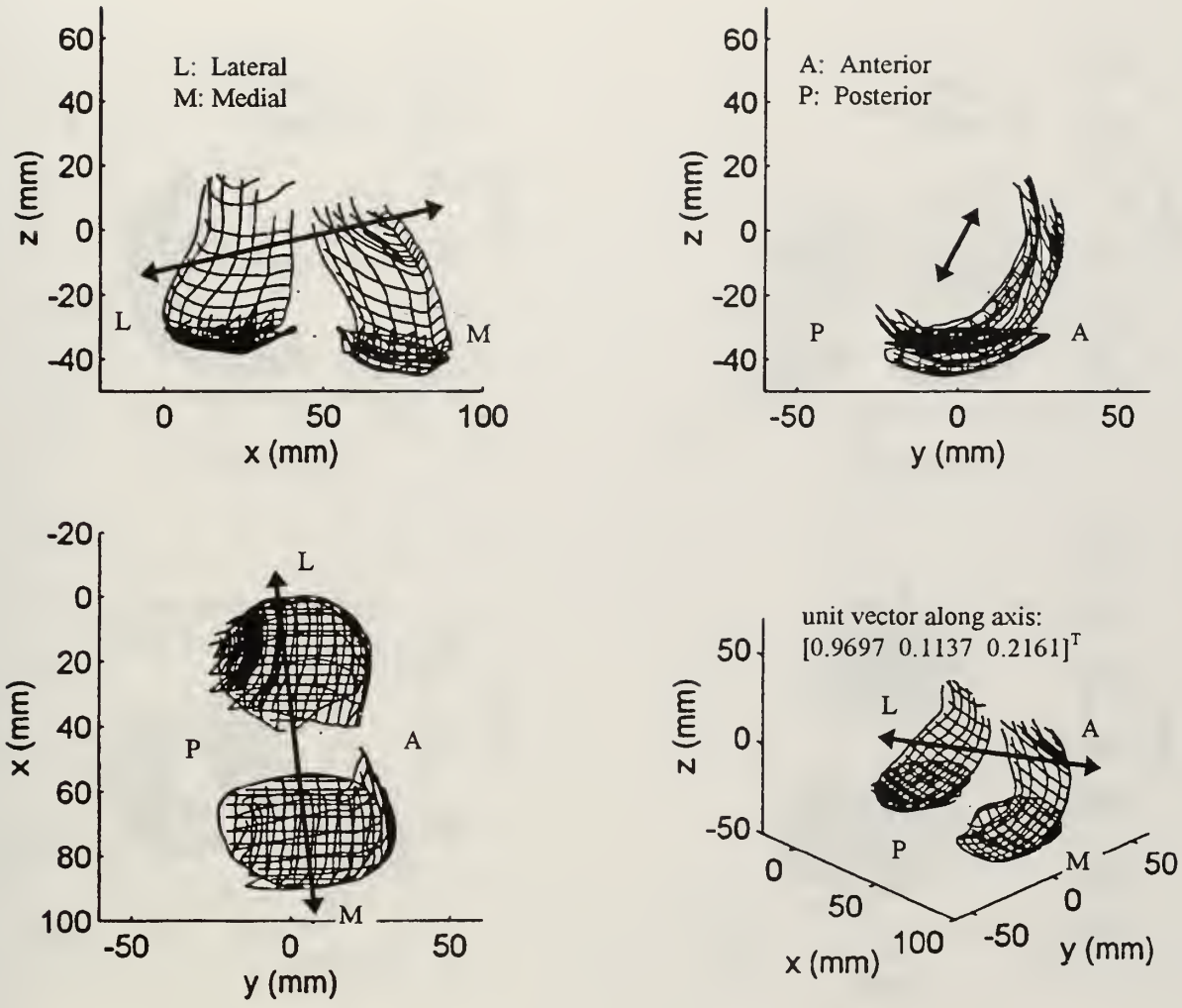


Figure 35: Instantaneous rotation axis, L210 knee, 10 degrees flexion

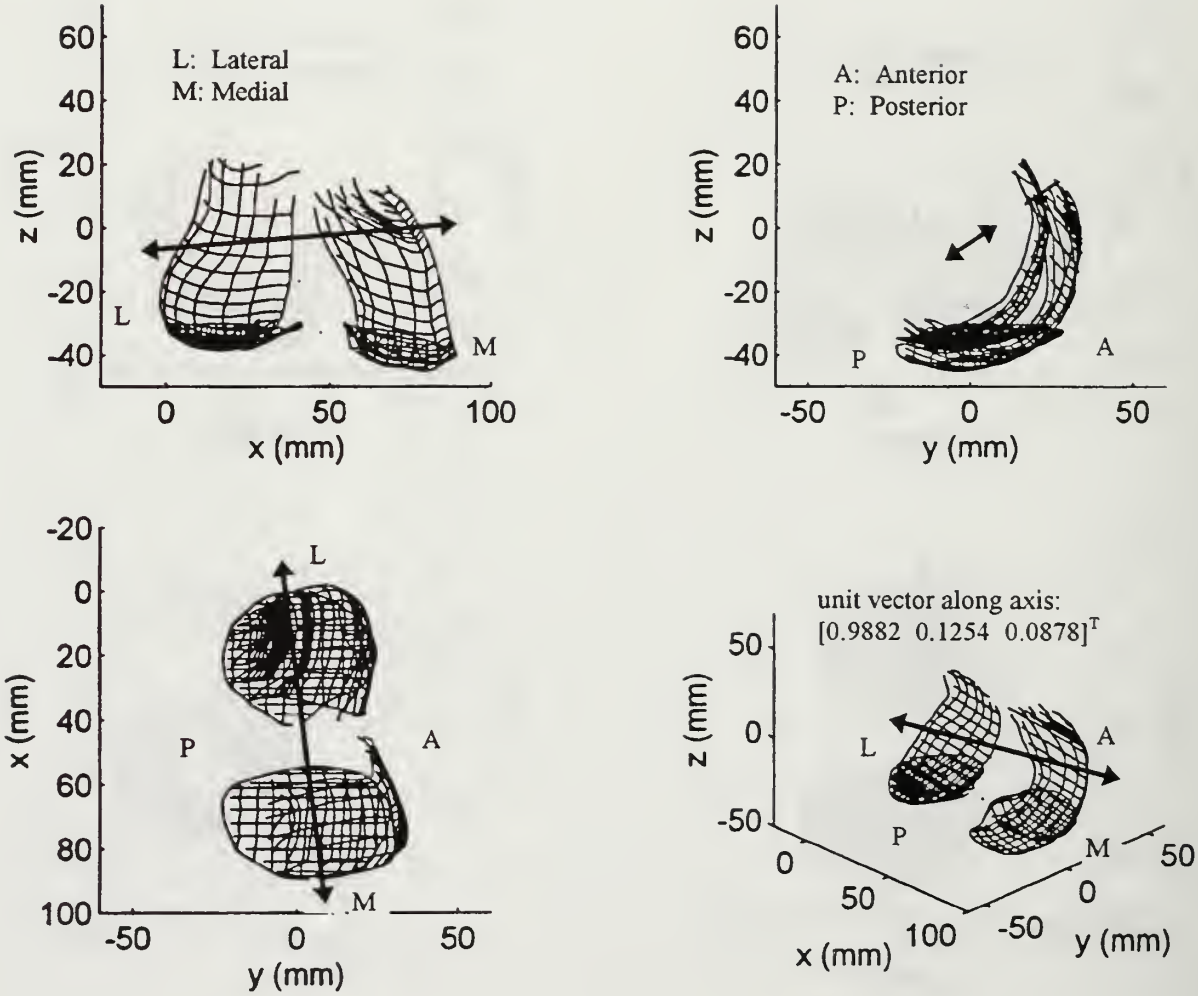


Figure 36: Instantaneous rotation axis, L210 knee, 20 degrees flexion

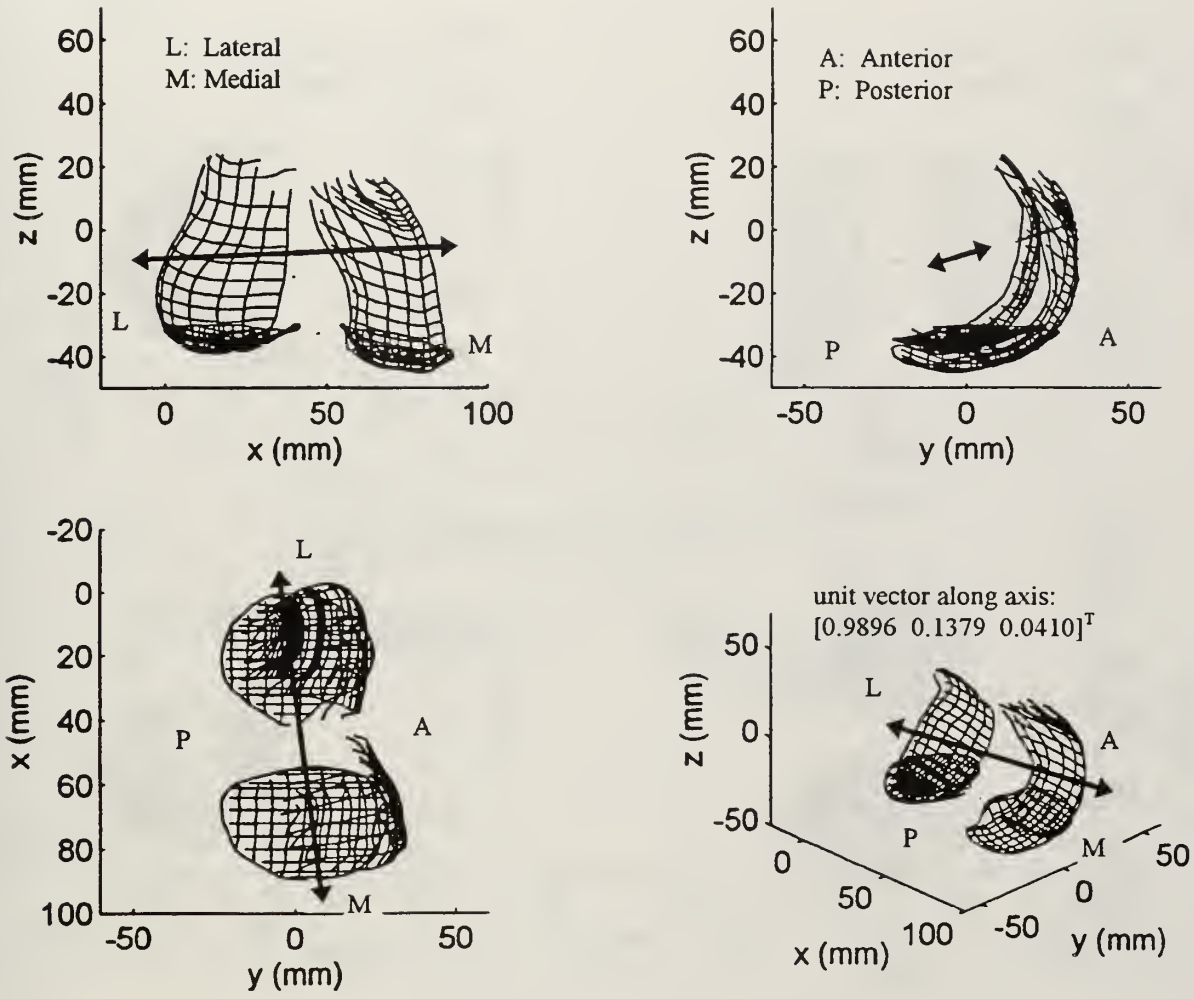


Figure 37: Instantaneous rotation axis, L210 knee, 30 degrees flexion

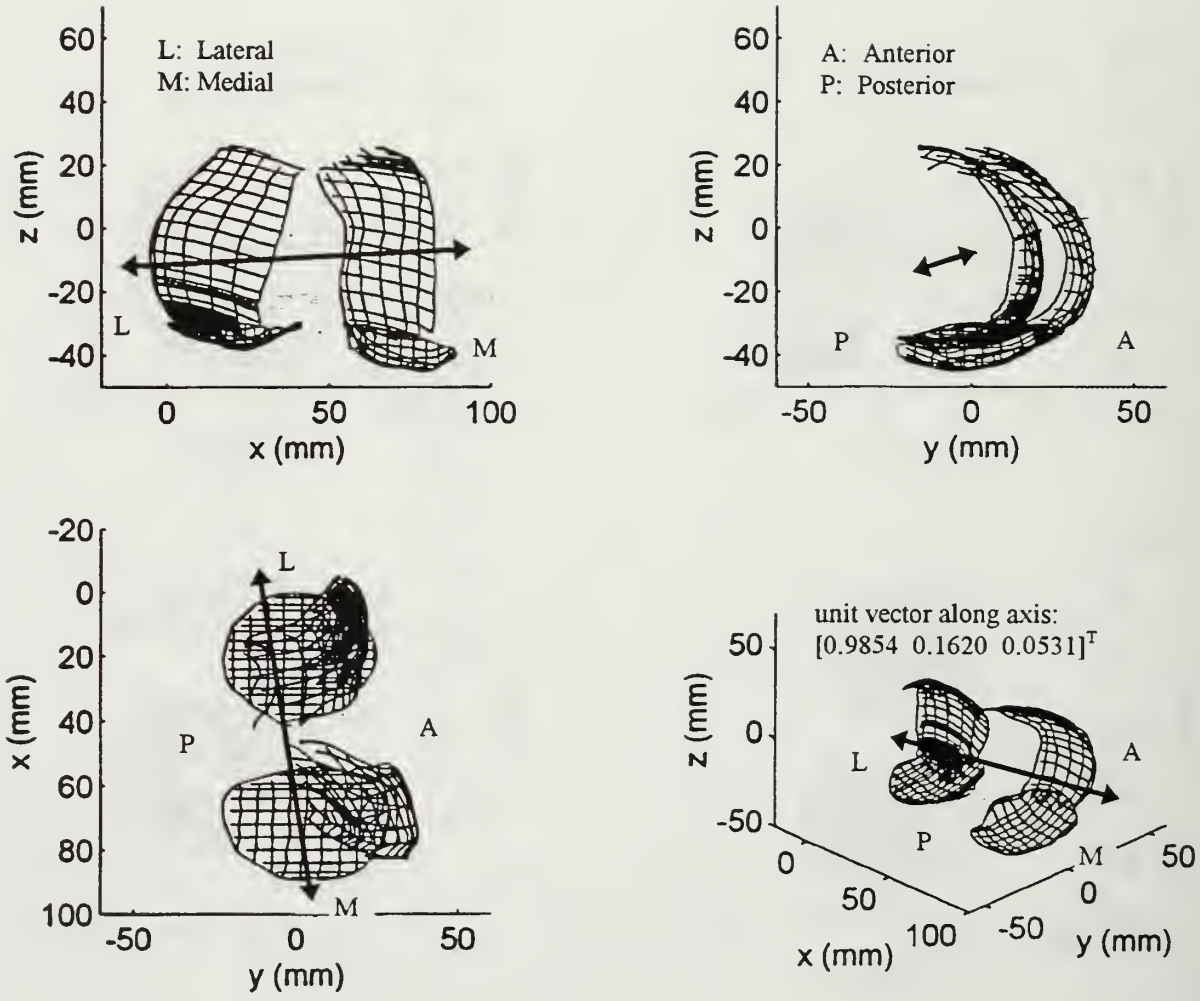


Figure 38: Instantaneous rotation axis, L210 knee, 90 degrees flexion

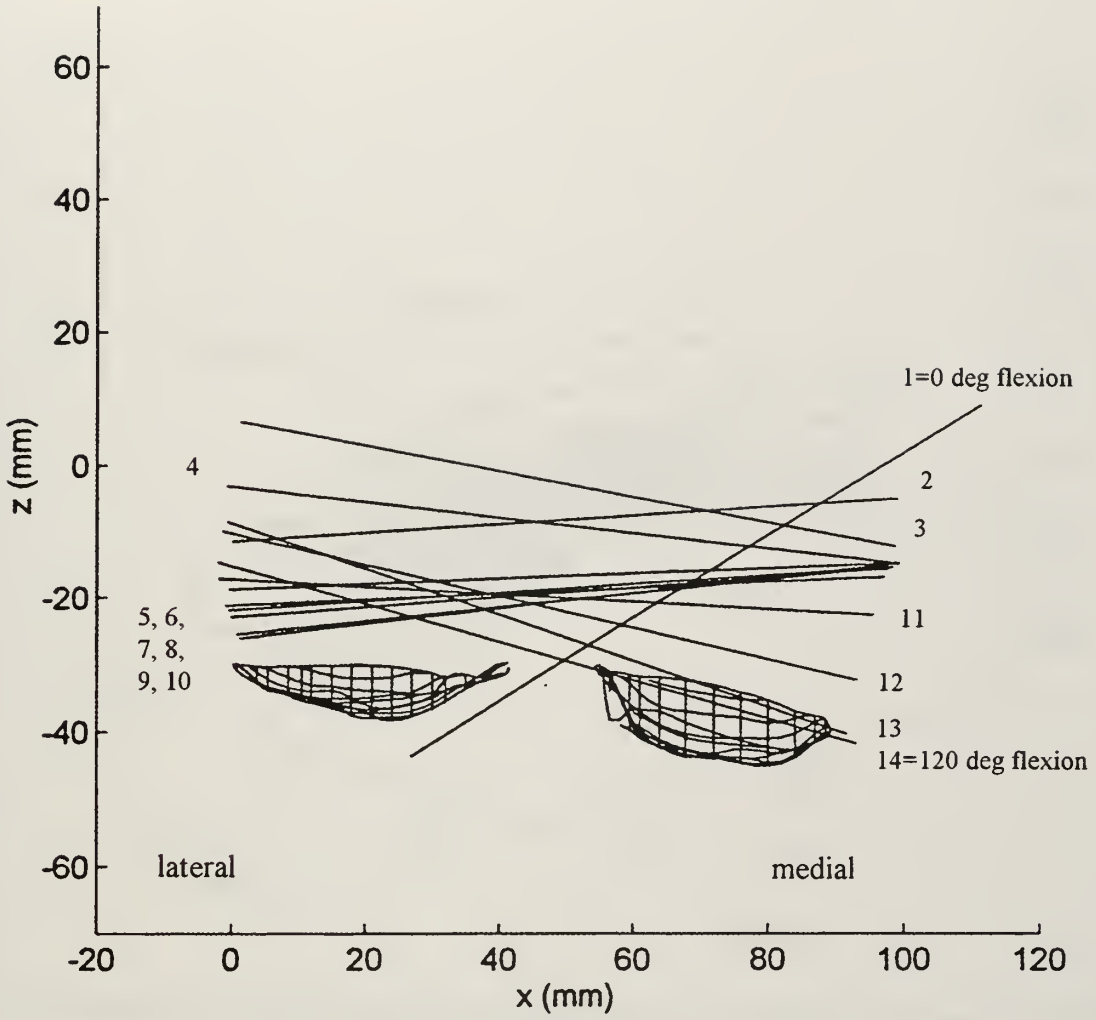


Figure 39: Knee L67 instantaneous axis of rotation. Each numbered axis represents the instantaneous axis calculated at approximately 8 degree increments. (coronal plane, posterior view)

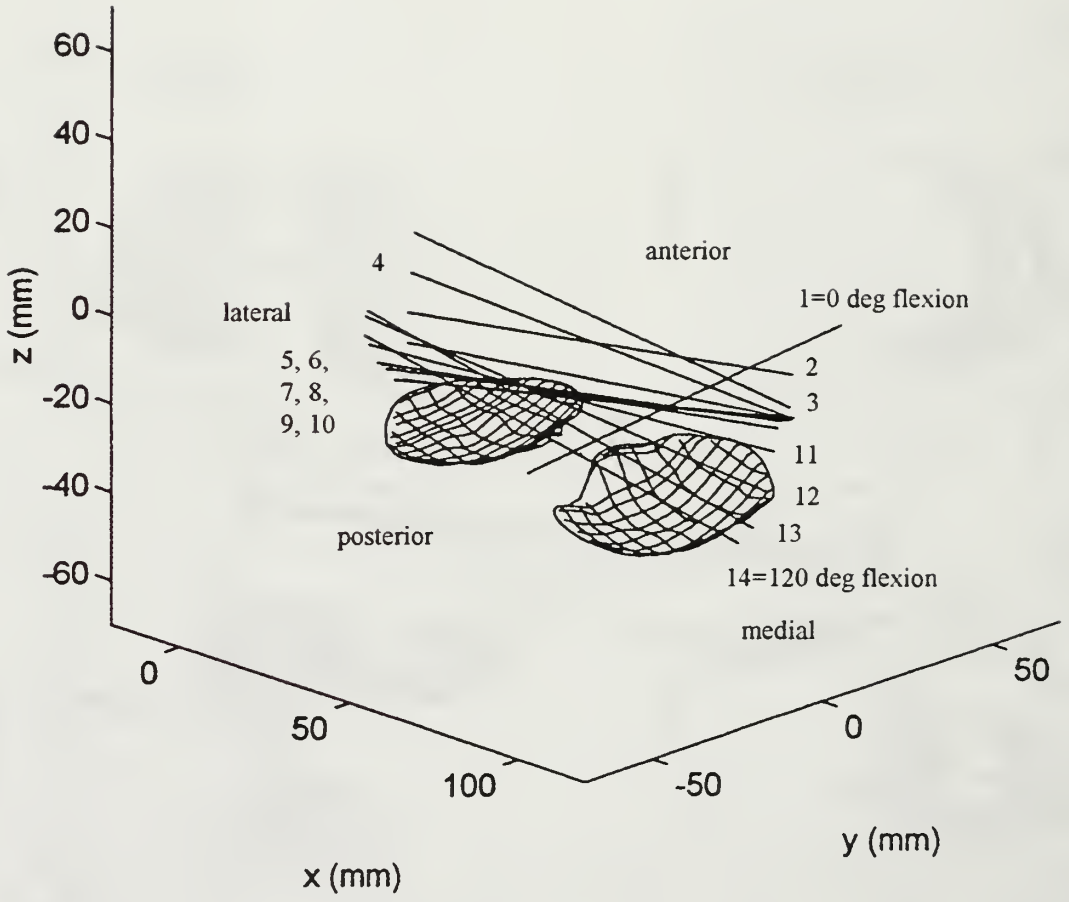


Figure 40: Knee L67 instantaneous axis of rotation. Each numbered axis represents the instantaneous axis calculated at approximately 8 degree increments. (oblique view, posteriomedial to anteriolateral)

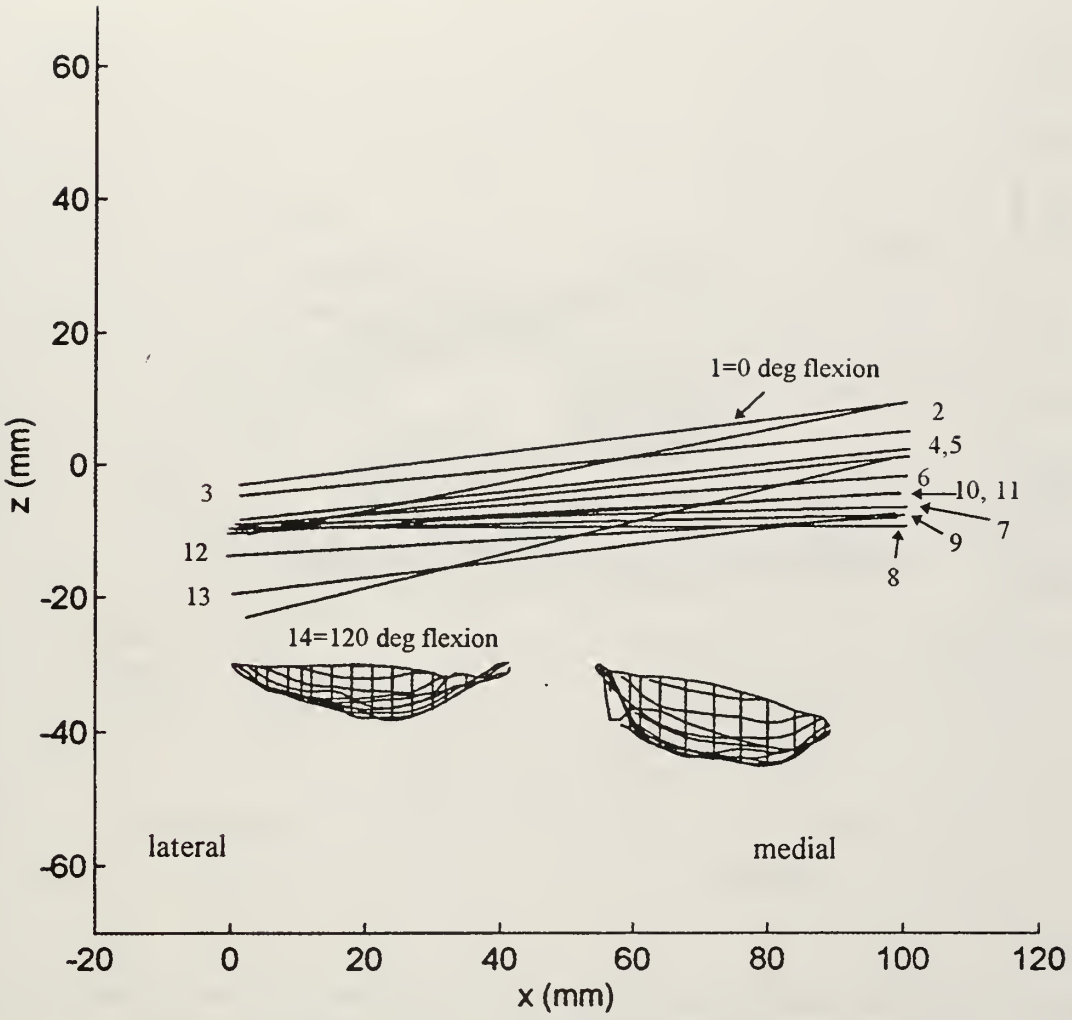


Figure 41: Knee L66 instantaneous axis of rotation. Each numbered axis represents the instantaneous axis calculated at approximately 8 degree increments. (coronal plane, posterior view)

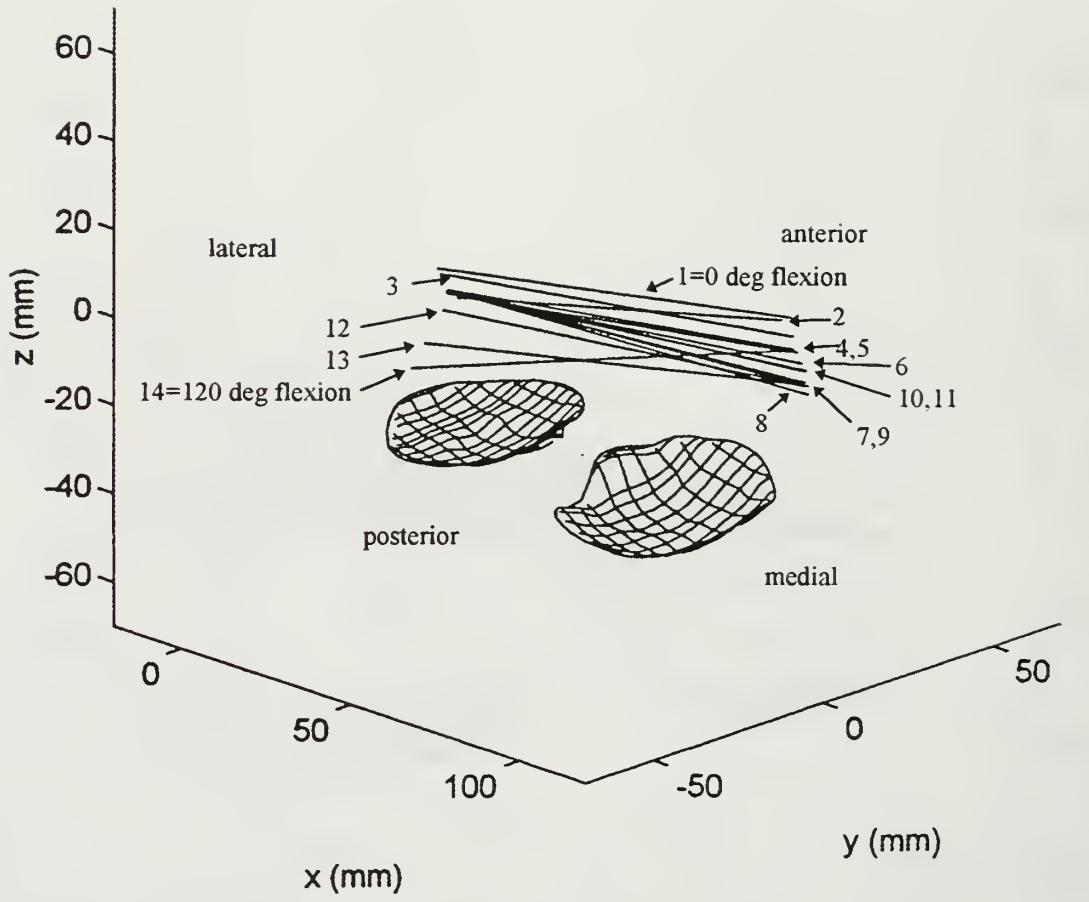


Figure 42: Knee L66 instantaneous axis of rotation. Each numbered axis represents the instantaneous axis calculated at approximately 8 degree increments. (oblique view, posteriomedial to anteriolateral)

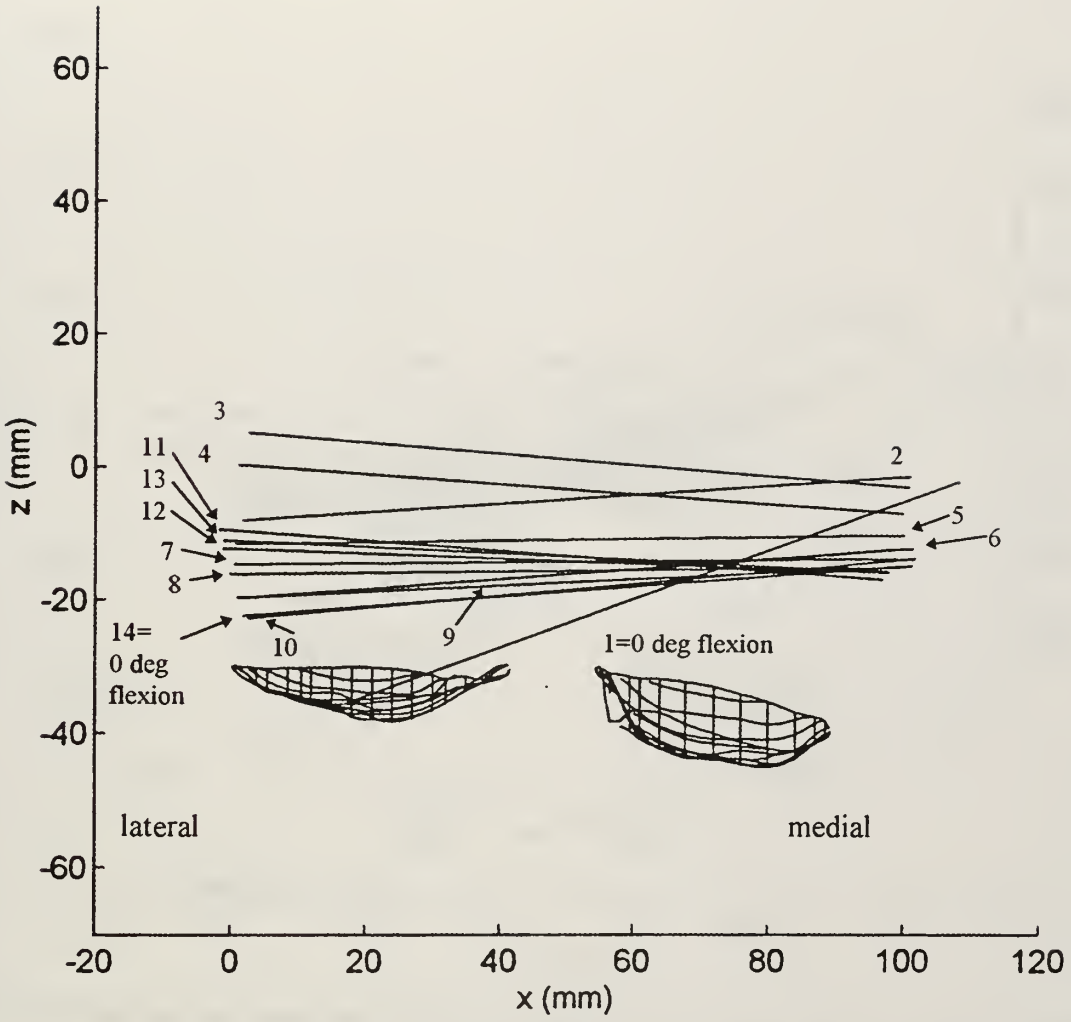


Figure 43: Knee L31 instantaneous axis of rotation. Each numbered axis represents the instantaneous axis calculated at approximately 8 degree increments. (coronal plane, posterior view)

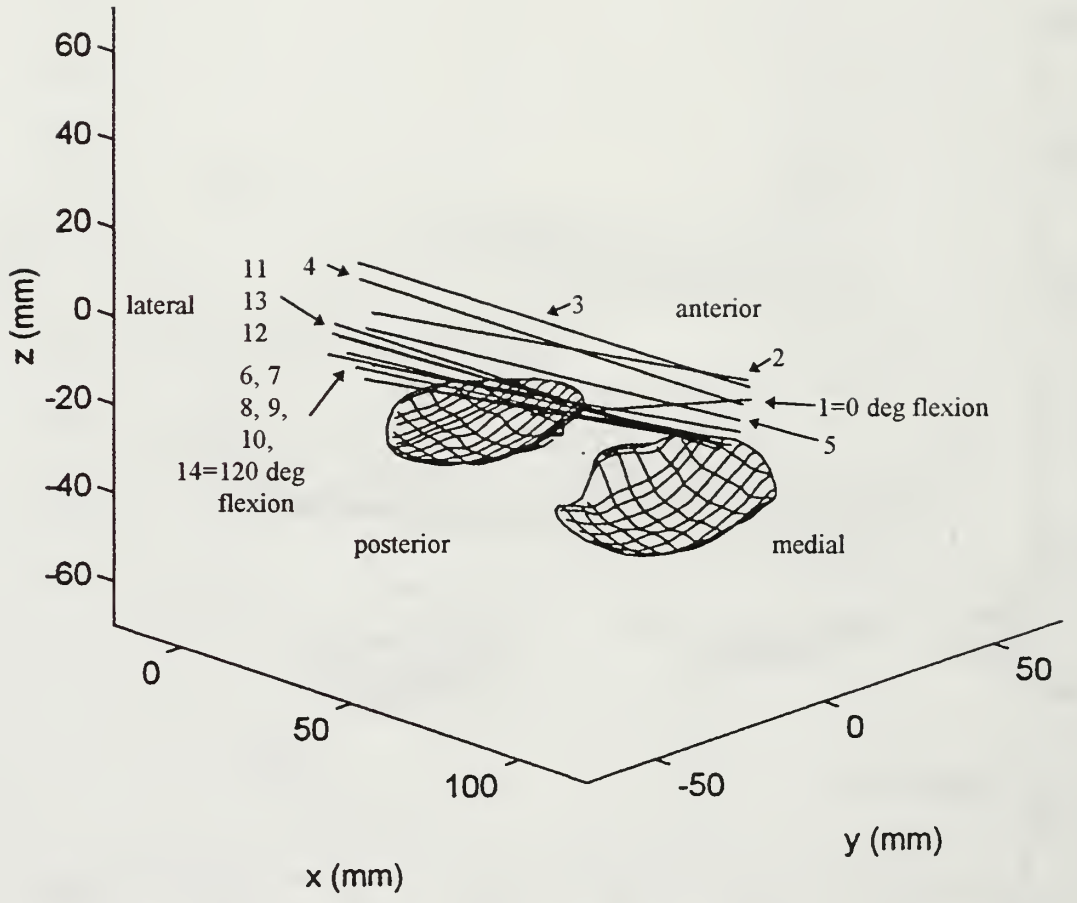


Figure 44: Knee L31 instantaneous axis of rotation. Each numbered axis represents the instantaneous axis calculated at approximately 8 degree increments. (oblique view, posteriomedial to anteriolateral)

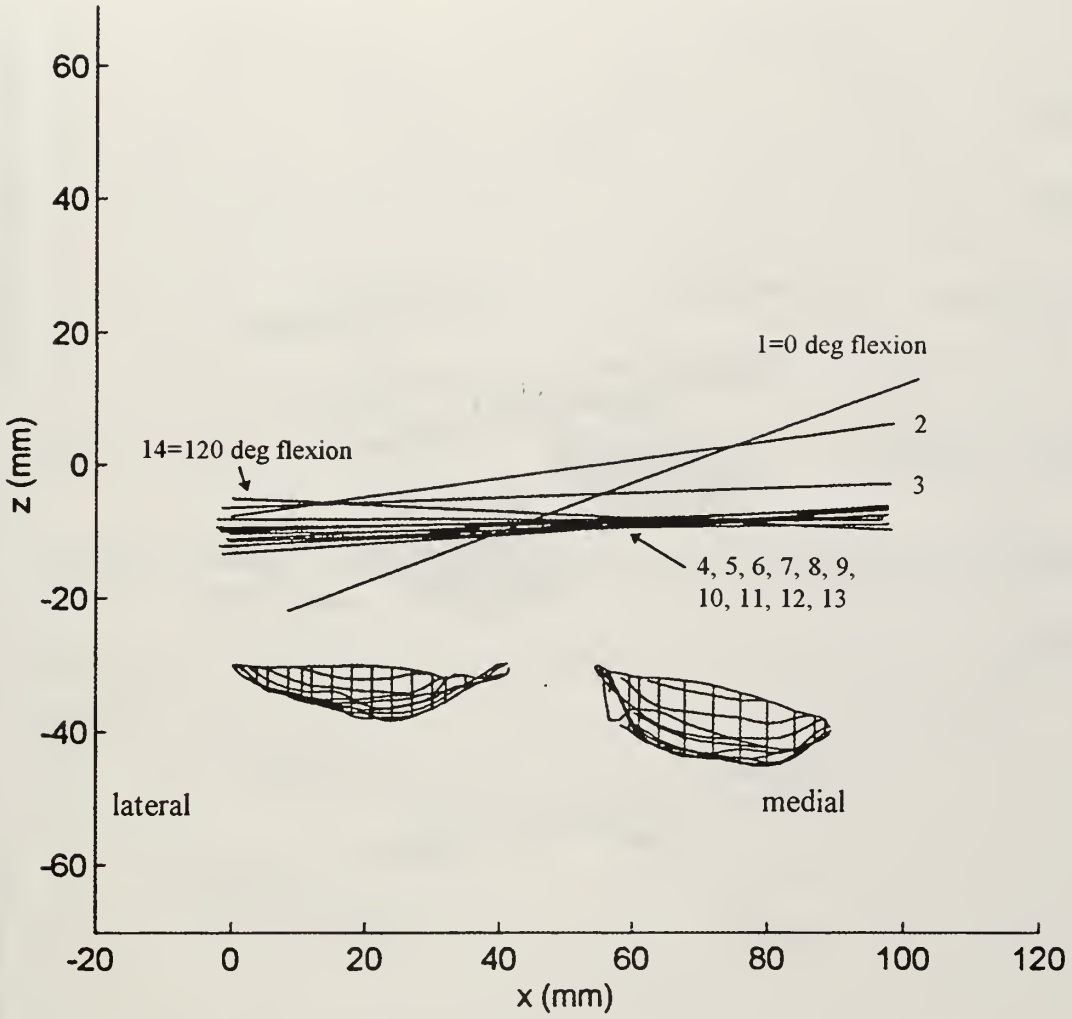


Figure 45: Knee L210 instantaneous axis of rotation. Each numbered axis represents the instantaneous axis calculated at approximately 8 degree increments. (coronal plane, posterior view)

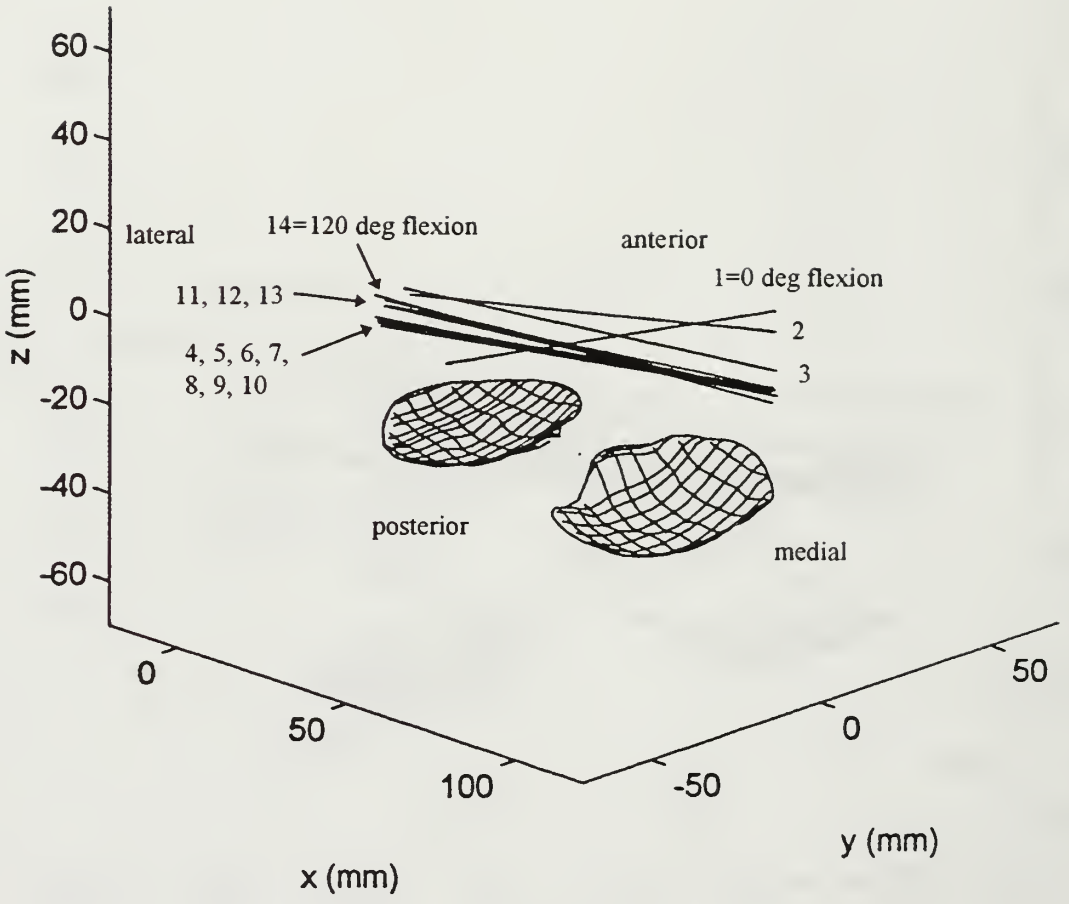


Figure 46: Knee L210 instantaneous axis of rotation. Each numbered axis represents the instantaneous axis calculated at approximately 8 degree increments. (oblique view, posteriomedial to anteriolateral)

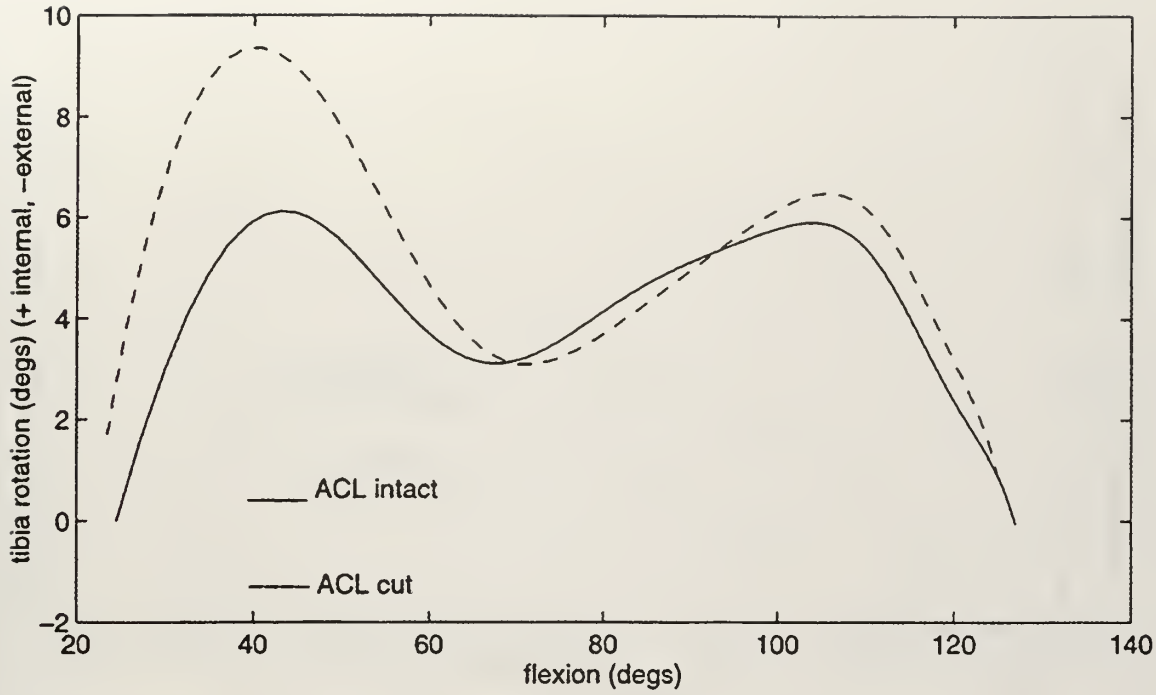


Figure 47: Knee L67 tibia rotation vs flexion for the ACL intact and ACL deficient conditions.

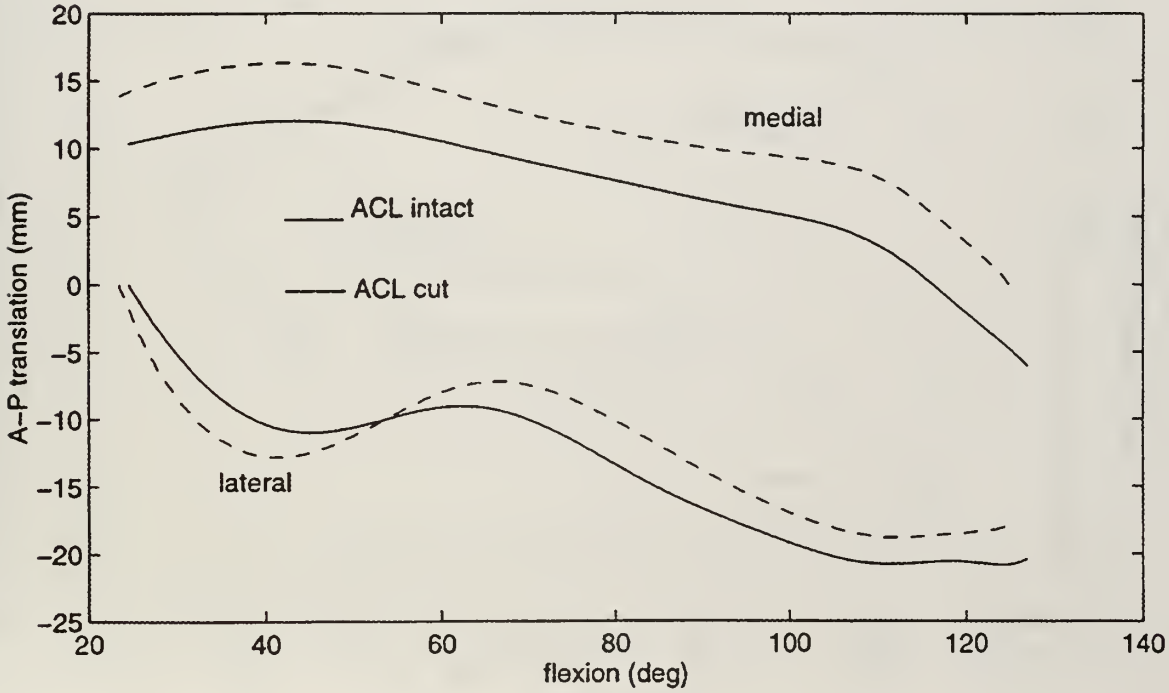


Figure 48: Apparent anterior-posterior (A-P) translation of the lateral and medial ends of the L67 knee transepicondylar axis vs flexion.

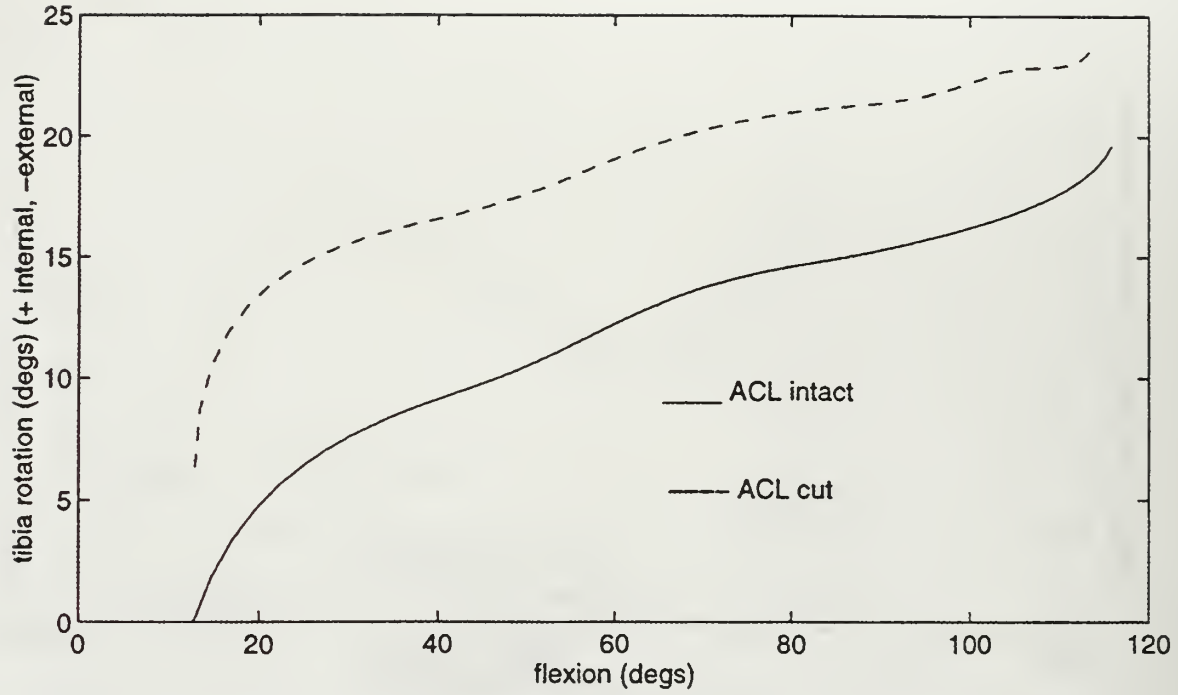


Figure 49: Knee L66 tibia rotation vs flexion for the ACL intact and ACL deficient conditions.

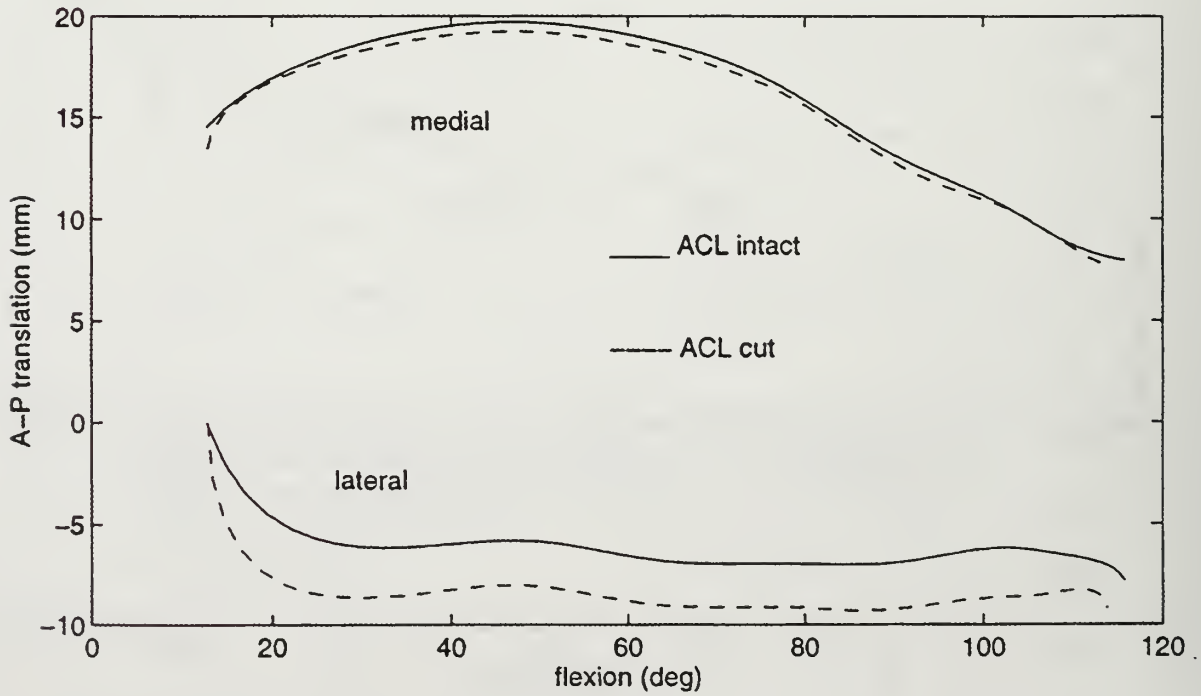


Figure 50: Apparent anterior-posterior (A-P) translation of the lateral and medial ends of the L66 knee transepicondylar axis vs flexion.

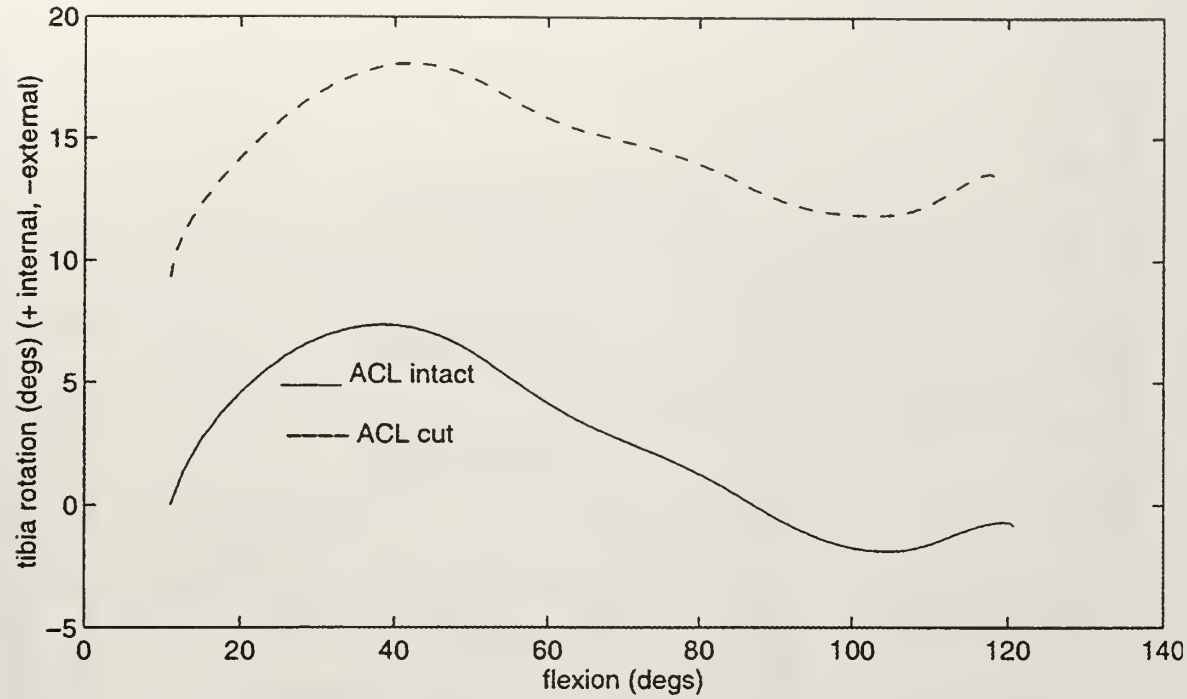


Figure 51: Knee L31 tibia rotation vs flexion for the ACL intact and ACL deficient conditions.

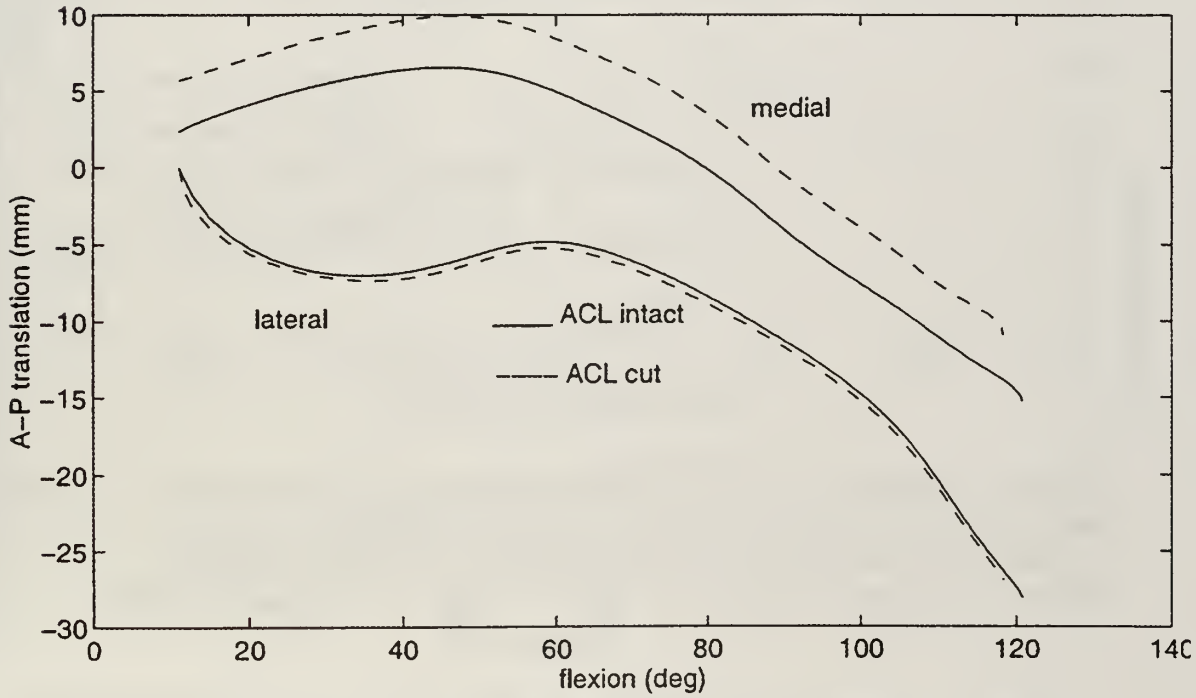


Figure 52: Apparent anterior-posterior (A-P) translation of the lateral and medial ends of the L31 knee transepicondylar axis vs flexion.

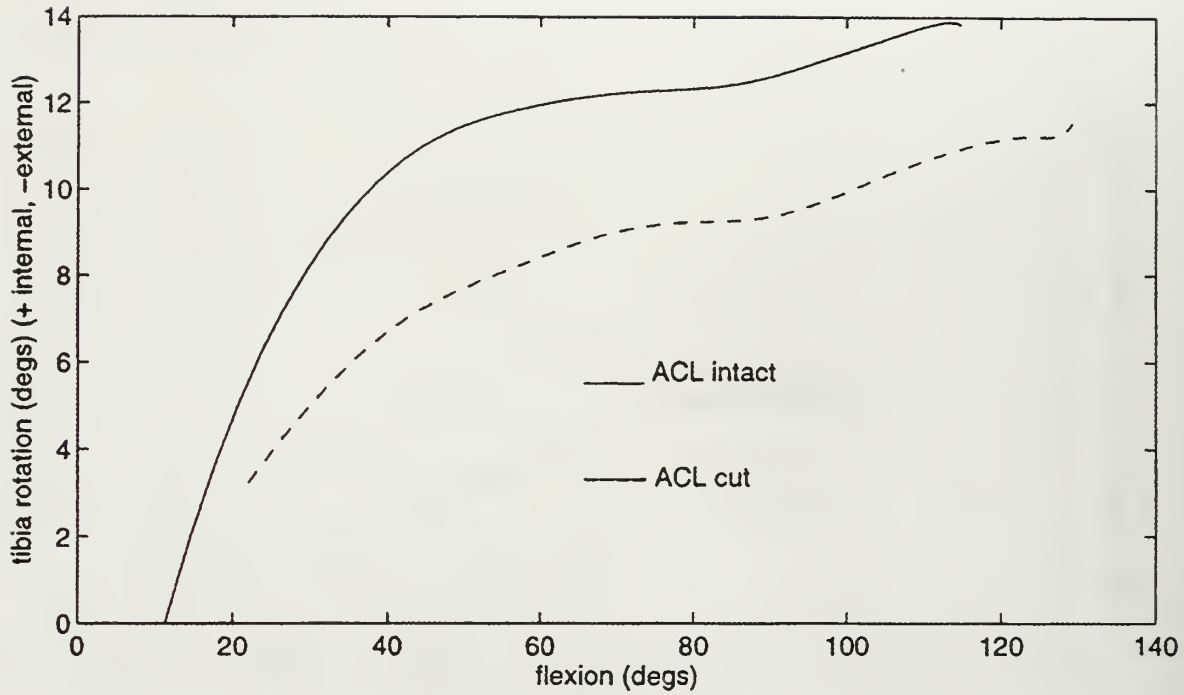


Figure 53: Knee L210 tibia rotation vs flexion for the ACL intact and ACL deficient conditions.

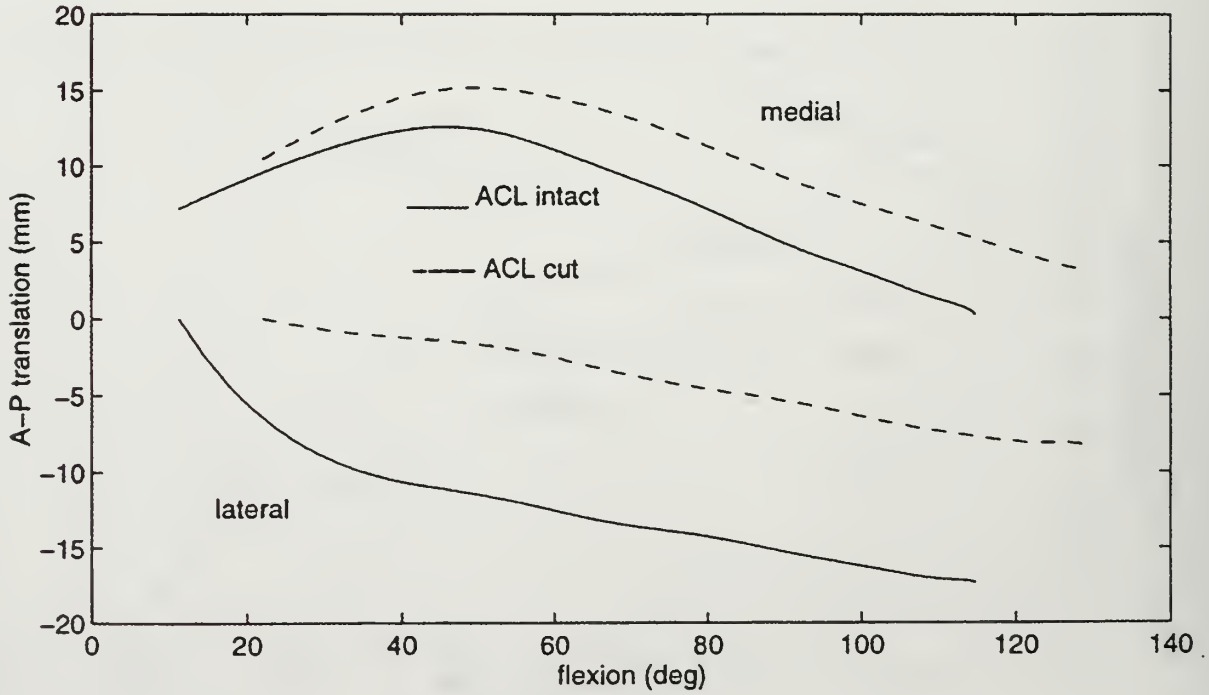


Figure 54: Apparent anterior-posterior (A-P) translation of the lateral and medial ends of the L210 knee transepicondylar axis vs flexion.

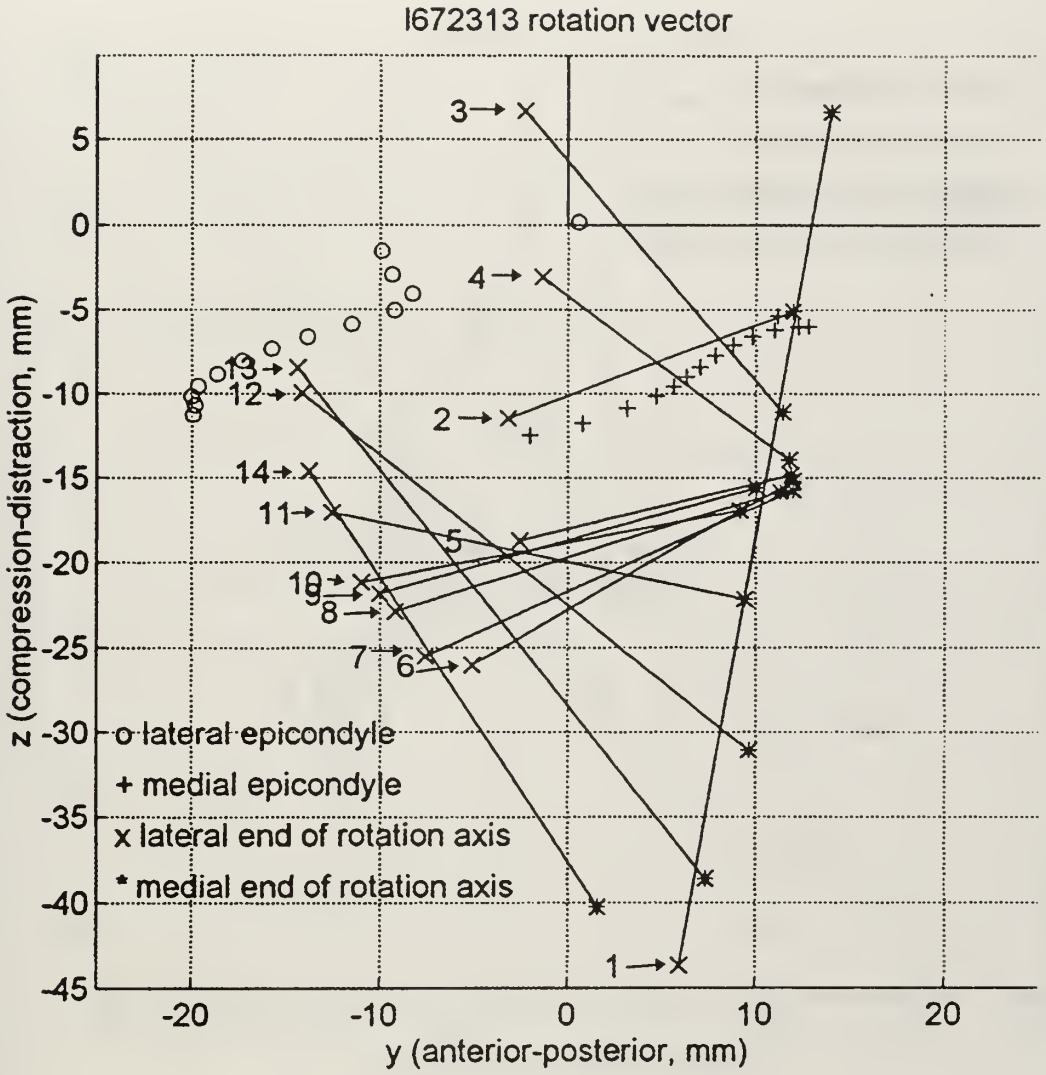


Figure 55: L67 knee instantaneous axis of rotation and epicondyle trajectories. Axis 1 corresponds to 0 degrees of flexion. Axis 14 corresponds to approximately 120 degrees of flexion. Intermediate axes are presented at approximately 10 degree increments.

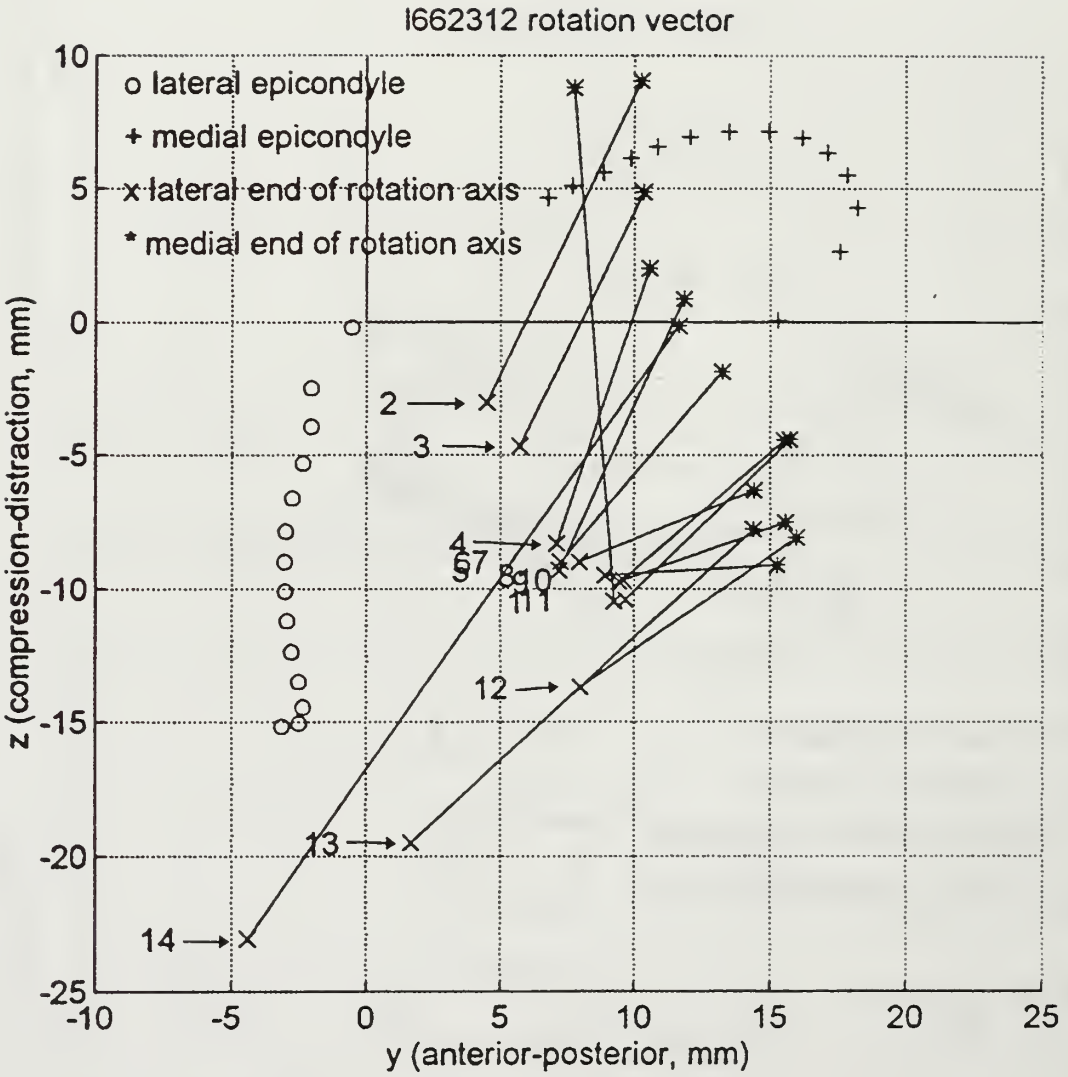


Figure 56: L66 knee instantaneous axis of rotation and epicondyle trajectories. Axis 1 corresponds to 0 degrees of flexion. Axis 14 corresponds to approximately 120 degrees of flexion. Intermediate axes are presented at approximately 10 degree increments.

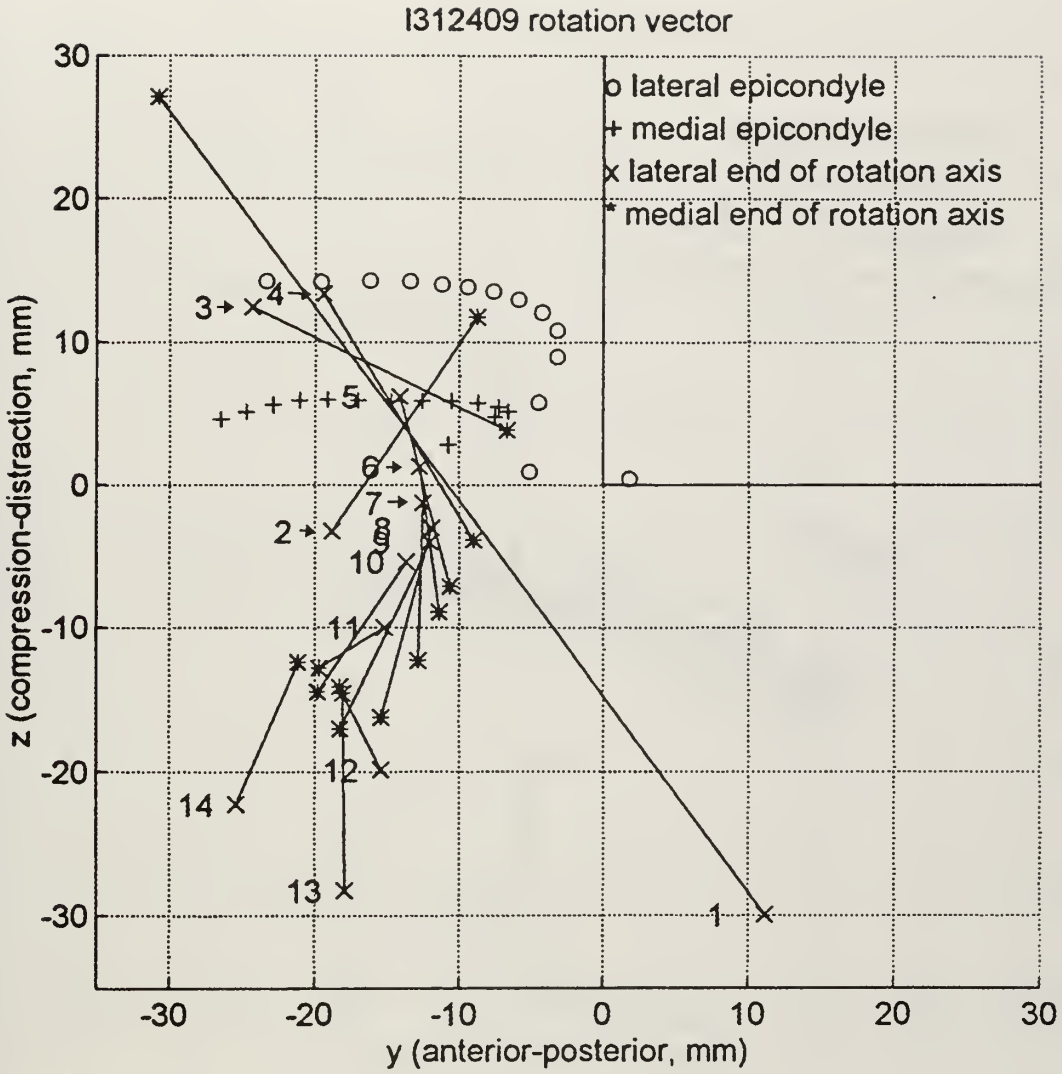


Figure 57: L31 knee instantaneous axis of rotation and epicondyle trajectories. Axis 1 corresponds to 0 degrees of flexion. Axis 14 corresponds to approximately 120 degrees of flexion. Intermediate axes are presented at approximately 10 degree increments.

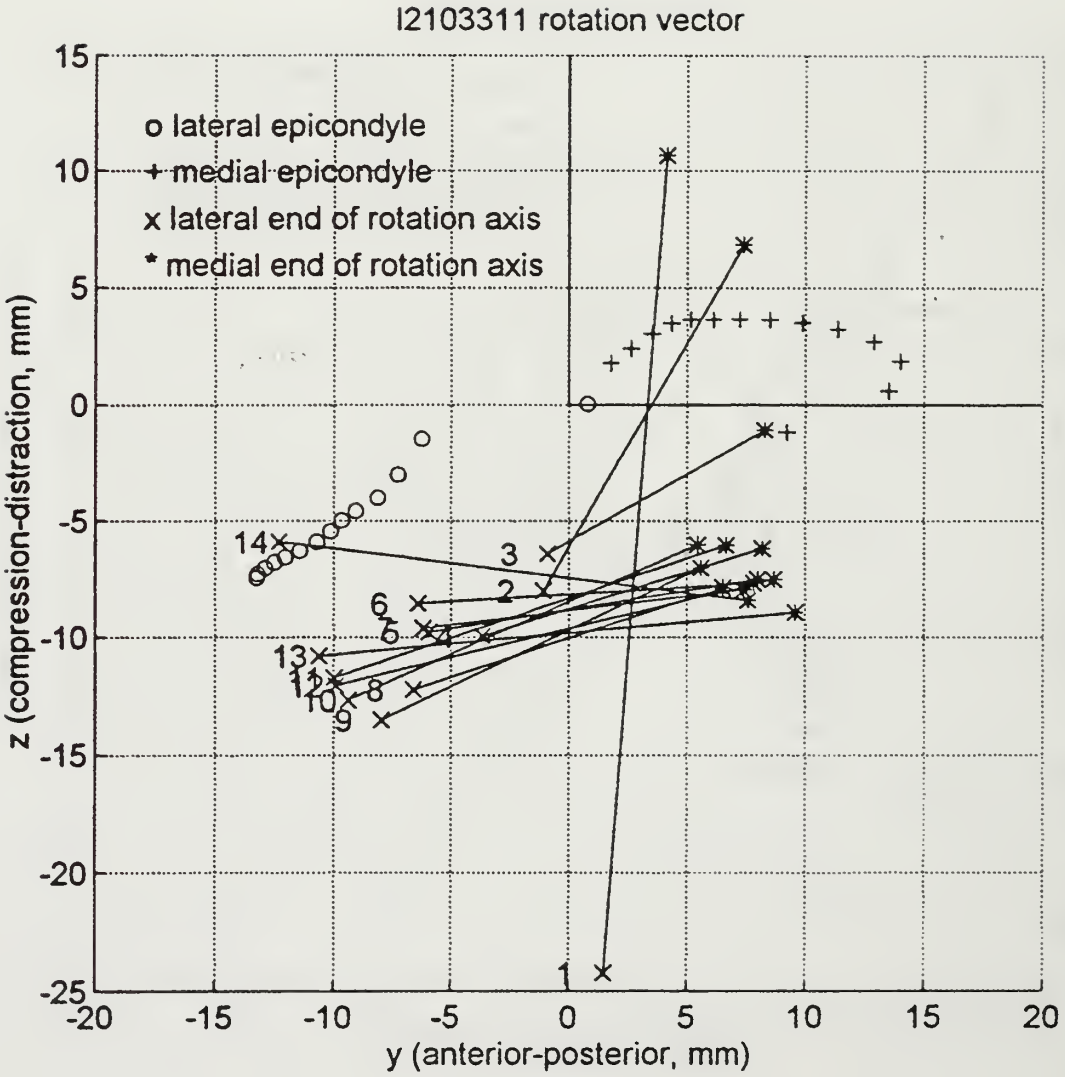


Figure 58: L210 knee instantaneous axis of rotation and epicondyle trajectories. Axis 1 corresponds to 0 degrees of flexion. Axis 14 corresponds to approximately 120 degrees of flexion. Intermediate axes are presented at approximately 10 degree increments.

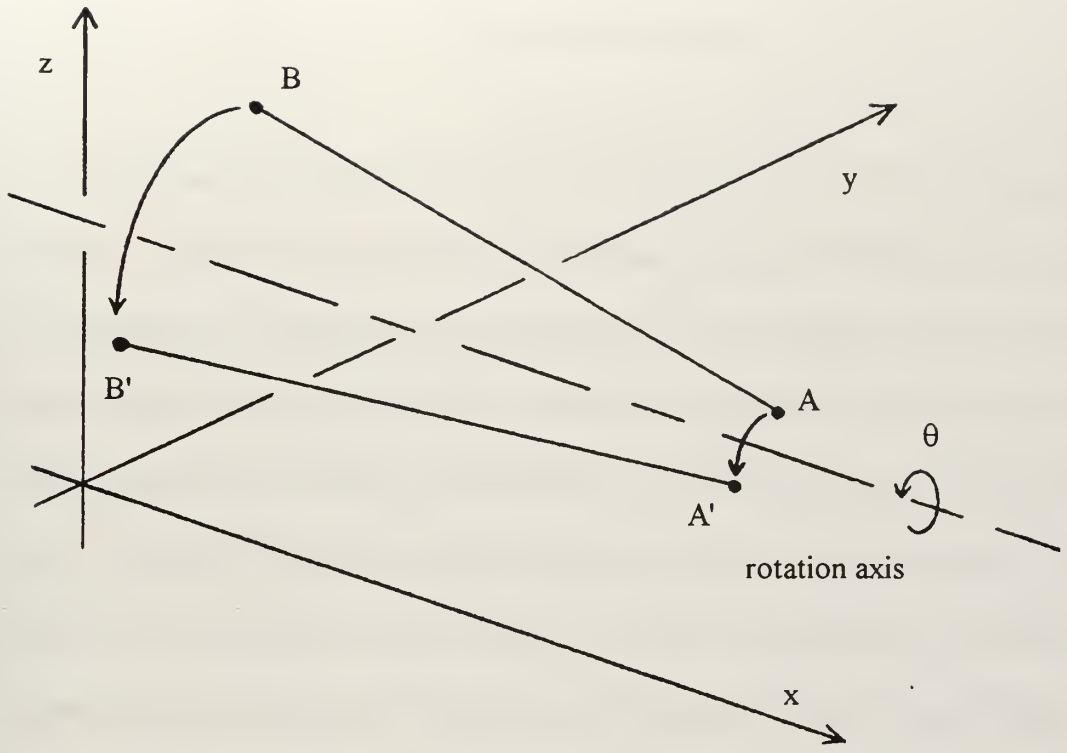


Figure 59: Rotation of an axis A-B about a separate rotation axis.

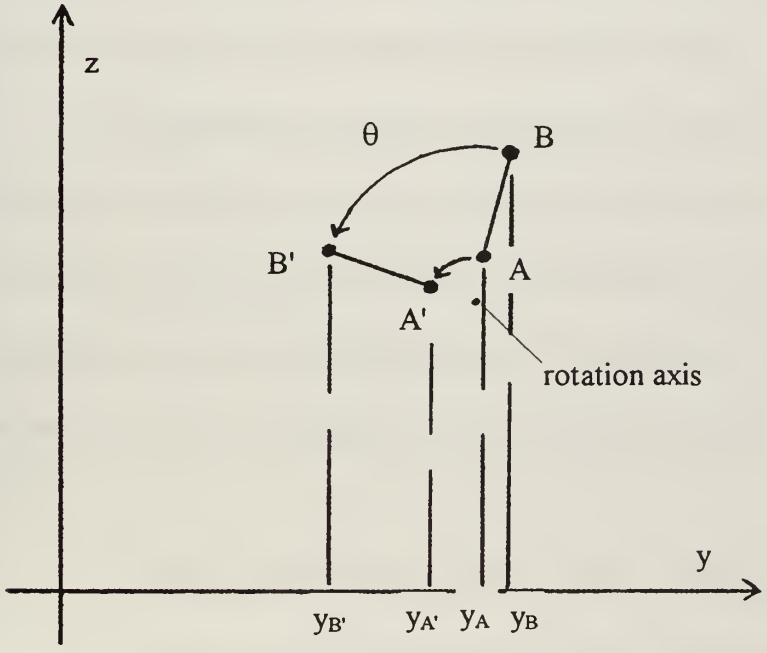


Figure 60: Apparent y translation of either end of the axis A-B due to rotation about a separate axis

VI. CONCLUSIONS

The continuous motion data collection scheme used in this study was adequate to determine an accurate approximation to the instantaneous axis of rotation for the joint. A 15 Hz sample rate resulted in data steps of no more than 0.3 degrees rotation per step. Such a small differential rotation allows small angle trigonometric approximations to be used to linearize the coordinate transformations required to calculate the instantaneous axis of rotation. The calculated instantaneous axis of rotation varied continuously as the knee was flexed forming a smooth surface in $\Re^3$ with no discontinuities. The common parameters for describing knee motion, internal/external tibia rotation, varus/valgus rotation, and flexion can be accurately calculated as the time integral of the z, y, and x components of the composite differential rotation vector developed by the model. These calculated parameters were consistent with observed values.

The instantaneous axis developed in this study agreed well with the FE axis developed by Hollister, *et al.*, using different analysis methods [Ref. 11]. In order to compare the results of the two studies, the component of internal/external tibia rotation in the instantaneous axis developed here must be neglected. Once this is done, the two different axes become analogous and the common characteristics become evident. These are:

- After the initial 20-30 degrees of flexion, the axis of rotation is relatively fixed.
- The axis is located below the epicondyles in the posterior femoral condyle.

- The lateral articulating surface of the joint is located closer to the axis of rotation than the medial articulating surface.

Each knee displayed its own unique motion path, however, similarities between knees were observed:

- Each knee displayed pronounced internal tibia rotation during the first 20° to 30° flexion.
- The instantaneous axis of rotation closely parallels the transepicondylar axis from approximately 40° flexion until the tibia begins to rotate off the posterior horn of the meniscus, occurring at about 90° -100° flexion.
- A varying ratio of articular surface rolling to articular surface sliding was observed in each knee. This varying ratio was evident as the instantaneous axis of rotation moved relative to the articulating surface between the femur and tibia.

After the ACL of each knee was cut, significantly different motion characteristics were observed. In every knee external tibia rotation was lost during extension resulting in failure of the knees to fully "screw home". Subsequent flexion data runs began from a starting position more internally rotated than with the ACL intact. In three of four knees the total amount of internal tibia rotation during flexion increased after the ACL was cut. Together, these two observations confirm the role of the ACL as a major secondary restraint to tibial internal rotation.

A comparison of the magnitude of tibia internal rotation and the initial valgus/varus orientation angle of each knee revealed a possible correlation between these parameters.

Two of the four knees tested were strongly valgus and displayed tibia internal rotation on the order of 14-18 degrees. The other two knees tested were either slightly valgus (2°) or varus. These knees displayed tibia internal rotation of 6-7 degrees, less than one half the total magnitude of the tibia internal rotation of the normal valgus knees. A detailed investigation of this finding was not performed. However, it is suspected that the magnitude of the tibia internal rotation component can be related to the initial varus/valgus orientation of the knee, and hence the shape of the articulating surfaces.

VII. RECOMMENDATIONS

The design of the motion measuring device allows continuous motion of the knee during data collection. Presently, the knee is loaded by external dead weights applied to the quadriceps tendon and the vector sum points of the hamstring and gastrocnemius muscle groups. Rotation and translation data is developed by sensors that are physically attached to the bones. This design possibly introduces forces and constraints that are not physiological. Several long term improvements in the design are recommended:

- An active control system should be developed to load the knee with muscle force patterns consistent with the activity to be simulated (i.e., sitting, standing, walking, etc.).
- A motion capture system should be procured or designed to record the motion of the knees without requiring direct contact.

Short term improvements are also recommended:

- The rotary sensor arrays should be redesigned to handle heavier loads.
- The present arrangement of pulleys and ropes places a constraining moment on the free rotation of the bones. The muscle force weight and pulley arrangement should be replaced by a pneumatic system to maintain a constant force at the muscle group vector sum points. The opposite end of each actuator should be fixed to supports that are free to rotate with the knee to remove the artificial constraining moment.

A detailed kinematic analysis should be performed to determine effects of the articulating surface shape on required internal or external tibia rotation. This study should attempt to define broad categories of knee motion characteristics and relate these characteristics to clinically observable parameters.

APPENDIX. ALTERNATIVE DERIVATIONS OF THE DIRECTION OF THE INSTANTANEOUS AXIS OF ROTATION

A. ANGULAR VELOCITY VECTOR CALCULATED UTILIZING DIFFERENTIAL EULER ANGLE DATA

Each data step is assumed to be an infinitesimal rotation and translation of the femur and tibia. This allows the collected position data to be treated as vector quantities, therefore, allowing direct numerical differentiation to calculate instantaneous angular and linear velocity vectors. The instantaneous rotation axis of the femur with respect to the tibia is the direction of the instantaneous angular velocity vector of the femur with respect to the tibia. The translation and rotation data was recorded by the measurement apparatus using a 15 Hz sample rate. After smoothing the raw data with a polynomial fit, the instantaneous time rate of change (velocity) of any parameter is calculated assuming a simple forward difference approximation.

$$\dot{y}_i = \frac{y_{i+1} - y_i}{h}$$

y is the parameter of concern and h is the time step 1/15 second. When carried out on the Euler angle data recorded by the measuring apparatus, these operations result in the time derivative of the Euler angles. These time derivatives must be transformed into the orthogonal tibial or femoral coordinate systems before they can be used to determine the instantaneous rotation axis.

The relationship between the time derivative of the Euler angles and the orthogonal angular rotation vector in the body fixed coordinate system has been determined to be [Ref. 13]:

$$\begin{Bmatrix} \omega_x \\ \omega_y \\ \omega_z \end{Bmatrix} = \begin{bmatrix} \cos(\theta)\cos(\phi) & \sin(\phi) & 0 \\ -\cos(\theta)\sin(\phi) & \cos(\phi) & 0 \\ \sin(\theta) & 0 & 1 \end{bmatrix} \begin{Bmatrix} \dot{\psi} \\ \dot{\theta} \\ \dot{\phi} \end{Bmatrix}$$

where ω_x, ω_y, and ω_z are the components of the velocity vector in the orthogonal body fixed coordinate system and $\dot{\psi}$, $\dot{\theta}$, and $\dot{\phi}$ are the time rates of change of the Euler angles of rotation about the x, y', and z'' axes respectively.

To calculate the angular velocity vector of the femur with respect to the tibia, the femoral angular velocity vector, which is defined in the body fixed femoral coordinate system, must be transformed to the tibial coordinate system. This is accomplished by premultiplication by the overall rotation matrix [T]. Following this transformation, both the tibial and the femoral angular velocity vectors are defined in the tibial coordinate system. The femoral angular velocity vector with respect to the tibia, $\omega_{f/t}$, is then calculated by subtracting the tibial angular velocity vector.

$$\{\omega_{f/t}\} = [T]\{\omega_f\} - \{\omega_t\}$$

The instantaneous rotation axis is the direction of the $\omega_{f/t}$ vector.

B. ANGULAR VELOCITY VECTOR CALCULATED UTILIZING THE TIME DERIVATIVE OF THE TRANSFORMATION MATRIX

The angular velocity of any rigid body defined in a particular reference coordinate system can be directly related to the time rate of change of the rigid body's transformation

matrix $\left([\dot{T}]\right)$, also defined in the same coordinate system [Ref. 21]. This relationship is given by the following equation:

$$[\dot{T}][T]^T = [\tilde{\omega}]$$

where [T] and $[\dot{T}]$ are the transformation matrix and the time derivative of the transformation matrix, respectively. The matrix, $[\tilde{\omega}]$, is skew symmetric and consists of the elements of the body's angular velocity vector in the reference coordinate system.

$$[\tilde{\omega}] = \begin{bmatrix} 0 & -\omega_3 & \omega_2 \\ \omega_3 & 0 & -\omega_1 \\ -\omega_2 & \omega_1 & 0 \end{bmatrix}$$

Because motion data is recorded at a high rate (15 Hz), the time derivative of the transformation matrix can be calculated by a finite forward difference approximation of the transformation matrix calculated for each time step.

$$[\dot{T}] = \frac{[T]_{i+1} - [T]_i}{\Delta t} \qquad \left(\Delta t = \frac{1}{15} \text{ sec}\right)$$

The angular velocity vector, $\vec{\omega}$, calculated for each finite time step of 1/15 second, can be considered a close approximation to the instantaneous angular velocity vector for that time step and can be considered the direction of the instantaneous rotation axis. The decomposition of the velocity of any point fixed with respect to the body will determine the location of the instantaneous rotation axis with respect to the body.

GLOSSARY OF MEDICAL TERMS

ANTERIOR - Directed toward the front.

ANTERIOR CRUCIATE LIGAMENT (ACL) - One of two ligaments which cross between the condyles of the femur holding the tibia and the femur together. The ACL is directed from posterio-lateral on the femur to anterio-medial on the tibia.

BICEPS FEMORIS MUSCLE - Long muscle directed along the posterior of the thigh from the proximal femur to the proximal tibia. One of the primary flexors of the knee.

CAPSULE - A tough, fibrous sac surrounding the knee joint containing synovial fluid.

CONDYLE - A rounded projection at the end of a bone that articulates with another bone.

DISTAL - Farthest point from a line of reference, typically the body center.

EPICONDYLE - Bony prominence found on either side of the femur corresponding to the femoral origin of the medial and lateral collateral ligaments.

FEMUR - The thigh bone which extends from the hip to the knee.

INFERIOR - Beneath; lower placement.

INTERNAL/EXTERNAL TIBIA ROTATION - The direction and magnitude of the rotation of the tibia around its long axis. Typically reported as the rotation of the tibia with respect to the femur. Internal rotation is rotation of the tibia toward the inside of the knee. External rotation is rotation of the tibia toward the outside of the knee.

LATERAL - Situated to the side or directed to the side.

LATERAL COLLATERAL LIGAMENT - The major ligament attaching the femur to the tibia on the lateral side of the knee.

LIGAMENT - A strong fibrous band of connecting tissue which binds the articular ends of bones to limit motion or to hold body organs in place.

MEDIAL - Situated to the middle or directed to the middle.

MEDIAL COLLATERAL LIGAMENT - The major ligament attaching the femur to the tibia on the medial side of the knee.

MEDULLARY CANAL - The canal in the interior of the bone containing the marrow.

MENISCUS - Fibrous cartilage on the surface of the tibia between the articulating surfaces of the femur and the tibia.

POPLITEAL FOSSA - The hollow in the posterior tibia directly beneath the meniscus.

POSTERIOR - Directed toward the rear.

POSTERIOR CRUCIATE LIGAMENT (PCL) - One of two ligaments which cross between the condyles of the femur holding the tibia and the femur together. The PCL is directed from anterio-medial on the femur to posterio-lateral on the tibia.

PROXIMAL - Closest point from a line of reference, typically the body center.

SEMIMEMBRANOSUS MUSCLE - Long muscle directed along the posterior of the thigh from the proximal femur to the proximal tibia. One of the primary flexors of the knee.

SUPERIOR - Above; higher placement.

TENDON - A fibrous cord of connective tissue by which a muscle is attached to bone or to cartilage.

TIBIA - The shin bone which extends from the knee to the ankle.

TIBIAL TUBERCLE - Bony prominence on the front of the tibia corresponding to the insertion site of the quadriceps tendon.

TRANSEPICONDYLAR AXIS - An axis directed through the knee passing through the medial and lateral femoral epicondyles.

VALGUS - The femur is bent outward with respect to the tibia. Knock kneed.

VARUS - The femur is bent inward with respect to the tibia. Bowlegged.

Definitions derived from *The New Webster's Medical Dictionary*, *The Knee: Form, Function, and Ligament Reconstruction* by W. Muller, and *Knee Ligaments: Structure, Function, Injury, and Repair* ed. D. Daniel, W. Akeson, and J. O'Connor.

GLOSSARY OF ENGINEERING TERMS

$\Re^3$ - Three dimensional real space.

CARTESIAN COORDINATE SYSTEM - Coordinate system where coordinates of points in space are given as distances from reference axes or planes.

DEGREE OF FREEDOM - Total number of degrees of freedom for a system is equal to the total number of coordinates required to specify the system configuration minus the number of independent equations of constraint.

GENERALIZED COORDINATES - Any set of parameters which serve to specify the configuration of a system.

HYSTERESIS - Path dependence of a process where the forward path is not the same as the return path.

INERTIAL REFERENCE FRAME - Any set of coordinate axes such that particle motion relative to these axes is governed by Newton's laws of motion.

NONHOLONOMIC CONSTRAINT - A restraint which must be expressed in terms of differentials of the coordinates and possibly time.

ORTHOGONAL - Two vectors $\bar{x}$ and $\bar{y}$ are orthogonal if $\bar{x}^T\bar{y} = \bar{0}$. In two dimensional and 3 dimensional real space, vectors which satisfy this relationship form 90° right angles to each other.

POTENTIOMETER - A variable resistor.

SKEW SYMMETRIC - A matrix form such that the components of a vector can be expressed in matrix form: $\begin{bmatrix} x \\ y \\ z \end{bmatrix} = \begin{bmatrix} 0 & -z & y \\ z & 0 & -x \\ -y & x & 0 \end{bmatrix}$

VISCOELASTIC - Time dependent elastic behavior.

Definitions derived from *Principles of Dynamics* by D. T. Greenwood and *Webster's Dictionary*.

LIST OF REFERENCES

1. Kurosawa, H., Walker, P. S., Abe, S., Garg, A., and Hunter, T., "Geometry and Motion of the Knee for Implant and Orthotic Design," *Journal of Biomechanics*, vol. 18, no. 7, pp. 487-499, 1985.

2. Muller, W., *The Knee - Form, Function, and Ligament Reconstruction*, pp. 8-17, Springer-Verlag, 1983.

3. Wismans, J., Veldpaus, F., Janssen, J., Huson, A., and Struben, P., "A Three-Dimensional Mathematical Model of the Knee-Joint," *Journal of Biomechanics*, vol. 13, pp. 677-685, 1980.

4. Crowninshield, R., Pope, M. H., Johnson, R. J., "An Analytical Model of the Knee," *Journal of Biomechanics*, vol. 9, pp. 397-405, 1976.

5. Woo, S. L-Y., Young, E. P., Kwan, M. K., "Fundamental Studies in Knee Ligament Mechanics," *Knee Ligaments: Structure, Function, Injury, and Repair*, Eds., Daniel, D., Akeson, W., O'Connor, J., chap. 7, pp. 115-134, Raven Press, Ltd., 1990.

6. Blankevoort, L., Huiskes, R., and de Lange, A., "Helical Axes of Passive Knee Motion," *Journal of Biomechanics*, vol. 23, no. 12, pp. 1219-1229, 1990.

7. Blankevoort, L., Huiskes, R., and de Lange, A., "The Envelope of Passive Knee Joint Motion," *Journal of Biomechanics*, vol. 21, no. 9, pp. 705-720, 1988.

8. Essinger, J. R., Leyvraz, P. F., Heegard, J. H., and Robertson, D. D., "A Mathematical Model for the Evaluation of the Behaviour During Flexion of Condylar-Type Knee Prostheses," *Journal of Biomechanics*, vol. 22, no. 11/12, pp. 1229-1241, 1989.

9. Biden, E., O'Connor, J., "Experimental Methods Used to Evaluate Knee Ligament Function," *Knee Ligaments: Structure, Function, Injury, and Repair*, Eds., Daniel, D., Akeson, W., O'Connor, J., chap. 8, pp. 135-151, Raven Press, Ltd., 1990.

10. Meriam, J. L., Kraige, L. G., *Engineering Mechanics: Dynamics*, p. 520, John Wiley & Sons, Inc., 1992.

11. Hollister, A. M., Jatana, S., Singh, A. K., Sullivan, W. W., and Lupichuk, A. G., "The Axes of Rotation of the Knee," *Clinical Orthopaedics and Related Research*, no. 290, pp. 259-268, 1993.

12. Netter, F.H., *Atlas of Human Anatomy*, plate 479, Ciba-Geigy Corp., 1994.

13. Nikravesh, P. E., *Computer-Aided Analysis of Mechanical Systems*, p. 351-352, Prentice Hall, Inc., 1988.

14. *DeMaio, M., *Adkison, D., and #Kwon, Y. W., "Continuous Motion Kinematics of the Loaded Human Cadaveric Knee: A Comparison Between the Posterior Cruciate Intact, Deficient, and Reconstructed States," (to be submitted for publishment at a future date). *Department of Orthopaedic Surgery, National Naval Medical Center, Bethesda, MD 20889. #Department of Mechanical Engineering, Naval Postgraduate School, Monterey, CA 93943.

15. Shabana, A. A., *Dynamics of Multibody Systems*, p. 16, John Wiley & Sons, 1988.

16. Greenwood, D. T., *Principles of Dynamics*, p. 300, Prentice Hall, Inc., 1988.

17. Greenwood, D. T., *Principles of Dynamics*, p. 352, Prentice Hall, Inc., 1988.

18. Shabana, A. A., *Dynamics of Multibody Systems*, p. 39, John Wiley & Sons, 1988.

19. O'Connor, J., Biden, E., Bradley, J., FitzPatrick, D., Young, S., Kershaw, C., Daniel, D. M., and Goodfellow, J., "The Muscle-Stabilized Knee," *Knee Ligaments: Structure, Function, Injury, and Repair*, Eds., Daniel, D., Akeson, W., O'Connor, J., chap. 12, pp. 239-277, Raven Press, Ltd., 1990.

20. Blacharski, P. A., Somerset, J. H., and Murray, D. G., "A Three-Dimensional Study of the Kinematics of the Human Knee," *Journal of Biomechanics*, vol. 8, pp. 375-384, 1975.

21. Nikravesh, P. E., *Computer-Aided Analysis of Mechanical Systems*, p. 172-174, Prentice Hall, Inc., 1988.

22. Shoemaker, S. C., Daniel, D. M., "The Limits of Knee Motion," *Knee Ligaments: Structure, Function, Injury, and Repair*, Eds., Daniel, D., Akeson, W., O'Connor, J., chap. 9, pp. 154-155, Raven Press, Ltd., 1990.

23. Muller, W., *The Knee - Form, Function, and Ligament Reconstruction*, pp. 60-68, Springer-Verlag, 1983.

24. Wang, C., Walker, P.S., and Wolf, B., "The Effects of Flexion and Rotation on the Length Patterns of the Ligaments of the Knee," *Journal of Biomechanics*, vol. 6, pp. 587-596, 1973.

INITIAL DISTRIBUTION LIST

1. Defense Technical Information Center 2
 8725 John J. Kingman Road., Ste 0944
 Ft. Belvoir, Va 22060-6218

2. Dudley Knox Library 2
 Naval Postgraduate School
 411 Dyer Rd.
 Monterey, CA 93943-5101

3. Naval Engineering Curricular Office (Code 34) 1
 Naval Postgraduate School
 Monterey, Ca 93943-5002

4. Department Chairman, Code ME 1
 Department of Mechanical Engineering
 Naval Postgraduate School
 Monterey, Ca 93943-5002

5. Professor Young W. Kwon, Code ME/Kw 2
 Department of Mechanical Engineering
 Naval Postgraduate School
 Monterey, Ca 93943-5002

6. CDR D. Adkison, MD 1
 Department Head, Orthopaedic Surgery
 National Naval Medical Center
 Bethesda, MD 20889

7. CDR M. DeMaio, MD 1
 Department of Orthopaedic Surgery
 National Naval Medical Center
 Bethesda, MD 20889

8. LT R. Carls, MD 1
 Department of Orthopaedic Surgery
 National Naval Medical Center
 Bethesda, MD 20889

9. LCDR Steven A. Parks 4
 111 Lake Tahoma Rd.
 Marion, NC 28752

DUDLEY KNOX LIBRARY
NAVAL POSTGRADUATE SCHOOL
MONTEREY CA 93943-5101

DUDLEY KNOX LIBRARY
3 2768 00339466 9